3-2-2021

Signal Optimization and Enhancement of Laser-Induced Breakdown Spectroscopy for Discrimination of Bacterial Organisms

Jeremy Calvin Marvin
University of Windsor

Signal Optimization and Enhancement of Laser-Induced Breakdown Spectroscopy for Discrimination of Bacterial Organisms

By

Jeremy C. Marvin

A Thesis
Submitted to the Faculty of Graduate Studies
through the **Department of Physics**
in Partial Fulfillment of the Requirements for
the Degree of **Master of Science**
at the University of Windsor

Windsor, Ontario, Canada

2020

Signal Optimization and Enhancement of Laser-Induced Breakdown Spectroscopy for Discrimination of Bacterial Organisms

By

Jeremy C. Marvin

APPROVED BY:

_____

Dr. D. Marquardt
Department of Chemistry and Biochemistry

_____

Dr. E. Maeva
Department of Physics

_____

S. J. Rehse, Advisor
Department of Physics

December 10, 2020

Declaration of Originality

I hereby certify that I am the sole author of this thesis and that no part of this thesis has been published or submitted for publication.

This thesis incorporates works that were the outcome of joint research in collaboration with Allie Paulick, Emma Blanchette and Sydney Sleiman under the supervision of Dr. Steven J. Rehse. This collaboration provided the basis for Chapters 5 and 6. The key ideas discussed in this thesis are primarily the work of the author, and the contributions of the co-authors were primarily in the act of sample preparation, data acquisition and refinement of the ideas taken from the results of those studies.

I certify that, to the best of my knowledge, my thesis does not infringe upon anyone's copyright nor violate any proprietary rights and that any ideas, techniques, quotations, or any other material from the work of other people included in my thesis, published or otherwise, are fully acknowledged in accordance with the standard referencing practices. Furthermore, to the extent that I have included copyrighted material that surpasses the bounds of fair dealing within the meaning of the Canada Copyright Act, I certify that I have obtained a written permission from the copyright owner(s) to include such material(s) in my thesis and have included copies of such copyright clearances to my appendix.

I declare that this is a true copy of my thesis, including any final revisions, as approved by my thesis committee and the Graduate Studies office, and that this thesis has not been submitted for a higher degree to any other University or Institution.

Abstract

Bacterial pathogens can be differentiated via an elemental analysis technique known as laser-induced breakdown spectroscopy (LIBS). This spectrochemical technique provides a near-instantaneous measurement of the elemental composition of a target. The aim of this work was to demonstrate the feasibility of LIBS for the rapid identification and discrimination of bacteria in simulated clinical specimens based on reproducible differences in the concentration of inorganic elements in bacterial cells. This research will describe the current experimental technique, including bacteria collection and mounting protocols, LIBS data acquisition, and spectral data analysis. These include methods for the collection, concentration, and separation of bacteria from unwanted biological matter, deposition of bacterial cells on a suitable ablation medium, the formation of high temperature laser-induced micro plasmas, collection, and analysis of the atomic emission spectra with a high-resolution spectrometer, and the differentiation of LIBS emission spectra from different bacterial species and genera using computerized chemometric algorithms. The construction of a spectral library database containing the LIBS emission spectra from hundreds of spectra obtained from highly diluted specimens of *Staphylococcus epidermidis, Escherichia coli, Mycobacterium smegmatis, Pseudomonas aeruginosa, Enterococcus cloacae* and sterile water control specimens is ongoing. Manipulation of this library with outlier elimination techniques, reduction of elemental contaminants contributing to extraneous background signals, and the addition of silver microparticles to enhance signal intensities are all being investigated to produce a standardized protocol that minimizes the bacterial limit of detection while maximizing classification accuracy.

Acknowledgements

This thesis would not have been possible without the help and support of my outstanding research group, my close friends, and my family.

I would like to sincerely thank my research advisor, Dr. Steven Rehse, for all of the knowledge he has passed on to me; for being a source of inspiration and motivation throughout my university career; and for always offering guidance, whether it was related to this research or not. None of this would have been possible without him.

I would also like to thank our group's previous Master's student, Allie Paulick for providing me with a groundwork to start my research and her countless hours spent teaching me about the LIBS project, equipment, and procedures. Thank you to Emma Blanchette and Sydney Sleiman for all of their help with experiments and whose assistance and insights were integral to the work of Chapter 5 and Chapter 6.

In addition, I would like to thank the other members of our research group Paul, Chris, Robert, Haiqa, Alayna, Griffin, Emily, Chloe and Archie for their assistance and support. A special thank you goes out to Rob as well, for sparking my interest in research.

Thank you to my brother Derrik, my amazing parents LouAnn and George, and my girlfriend Marisa who have given me love and support during the best and most difficult times over the course of my graduate studies. Without them I would not be where I am today. I would also like to thank my best friends Jordyn, Zac and Riley.

Table of Contents

List of Tables

List of Figures

List of Abbreviations

ANN: artificial neural network

CCD: charge coupled device

CFU: colony forming units

CSF: cerebrospinal fluid

DF: discriminant function

DFA: discriminant function analysis

DI: deionized

DNA: deoxyribonucleic acid

FWHM: full width at half maximum

GLIER: Great Lakes Institute for Environmental Research

ICCD: intensified charge coupled device

LIBS: laser-induced breakdown spectroscopy

LIP: laser induced plasma

LOD: limit of detection

LOI: limit of identification

LTE: local thermodynamic equilibrium

LV: latent variable

MALDI-TOF-MS: matrix assisted laser desorption/ionization time-of-flight mass spectrometry

MCE: mixed cellulose esters

MCP: microchannel plate

MP: microparticle

MPLIBS: microparticle enhanced laser-induced breakdown spectroscopy

MRSA: methicillin resistant *Staphylococcus aureus*

Nd:YAG: neodymium-doped yttrium aluminum garnet

NELIBS: nanoparticle enhanced laser-induced breakdown spectroscopy

NIST: National Institute of Standards and Technology

NN: neural network

NP: nanoparticle

PCA: principal component analysis

PCR: polymerase chain reaction

PFGE: pulse-field gel electrophoresis

PLS-DA: partial least squares discriminant analysis

PPB: parts per billion

PPM: parts per million

PVDF: Polyvinylidene Fluoride

RFLP: restriction fragment length polymorphism

RM: ratio model

ROI: region of interest

SCFH: standard cubic feet per hour

SEM: scanning electron microscope

SVM: support vector machine

TB: tuberculosis

TSA: tryptic soy agar

TSP: total spectral power

UTI: urinary tract infection

UV: ultraviolet

WHO: World Health Organization

List of Appendices

Chapter 1: Introduction

1.1 Motivation

Laser-induced breakdown spectroscopy (LIBS) is a laser-based spectrochemical technique that allows a near-instantaneous measurement of the elemental composition of a target (including bacterial pathogens).[1] If the elemental composition of that target is repeatable and stable through time, a careful spectroscopic measurement of that composition can be used to uniquely identify the target.

Our lab has been investigating the use of LIBS for the rapid detection, identification and diagnosis of bacteria in clinical specimens.[2,3,4] To identify bacteria, subtle yet reproducible differences in the concentration of inorganic elements like phosphorous, magnesium, calcium, and sodium in the bacterial cell allow a differentiation of the bacteria on the basis of their atomic emission spectrum alone.[5]

The measured intensities of emission lines in the LIBS spectrum provide a unique elemental "spectral fingerprint" for each type of bacteria, which can be classified using computerized chemometric algorithms. Our goal is to accurately identify and classify as small a number of bacterial cells as possible (lowering the limits of detection), while maximizing the rates of true positives and minimizing the rates of false positives. Our experimental protocols were designed to more closely resemble clinical environments along with diagnostic tools that would be readily available in such settings. In Chapter 2 the specific types of medically relevant bacteria currently being experimented on, important details about bacterial growth and preparation protocols, and how a clinical specimen is simulated in our laboratory will be described. The ability to rapidly identify harmful pathogens in such specimens is crucial for initiating appropriate treatment of infectious diseases that can kill within hours of the onset of symptoms.[6] Current laboratory techniques can take as long as 24-72 hours for a positive identification. Our research program is attempting to reduce that time to minutes.

The rapid bacterial measurements provided by the LIBS technique could lead to significant advancements and improvements in many areas interested in bacterial

detection diagnosis, including environmental, food and water, medical and military applications.[7] Disease, infection and illnesses caused by bacteria and harmful pathogens lead to millions of deaths worldwide every year.[8] Providing health care facilities with the means to begin targeted treatment immediately would save lives, reduce health care costs, improve patient outcomes, and aid in preventing the rise of antibiotic-resistant strains of bacteria.

1.2 A Review of Laser-Induced Breakdown Spectroscopy

Laser-induced breakdown spectroscopy (LIBS) is a rapid elemental analysis technique that involves focusing a high energy pulsed laser onto a target medium in order to produce a weakly ionized plasma. The physics of how this occurs and how it is experimentally realized in a laboratory environment will be discussed in detail in Chapter 3. The plasma consists of highly excited atoms, ions and free electrons that reach temperatures up to approximately 50000 K, before quickly cooling.[9] As the plasmas cool, excited electrons transition to lower energy levels in the atoms and ions, which emit characteristic photons. These photons are collected by a spectrometer and analyzed in order to identify the presence and abundance of specific elements contained in the ablated material. The entire process of ablating a sample medium and detecting its atomic content can be accomplished on a time scale shorter than one second.

Aside from being an extremely fast elemental analysis technique, LIBS holds numerous other advantages as a promising diagnostic tool. LIBS requires very little sample preparation, all of which requires little to no expertise in the fields of medicine or microbiology and could be combined with items readily available in a medical environment. LIBS can be performed on solid,[10] liquid[11] or gaseous samples,[12] which provides countless targets such as metals,[13] blood,[14] urine,[15] ground and hazardous materials.[16]

LIBS is a destructive technique but uses only micrograms of sample material and detects all elements listed in the periodic table simultaneously.[17] This technique can be deployed remotely allowing LIBS to be utilized in potentially dangerous or

inaccessible locations.[18] Another benefit is the ability to generate highly excited atoms, which require large amounts of energy and are difficult to produce in other elemental analysis techniques.[19]

A LIBS spectrum yields a reproducible spectral fingerprint that is unique to the ablated material. The spectra contain narrow well-resolved atomic emission lines with high signal to noise ratios. The spectra display the recorded optical emission intensities as a function of wavelength. If the spectrometer has sufficient resolution, peak positions can be easily measured to precisely identify key elements. An example of an optical emission spectrum produced by a LIBS plasma is shown in Figure 1.1.

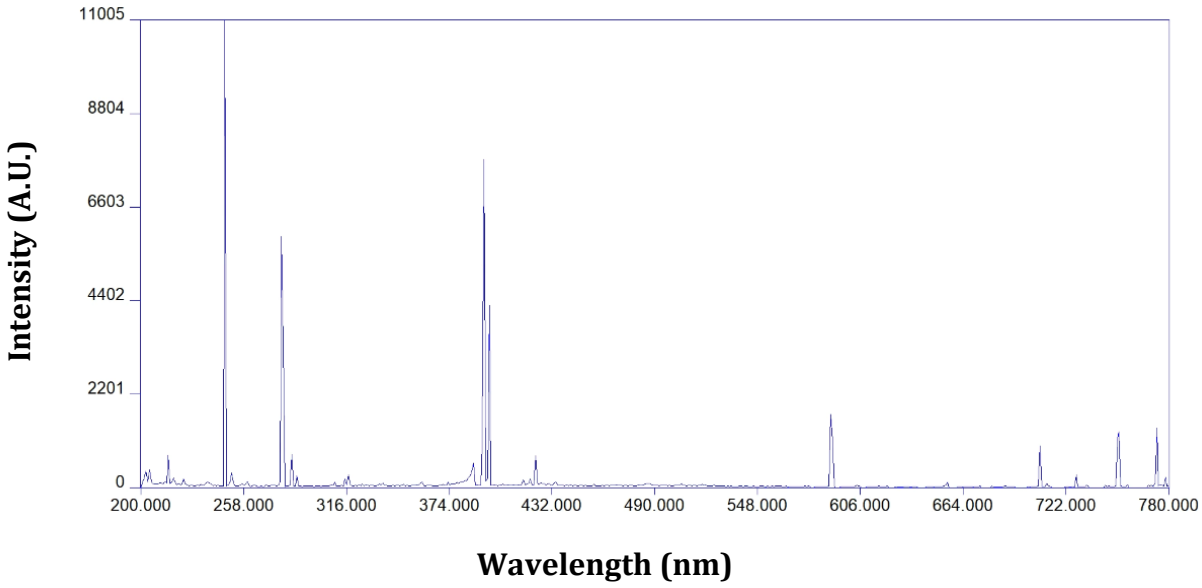

Figure 1.1: LIBS spectrum acquired from an E. coli specimen mounted on nitrocellulose filter ablated in an argon environment at atmospheric pressure.

1.3 Specific Work Relating to LIBS on Bacteria

Laser-induced breakdown spectroscopy has gained increasing popularity since the early 21st century with its ability to identify different biomaterials solely based on their elemental compositions. In 2003 Kiel et al. tested the identification of spores and bacterial insecticide using LIBS by tagging samples with rare earth metals that could be easily detected.[20] Tracking coatings and taggants was an important initial step towards spurious detection with LIBS. Bacteria and other biomaterials such as molds and pollens were successfully discriminated from one another using LIBS

combined with a chemometric algorithm known as Principal Component Analysis (PCA) as shown by Samuels et al. in 2003.[21] These tests emphasized the potential of LIBS being used to detect biohazards that could cause large scale exposures in order to provide quick responses and protective measures. Hybl et al. were able to combine PCA with LIBS to detect and classify biological aerosols that simulate bio-warfare agent stimulants and environmental interferents.[22] Linear combinations of atomic emission lines were combined in different ratios to provide a more sensitive measurement against background aerosol signals. Morel et al. showed that different types of bacteria and pollens could be discriminated using ratios calculated from the elemental emission intensities.[23] In preliminary studies LIBS provided reproducibility in its ability to sort different species and a means to establish a database of spectral signals.

In 2004 Leone et al. tested the detection of bacterial deposits in pellet form along with bio-aerosols in droplets to illustrate the capability of LIBS for precise diagnoses.[24] The results from these experiments outlined the advantage of the real time capabilities of LIBS as an elemental classification technique. Kim et al. plotted the major chemical components of five non-pathogenic bacterial strains to distinguish between spectral fingerprints using LIBS technology.[25] The diverse emissions of elements accumulated in different bacteria as they uptake nutrients from their surroundings are enough to provide a rapid means of classification with minimal sample preparation. In 2005 Hahn et al. used LIBS to measure trace element emission lines such as calcium, magnesium and sodium as well as carbon, after removing CO_2 from the shooting conditions, to detect and identify bacterial spores.[26] This work addressed the necessity to study LIBS as an analytical technique and assess its limitations in terms of single shot feasibility in real world environments and inherent detection limits. DeLucia et al. highlighted the versatility of LIBS to detect hazardous materials both biological and chemical, including explosives and other warfare simulants in 2005.[27] Real time analysis, high sensitivity, minimal sample preparation and the ability to detect virtually all elements and hazards highlighted laser-induced breakdown spectroscopy as a potential candidate for military, security and environmental applications against terrorism and warfare.

In 2007 Baudelet et al. presented spectra with emphasis on emissions from organic elements N, O and the CN molecular bonds in order to specify different organic and biological materials with LIBS.[28] While many groups had placed emphasis on inorganic elements and trace metals, this work focused on organic elements, which provide a basis for most organic materials. In 2008, Gottfried et al. demonstrated the detection and discrimination of biological warfare agents at standoff distances using LIBS combined with Partial Least Squares Discriminant Analysis (PLS-DA) chemometrics.[29] LIBS was able to effectively distinguish agents such as anthrax and ricin at distances of up to 20 meters and explosive residues at distances up to 50 meters, pushing towards universal hazardous materials detection. Snyder et al. modeled biological agents for quantification of detection limits in 2008, illustrating LIBS to be more sensitive than methods currently available to first responders, who may come across unknown powders and compounds.[30] In an effort to address the need for cost effective, easy to use techniques, portable LIBS detector systems were developed.

Since 2010 many groups have made advancements within the LIBS community towards analyzing bacteriological samples. Yao et al. compared the spectral intensity and trace elements of nutritional media, filter papers and *E. coli.*[31] LIBS was able to properly discriminate *E. coli,* a bacterium that is commonly found in humans, mammals and birds, some strains of which can cause food poisoning and harmful infections.[32] Cremers et al. successfully matched bacterial species and strains using chemometric analysis of LIBS data collected during a blind study.[33] When combined with the appropriate chemometric model, LIBS can be used to identify unknown pathogens of both strain and species when tested against a well-defined library set of pathogens. In 2011, three groups Lewis et al., Barnett et al., and Marcos-Martinez et al. researched the discrimination of bacteria in soil samples, detection of bacteria in food samples and identification of bacterial strains using neural networks (NN) respectively.[34,35,36] These experiments provided accurate sample analysis obtained by LIBS over long periods of time. The conclusions were stable even with minor changes in experimental conditions, variations in culture media and differences in the sampling environment. Cisewski et al. combined several methods of predictive

performance models utilizing support vector machine classification with LIBS to determine if unknown powder samples contained bacterial spores.[37] The data was analyzed with respect to eight key elements to focus on important regions of the LIBS spectrum that can be used to identify the spores.

The use of laser-induced breakdown spectroscopy was shown to differentiate between pathogens and viruses. This was shown in 2012, when Multari et al. used both glass and agar substrates to build chemometric models for sample differentiation between live pathogen samples as well as UV-killed virus samples.[38] The choice of substrate, target species and atmosphere were all important parameters that should be optimized for different situations. In 2014 Farooq et al. supported LIBS identification and discrimination[39] and Manzoor et al. achieved rapid identification and discrimination of bacterial strains of the same species, including single gene variations and those exhibiting resistance to antibiotics based on spectral fingerprints using LIBS and neural network analysis.[40] These results all illustrate the capabilities of LIBS as a bacterial identification technique in ideal laboratory settings.

Sivakumar et al. successfully monitored cellular health of bacterial organisms by detecting and classifying living and dead bacteria specimens.[41] This difference in the spectra obtained from dead cells was hypothesized to be due to the leakage of cellular contents that are lost as the cellular membranes are ruptured. Loss of cellular components reduces elemental compositions in the cells that are measured in LIBS spectra. Further research included investigating the liquid media and sample preparation of bacterial samples and the effect pH and other parameters have on the elemental composition of bacterial cells.[42] This was shown by Gamble et al. who concluded DI water as the preferred source to prepare bacterial samples in order to decrease variations in pH and limit ion exchange mechanisms. All of this research in the field of LIBS has provided a compelling and convincing demonstration of the equipment and methods that can be developed for robust, automatic, and reliable real time measurements, specifically when used for bacterial identification.

1.4 Overview of Previous Results of LIBS Performed on Bacterial Samples by the Rehse Group

The Rehse research group has conducted extensive research with the ultimate goal of evolving the LIBS method into a diagnostic technique for rapid pathogen identification that can be used in a medical environment or clinical setting. In 2007, Rehse et al. showed that it was possible to identify and discriminate bacteria strains grown on different nutritional media with LIBS and Discriminant Function Analysis (DFA).[43] This research was conducted with samples of *Pseudomonas aeruginosa* as well as four strains of *E. coli*, supporting the ability of LIBS to discriminate strains prepared with differing environmental conditions. Further experiments were performed to address issues relating to sample dilution, sample mixing, contamination and reducing limits of detection.

In 2009 Rehse et al. performed enhanced discrimination between Gram-positive and Gram-negative bacteria in two different noble gas environments.[44] LIBS with the use of helium and argon atmospheres combined with DFA achieved 100% categorization accuracy of the bacteria samples. Noble gases, specifically argon improve the emission and reproducibility of generated plasmas during laser ablation of target materials, by increasing both plasma temperature and electron density. In a separate study it was also concluded that the membrane biochemistry of the bacteria contributes towards the identification of samples performed with LIBS and DFA.[45] More importantly it was shown that different genera of bacteria (i.e. Staphylococcus, Streptococcus, Escherichia, and Pseudomonas) display more variation in LIBS spectra than that of different strains of the same species, with or without altering membrane biochemistry. This evidence supports LIBS as a viable technique regardless of alterations in environmental conditions.

After testing laser-induced breakdown spectroscopy of bacterial cells exposed to different growth media, atmospheric conditions, and environmental variations, LIBS was tested on mixed and dilute samples. This was shown in 2010, when Rehse et al. used mixtures of two bacteria as well as dilutions by a factor of two and factor of three compared to the control concentration.[46] LIBS was able to accurately identify

these dilutions and mixing ratios down to a mixing ratio of 80:20 before loss of sensitivity. In 2011 Mohaidat et al. showed that it was possible to discriminate between bacteria whether live, autoclaved, inactivated by UV exposure or deprived of nutrition for several days.[47] The collected LIBS spectra were not significantly altered by these common bactericidal techniques and classified correctly. Many of these processes reduce water content within the sample cells, however LIBS classification does not rely upon H or O composition in a fundamental way and the cells were not destroyed at a level that would disrupt accurate classification. Bacteria survive within very narrow real world environmental conditions, relying on specific pH levels, temperatures, pressures and ionic concentrations.[48] Testing these samples in realistic chemical environments with a variety of stressors likely to be encountered by the cells provides assurance that LIBS retains its selectivity and sensitivity as a diagnostic technique in these ranges.

Since 2011, our research group at the University of Windsor has been devoted to developing LIBS as a real world biomedical application. Putnam et al. obtained the spectral fingerprints of living specimens from thirteen different taxonomic bacterial classes spanning five bacterial genera.[49] Three models were constructed combining sums, ratios and complex ratios of measured atomic emission line intensities using discriminant function analysis along with partial least squares discriminant analysis. The models were studied to compare the performance abilities and determine the effectiveness of each technique with regards to sensitivity, specificity and accuracy. Although based on fundamentally different mathematical principles, both multivariate techniques provided effective classification of the unknown bacterial LIBS spectra and could be combined to simultaneously classify samples against a pre-compiled library of data as depicted in Figure 1.2 below.

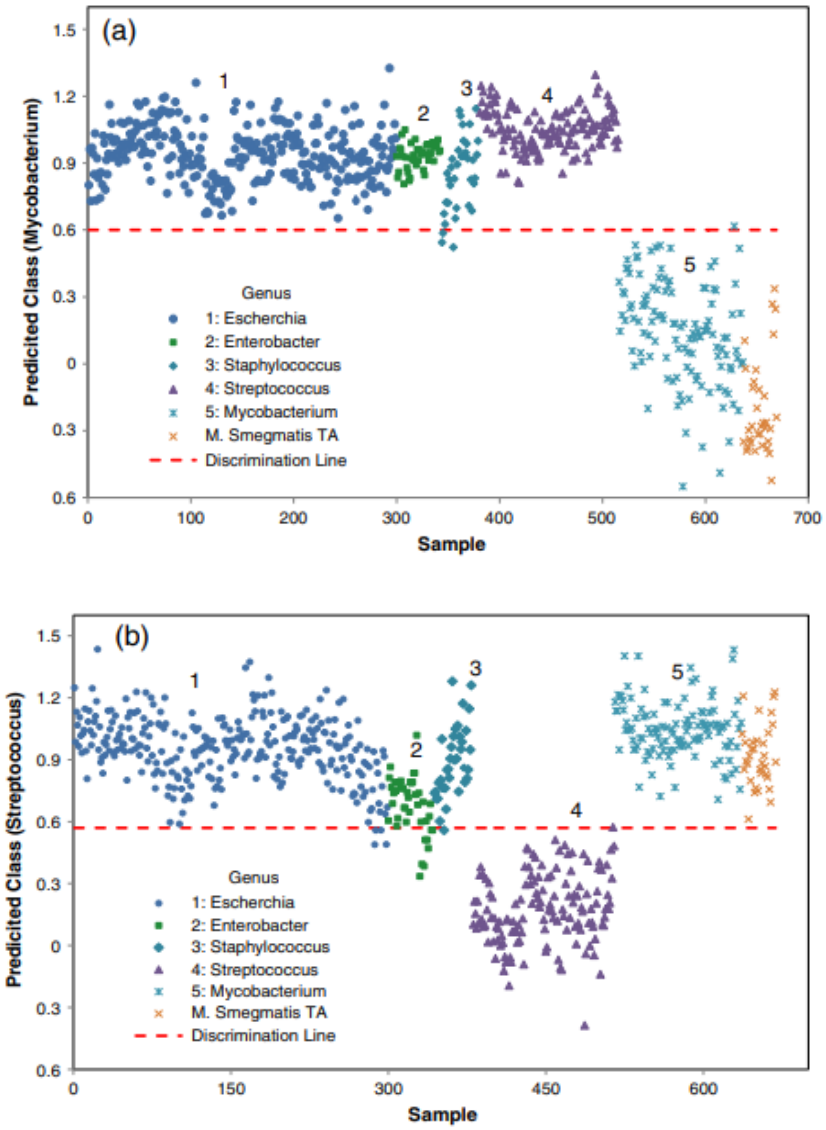

Figure 1.2: Graphical representation of PLS-DA external validation performed on M. smegmatis strain TA. (a) All unknown spectra depicted with 'x' symbols were correctly classified as Mycobacterium (true positives). (b) All unknown spectra depicted with 'x' symbols were correctly classified as not belonging to genus Streptococcus (true negatives). Image adapted from R.A. Putnam et al. / Spectrochimica Acta Part B 87 (2013) 161–167

Malenfant et al. designed and constructed a filtration device that could be combined with centrifugation to rapidly concentrate bacteria collected in liquid suspensions upon filtration media.[2] The choice of pore size of the filters and a two-stage insert allowed for separation of larger contaminants from collected samples based on size, with the smaller bacterial cells passing through to a second filter. Upwards of 90% of cells in suspension could be captured and concentrated with this

new technique and easily removed for subsequent LIBS analysis within minutes. This work also quantified a limit of detection of 90,000 cells per laser shot, reducing the sample size towards a comparable amount that would be encountered when collecting patient samples such as saliva, urine or blood. The collection procedures and apparatus used in this mounting protocol closely resemble that by which clinicians or microbiologists would be familiar with outside of an ideal lab setting. This filtration device was used extensively in the work described in this thesis.

As an extension of this work, Paulick et al. built a custom fabricated metal cone device that could be combined with the filtration device in order to concentrate collected bacteria into a smaller circular spot size with diameter of 1mm, centered on a flat disposable nitrocellulose filtration medium.[3] This metal cone device was also used extensively in the work described in this thesis and will be described in detail and shown schematically in chapter 3. Recorded optical densitometry measurements of prepared specimens observed a reduction by factor of 50 for the limit of detection which can be displayed in Figure 1.3.

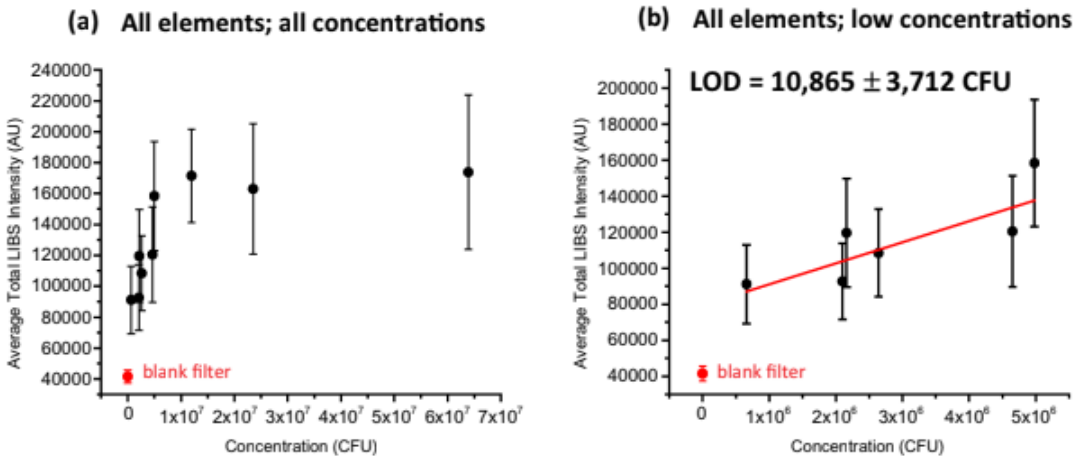

Figure 1.3: (a) Plot of average total LIBS intensity as a function of colony forming units (CFU) deposited on the filter for nine different initial concentrations and one blank filter. Error bars represent one standard deviation in the forty measurements. (b) Linear fit to the six concentrations which lie in the linear regime of the curve shown in (a). The LOD was calculated using the value of 3σ/m.

While more research focused on the capability of LIBS to detect and identify bacteria at clinically relevant levels is required, this technique has proven to be a convenient measure of cellular elemental composition with preparation and testing procedures that can be done safely and rapidly with bacterial specimens. Specimens obtained from patients in clinical environments should be tested via LIBS and other competing modalities to compare the accuracy of all available methods in order to gain valuable insight into the development of immediate targeted treatments. The LIBS technique will continue to benefit from technological advancements in the field of lasers, spectrometers and detectors. Laser-induced breakdown spectroscopy will require the collaboration of physicists, microbiologists and signal processing experts in order to convince medical practitioners to utilize LIBS as a gold standard diagnostic method, which could be commercialized. The results to date indicate the revolutionary impact that a rapid point of care diagnostic instrument with the ability to detect and identify harmful pathogens at a cellular level with extreme accuracy could have for the field of medical science.

1.5 Scope of Work and Outline of Thesis

My thesis describes the construction of a spectral library database containing the LIBS emission spectra from hundreds of spectra collected by using the previously mentioned centrifuge device and cone device along with a standardized protocol that minimizes the bacterial limit of detection while maximizing classification accuracy. Clinical swabs are used for the first time to collect bacteria, simulating clinical diagnostic testing. Several methods of reducing background noise and enhancing plasma emissions were explored in order to reduce the limit of identification to resemble that of clinical samples.

Specifically, this thesis describes our current experimental techniques including bacteria collection and mounting protocols, LIBS data acquisition, and spectral data analysis. This will include methods for the collection, concentration, and separation of bacteria from unwanted biological matter, deposition of bacterial cells on a suitable ablation medium, the formation of high temperature laser-induced microplasmas,

collection and analysis of the atomic emission spectra with a high-resolution spectrometer, and the differentiation of LIBS emission spectra from different bacterial species and genera using computerized chemometric algorithms.

The remainder of this thesis is organized as follows:

Chapter 2 is dedicated to a detailed description of bacterial characteristics including types, physiology, and anatomy. Then the culture media, growth and harvesting of the bacteria utilized in our laser ablated targets will be explored. This will lead into the testing of experimental parameters in order to establish optimal sample collection and preprocessing during sample preparation.

Chapter 3 provides a comprehensive analysis of the theory, apparatus and experimental conditions behind laser-induced breakdown spectroscopy and plasma formation. This will include the emission and observation of distinct and characteristic elemental spectra used to differentiate between specific bacterial species and mounting surfaces.

Chapter 4 is devoted to chemometric algorithms and their ability to externally classify spectra based on their similarity to a reference library. Two algorithms known as DFA and PLS-DA will be explored in detail, outlining their respective methods of analyzing unique variables, predicting classifications of samples, and defining accuracy.

Chapter 5 will present experimental findings related to the ability to detect and discriminate bacteria collected from swabbed samples. Moreover, research related to quantifying the true detection capability of our current procedure will be described along with a technique for the separation of bacterial targets from collected samples, in order to minimize the bacterial concentration levels required for detection and identification.

Chapter 6 contains various studies pertaining to the elimination of undesired contaminants from bacterial LIBS spectra, the reduction of background signal, and the implemented pre-processing steps to improve data rejection of unwanted or misclassified spectra. Serial dilutions are tested to construct and analyze a LIBS bacterial curve of growth.

Chapter 7 focuses on the use of cheap and readily available metal microparticles to boost spectral emissions in order to enhance LIBS signals. In addition, we investigate the opportunity to eliminate blank spectra from occurring during LIBS on bacteria and the potential to improve the overall limit of detection.

Chapter 8 will include an overview of the main results and conclusions gathered throughout the course of the research. Several perspectives for future work will be discussed including LIBS on viruses, combining LIBS with Raman spectroscopy, the utilization of metal nanoparticles and the analysis of samples that would be collected from patients in a clinical environment.

References

[1] Singh, J. P., & Thakur, S. N. (Eds.). (2020). *Laser-induced breakdown spectroscopy*. Elsevier.

[2] Malenfant, D. J. (2016). *Influences on the Emissions of Bacterial Plasmas Generated through Nanosecond Laser-Induced Breakdown Spectroscopy*, Master's thesis, University of Windsor. https://scholar.uwindsor.ca/etd/5843

[3] Paulick, A. E. (2018). *Development of Laser-Induced Breakdown Spectroscopy as a Rapid Diagnostic Tool for Bacterial Infection*, Master's thesis, University of Windsor. https://scholar.uwindsor.ca/etd/7653

[4] Rehse, S. J. (2019). A review of the use of laser-induced breakdown spectroscopy for bacterial classification, quantification, and identification. *Spectrochimica Acta Part B: Atomic Spectroscopy*, *154*, 50-69. https://doi.org/10.1016/j.sab.2019.02.005

[5] Dixon, P. B., & Hahn, D. W. (2005). Feasibility of detection and identification of individual bioaerosols using laser-induced breakdown spectroscopy. *Analytical chemistry*, *77*(2), 631-638. https://doi.org/10.1021/ac048838i

[6] Schaechter, M., Medoff, G., & Eisenstein, B. I. (Eds.). (1993). *Mechanisms of microbial disease*. Lippincott Williams & Wilkins.

[7] Pathak, A. K., Kumar, R., Singh, V. K., Agrawal, R., Rai, S., & Rai, A. K. (2012). Assessment of LIBS for spectrochemical analysis: a review. *Applied Spectroscopy Reviews*, *47*(1), 14-40. https://doi.org/10.1080/05704928.2011.622327

[8] The World Health Organization, The World Health Report 1996: fighting disease, fostering development, (Geneva, Switzerland, 1996)

[9] Thakur, S. N., & Singh, J. P. (2007). Fundamentals of laser induced breakdown spectroscopy. In *Laser-induced breakdown spectroscopy* (pp. 3-21). Elsevier.

[10] Jantzi, S. C., Motto-Ros, V., Trichard, F., Markushin, Y., Melikechi, N., & De Giacomo, A. (2016). Sample treatment and preparation for laser-induced breakdown spectroscopy. *Spectrochimica Acta Part B: Atomic Spectroscopy*, *115*, 52-63. https://doi.org/10.1016/j.sab.2015.11.002

[11] Lazic, V., & Jovićević, S. (2014). Laser induced breakdown spectroscopy inside liquids: processes and analytical aspects. *Spectrochimica Acta Part B: Atomic Spectroscopy*, *101*, 288-311. https://doi.org/10.1016/j.sab.2014.09.006

[12] Haisch, C., Niessner, R., Matveev, O. I., Panne, U., & Omenetto, N. (1996). Element-specific determination of chlorine in gases by laser-induced-breakdown-

spectroscopy (LIBS). *Fresenius' journal of analytical chemistry*, *356*(1), 21-26. https://doi.org/10.1007/s0021663560021

[13] Essington, M. E., Melnichenko, G. V., Stewart, M. A., & Hull, R. A. (2009). Soil metals analysis using laser-induced breakdown spectroscopy (LIBS). *Soil Science Society of America Journal*, *73*(5), 1469-1478. https://doi.org/10.2136/sssaj2008.0267

[14] Chen, X., Li, X., Yang, S., Yu, X., & Liu, A. (2018). Discrimination of lymphoma using laser-induced breakdown spectroscopy conducted on whole blood samples. *Biomedical optics express*, *9*(3), 1057-1068. https://doi.org/10.1364/BOE.9.001057

[15] Rehse, S. J. (2014). Biomedical applications of LIBS. In *Laser-Induced Breakdown Spectroscopy* (pp. 457-488). Springer, Berlin, Heidelberg. https://doi.org/10.1007/978-3-642-45085-3_17

[16] Moros, J., Lorenzo, J. A., & Laserna, J. J. (2011). Standoff detection of explosives: critical comparison for ensuing options on Raman spectroscopy–LIBS sensor fusion. *Analytical and bioanalytical chemistry*, *400*(10), 3353-3365. https://doi.org/10.1007/s00216-011-4999-y

[17] De Lucia Jr, F. C., & Gottfried, J. L. (2011). Rapid analysis of energetic and geo-materials using LIBS. *Materials today*, *14*(6), 274-281. https://doi.org/10.1016/S1369-7021(11)70142-0

[18] Knight, A. K., Scherbarth, N. L., Cremers, D. A., & Ferris, M. J. (2000). Characterization of laser-induced breakdown spectroscopy (LIBS) for application to space exploration. *Applied Spectroscopy*, *54*(3), 331-340.

[19] Rehse, S. J., & Ryder, C. A. (2009). Laser-induced breakdown spectroscopy for branching ratio and atomic lifetime measurements in singly-ionized neodymium and gallium. *Spectrochimica Acta Part B: Atomic Spectroscopy*, *64*(10), 974-980. https://doi.org/10.1016/j.sab.2009.07.024

[20] Kiel, J. L., Holwitt, E. A., Parker, J. E., Vivekananda, J., Franz, V., Sloan, M. A., ... & Mattley, Y. D. (2005, May). Specific biological agent taggants. In *Chemical and Biological Sensing VI* (Vol. 5795, pp. 39-45). International Society for Optics and Photonics. https://doi.org/10.1117/12.597640

[21] Samuels, A. C., DeLucia, F. C., McNesby, K. L., & Miziolek, A. W. (2003). Laser-induced breakdown spectroscopy of bacterial spores, molds, pollens, and protein: initial studies of discrimination potential. *Applied optics*, *42*(30), 6205-6209. https://doi.org/10.1364/AO.42.006205

[22] Hybl, J. D., Lithgow, G. A., & Buckley, S. G. (2003). Laser-induced breakdown spectroscopy detection and classification of biological aerosols. *Applied spectroscopy*, *57*(10), 1207-1215.

[23] Morel, S., Leone, N., Adam, P., & Amouroux, J. (2003). Detection of bacteria by time-resolved laser-induced breakdown spectroscopy. *Applied optics*, *42*(30), 6184-6191. https://doi.org/10.1364/AO.42.006184

[24] Leone, N., D'Arthur, G., Adam, P., & Amouroux, J. (2004). Detection of Bacterial Deposits and Bio aerosols by Time-Resolved Laser-Induced Breakdown Spectroscopy (TRELIBS). *High Temperature Material Processes: An International Quarterly of High-Technology Plasma Processes*, *8*(1). https://doi.org/10.1615/HighTempMatProc.v8.i1.10

[25] Kim, T., Specht, Z. G., Vary, P. S., & Lin, C. T. (2004). Spectral fingerprints of bacterial strains by laser-induced breakdown spectroscopy. *The Journal of Physical Chemistry B*, *108*(17), 5477-5482. https://doi.org/10.1021/jp031269i

[26] Dixon, P. B., & Hahn, D. W. (2005). Feasibility of detection and identification of individual bioaerosols using laser-induced breakdown spectroscopy. *Analytical chemistry*, *77*(2), 631-638. https://doi.org/10.1021/ac048838i

[27] DeLucia, F. C., Samuels, A. C., Harmon, R. S., Walters, R. A., McNesby, K. L., LaPointe, A., ... & Miziolek, A. W. (2005). Laser-induced breakdown spectroscopy (LIBS): a promising versatile chemical sensor technology for hazardous material detection. *IEEE Sensors Journal*, *5*(4), 681-689. DOI: 10.1109/JSEN.2005.848151

[28] Baudelet, M., Boueri, M., Yu, J., Mao, S. S., Piscitelli, V., Mao, X., & Russo, R. E. (2007). Time-resolved ultraviolet laser-induced breakdown spectroscopy for organic material analysis. *Spectrochimica Acta Part B: Atomic Spectroscopy*, *62*(12), 1329-1334. https://doi.org/10.1016/j.sab.2007.10.043

[29] Gottfried, J. L., De Lucia, F. C., Munson, C. A., & Miziolek, A. W. (2008). Standoff detection of chemical and biological threats using laser-induced breakdown spectroscopy. *Applied spectroscopy*, *62*(4), 353-363.

[30] Snyder, E. G., Munson, C. A., Gottfried, J. L., De Lucia Jr, F. C., Gullett, B., & Miziolek, A. (2008). Laser-induced breakdown spectroscopy for the classification of unknown powders. *Applied optics*, *47*(31), G80-G87. https://doi.org/10.1364/AO.47.000G80

[31] Yao, M., Lin, J., Liu, M., Li, Q., Lei, Z., & Huang, L. (2010, October). Identification of escherichia coli by laser induced breakdown spectroscopy. In *2010 3rd International Conference on Biomedical Engineering and Informatics* (Vol. 1, pp. 302-305). IEEE. DOI: 10.1109/BMEI.2010.5639492

[32] Salyers, A. A., Whitt, D. D., & Whitt, D. D. (1994). *Bacterial pathogenesis: a molecular approach* (Vol. 1). Washington, DC: ASM press.

[33] Multari, R. A., Cremers, D. A., Dupre, J. M., & Gustafson, J. E. (2010). The use of laser-induced breakdown spectroscopy for distinguishing between bacterial pathogen species and strains. *Applied spectroscopy*, *64*(7), 750-759.

[34] Lewis, D. E., Martinez, J., Akpovo, C. A., Johnson, L., Chauhan, A., & Edington, M. D. (2011). Discrimination of bacteria from Jamaican bauxite soils using laser-induced breakdown spectroscopy. *Analytical and bioanalytical chemistry*, *401*(7), 2225. https://doi.org/10.1007/s00216-011-5274-y

[35] Barnett, C., Bell, C., Vig, K., Akpovo, A. C., Johnson, L., Pillai, S., & Singh, S. (2011). Development of a LIBS assay for the detection of Salmonella enterica serovar Typhimurium from food. *Analytical and bioanalytical chemistry*, *400*(10), 3323-3330. https://doi.org/10.1007/s00216-011-4844-3

[36] Marcos-Martinez, D., Ayala, J. A., Izquierdo-Hornillos, R. C., de Villena, F. M., & Caceres, J. O. (2011). Identification and discrimination of bacterial strains by laser induced breakdown spectroscopy and neural networks. *Talanta*, *84*(3), 730-737. https://doi.org/10.1016/j.talanta.2011.01.069

[37] Cisewski, J., Snyder, E., Hannig, J., & Oudejans, L. (2012). Support vector machine classification of suspect powders using laser-induced breakdown spectroscopy (LIBS) spectral data. *Journal of Chemometrics*, *26*(5), 143-149. https://doi.org/10.1002/cem.2422

[38] Multari, R. A., Cremers, D. A., & Bostian, M. L. (2012). Use of laser-induced breakdown spectroscopy for the differentiation of pathogens and viruses on substrates. *Applied optics*, *51*(7), B57-B64. https://doi.org/10.1364/AO.51.000B57

[39] Farooq, W. A., Atif, M., Tawfik, W., Alsalhi, M. S., Alahmed, Z. A., Sarfraz, M., & Singh, J. P. (2014). Study of bacterial samples using laser induced breakdown spectroscopy. *Plasma Science and Technology*, *16*(12), 1141.

[40] Manzoor, S., Moncayo, S., Navarro-Villoslada, F., Ayala, J. A., Izquierdo-Hornillos, R., de Villena, F. M., & Caceres, J. O. (2014). Rapid identification and discrimination of bacterial strains by laser induced breakdown spectroscopy and neural networks. *Talanta*, *121*, 65-70. https://doi.org/10.1016/j.talanta.2013.12.057

[41] Sivakumar, P., Fernández-Bravo, A., Taleh, L., Biddle, J. F., & Melikechi, N. (2015). Detection and classification of live and dead Escherichia coli by laser-induced breakdown spectroscopy. *Astrobiology*, *15*(2), 144-153. https://doi.org/10.1089/ast.2014.1181

[42] Gamble, G. R., Park, B., Yoon, S. C., & Lawrence, K. C. (2016). Effect of sample preparation on the discrimination of bacterial isolates cultured in liquid nutrient media using laser-induced breakdown spectroscopy (LIBS). *Applied Spectroscopy*, *70*(3), 494-504. https://doi.org/10.1177/0003702815626679

[43] Diedrich, J., Rehse, S. J., & Palchaudhuri, S. (2007). Escherichia coli identification and strain discrimination using nanosecond laser-induced breakdown spectroscopy. *Applied Physics Letters*, *90*(16), 163901. https://doi.org/10.1063/1.2723659

[44] Rehse, S. J., Jeyasingham, N., Diedrich, J., & Palchaudhuri, S. (2009). A membrane basis for bacterial identification and discrimination using laser-induced breakdown spectroscopy. *Journal of Applied Physics*, *105*(10), 102034. https://doi.org/10.1063/1.3116141

[45] Rehse, S. J., & Mohaidat, Q. I. (2009). The effect of sequential dual-gas testing on laser-induced breakdown spectroscopy-based discrimination: Application to brass samples and bacterial strains. *Spectrochimica Acta Part B: Atomic Spectroscopy*, *64*(10), 1020-1027. https://doi.org/10.1016/j.sab.2009.07.012

[46] Rehse, S. J., Mohaidat, Q. I., & Palchaudhuri, S. (2010). Towards the clinical application of laser-induced breakdown spectroscopy for rapid pathogen diagnosis: the effect of mixed cultures and sample dilution on bacterial identification. *Applied Optics*, *49*(13), C27-C35. https://doi.org/10.1364/AO.49.000C27

[47] Mohaidat, Q., Palchaudhuri, S., & Rehse, S. J. (2011). The effect of bacterial environmental and metabolic stresses on a laser-induced breakdown spectroscopy (LIBS) based identification of Escherichia coli and Streptococcus viridans. *Applied spectroscopy*, *65*(4), 386-392.

[48] De Lucia Jr, F. C., & Gottfried, J. L. (2011). Influence of variable selection on partial least squares discriminant analysis models for explosive residue classification. *Spectrochimica Acta Part B: Atomic Spectroscopy*, *66*(2), 122-128. https://doi.org/10.1016/j.sab.2010.12.007

[49] Putnam, R. A., Mohaidat, Q. I., Daabous, A., & Rehse, S. J. (2013). A comparison of multivariate analysis techniques and variable selection strategies in a laser-induced breakdown spectroscopy bacterial classification. *Spectrochimica Acta Part B: Atomic Spectroscopy*, *87*, 161-167. https://doi.org/10.1016/j.sab.2013.05.014

Chapter 2: Bacteria

2.1 Bacteria Types and Physiology

Bacteria are omnipresent microorganisms found throughout the world's environments, living creatures and the human body. There are thousands of species of bacteria that have been discovered and investigated, of which only a small fraction cause disease. Harmful bacteria infect millions of people every year leading to public health issues, illness and mortality.[50] According to the World Health Organization (WHO) 1996 World Health Report, infectious diseases were the leading cause of premature death worldwide.[51] Bacteria live in symbiotic relationships with plants and animals providing important enzymes, reactions and processes that help synthesize and metabolize key components for cellular survival.[52] However, several species of bacteria are pathogenic and cause infectious diseases such as cholera, syphilis, anthrax, leprosy, tuberculosis and respiratory infections.[53]

Newer, more reliable, and time-sensitive methods to prevent and combat water-borne infections, food-borne infections, antibiotic resistant bacteria, and hospital-acquired infections are very important. Current techniques used for bacterial identification are time-consuming, labor-intensive, require an expertise in microbiology and are only useful to specific types of bacteria. Examples of these include culture-based methods, polymerase chain reaction (PCR), restriction fragment length polymorphism (RFLP), pulse-field gel electrophoresis (PFGE), and matrix-assisted laser desorption/ionization time-of-flight mass spectrometry (MALDI-TOF-MS).[54,55,56] Culturing, growing and testing bacteria over days and even weeks is a major drawback to identify harmful bacteria, administer proper treatment in time-sensitive scenarios, and reduce the widespread use of general antibiotics that give rise to antibiotic resistant strains. Another major issue being that only about 27 percent of bacterial phyla have species that can be grown in a laboratory.[57] There are many structural and genetic differences between bacteria, the types and physiology will be described in this section.

Bacteria are prokaryotes, single celled microbes of the kingdom Monera, that lack a nucleus or membrane bound organelles.[58] These organisms, much like eukaryotic

cells, do still contain a plasma membrane, cytoplasm, DNA and ribosomes. There are five main shapes of bacteria that include coccus which are spherical, bacillus which are rod-like, spirillum which are spiraled, spirochaete which resemble a corkscrew and vibrios which are comma shaped.[59] These shapes can form pairs, chains and clusters within colonies. Bacterial cells are also comprised of a cell envelope that consists of the cellular membrane along with an outer cell wall. The cell wall is largely responsible for the rigidity and overall shape of a bacteria.

Most bacteria can be divided into two main categories based on the composition of the cell wall and its reaction to the Gram stain test. This staining method utilizes chemicals and dyes that stain bacteria a certain colour depending on the presence or absence of specific substances unique to bacteria. A bacterium that contains cell walls composed of peptidoglycan is categorized as Gram-positive and will appear purple after Gram staining while a bacterium that contains an outer membrane of lipopolysaccharides is categorized as Gram-negative and appears more pink or red after Gram staining.[60] There is a third category of bacteria known as acid fast bacteria that contain complex hydrocarbon chains interwoven throughout the cell wall. Acid fastness refers to the physical property in which a bacterium resists the decolorization caused by acids during the staining procedure.

Gram-positive bacteria have a thick cell wall that protects and surrounds the cytoplasmic membrane. This wall is built up with peptidoglycan also known as murein. Murein is a complex polymer composed of altering units of N-acetyl glucosamine and N-acetyl muramic acid, which are in turn bonded to peptides. The peptides link across strands of murein in order to form highly polar, dense hydrophilic barriers built up of sugars and charged amino acids. This barrier protects the bacterium from harmful hydrophobic chemicals such as bile salts and maintains structural integrity in order to prevent pressure along the membrane from collapsing the cell. [60] This layer is also responsible for retaining the crystal violet dye during the Gram staining process, which in turn produces a purple stained coloration in this type of bacterial cell.[60]

Gram-negative bacteria contain a much thinner peptidoglycan layer surrounded by an outer membrane. This membrane is built up with a phospholipid bilayer

structure composed of phospholipids facing inwards and lipopolysaccharides facing outwards. This bilayer prevents large compounds from passing through and contains porins, special channels that enable small hydrophilic molecules to enter. Hydrophobic compounds being too large to pass through the porins, are repelled by the polar regions of the bilayer and instead pass though the membrane via specific transport mechanisms.[60] Between the inner and outer membrane there are degradative enzymes that break down larger molecules as well as binding proteins that aid in the collection of sugars and amino acids. Gram-negative bacteria contain compounds in this phospholipid bilayer structure that make them unique and especially dangerous including endotoxins, which in large doses can cause fever and death, along with O antigens that aid to avoid immune responses from infected hosts as well as β-lactamases that inactivate certain antibiotics.[61] During a Gram stain procedure, a counter stain known as safranin is used which does not affect the purple colour of Gram-positive cells but causes Gram-negative cells to turn pink.[60]

Acid fast bacteria have a unique feature that allows them to resist decolourization during the staining procedures. This means that once a dye is introduced to a cell that is acid-fast or acid resistant, the stain cannot be removed with dilute acids. These bacteria contain complex hydrocarbon chains known as waxes throughout the murein in the cell wall. This waxy lipoid capsule stains with carbol-fuchsin, methylene blue and various other dyes due to the presence of membrane glycolipids and abundance of mycolic acids.[62] The acid-fast envelope also uniquely contains arabinogalactan polysaccharides that are covalently linked to the peptidoglycan. The waxy coating acts as a protective layer against harsh chemicals for the cell but also reduces the ability of the bacteria to bring in nutrients, which causes many acid-fast types to divide and grow more slowly.[63]

2.2 Bacterial Species Tested with LIBS

The names of bacteria are italicized and contain the genus followed by the species. For example, the bacterium *Streptococcus pneumoniae* refers to the genus *streptococcus* and the species *pneumoniae*. For simplification, the genus name is

regularly shortened to the first letter. Five types of bacteria with different physiological properties from different genera were used in this work: *Escherichia coli, Staphylococcus aureus, Pseudomonas aeruginosa, Mycobacterium smegmatis* and *Enterobacter cloacae.* These bacteria have been chosen by our group for the purpose of investigating the ability of LIBS to identify and discriminate bacterial species of different groups. They are discussed in this section below. A complete list of all the bacterial species ever tested by LIBS was compiled by Rehse (2019) and is presented in **Appendix A** as a reference for the reader.

E. coli is a Gram-negative rod shaped, motile, coliform bacterium commonly found in the intestines of warm-blooded animals and humans. Harmless non-pathogenic strains are beneficial and help produce vitamins and prevent other pathogenic bacteria from colonizing in the intestinal areas. However, pathogenic strains of *E. coli* can cause health issues including food poisoning, diarrhea, kidney failure, urinary tract infections (UTI's), septicemia, pneumonia and meningitis.[64] Early work on the identification of bacteria by our group using LIBS focused on strains of *E. coli* because it has been well studied as a model prokaryotic organism and can be grown and cultured easily and inexpensively in a laboratory setting. *E. coli* exhibit both a high degree of genetic and phenotypic diversity and are surrounded by a cell wall that protects it from certain antibiotics including penicillin. Pathogenic *E. coli* is the most common cause of community-acquired UTI's and is commonly found on contaminated slaughtered meat products.[65] Rapidly identifying pathogenic strains of this bacteria in food and urine samples with LIBS could save lives, food products and money. In the context of our laboratory work, extensive work is performed with non-pathogenic strains of *E. coli* because they are easy to grow, safe to experiment on and dispose of, and robust through time.

S. aureus is a Gram-positive coccal shaped nonmotile bacterium commonly found on skin, inside the nostrils and in the upper respiratory tract. Harmless non-pathogenic strains act as commensal bacteria organisms and also help with catalase and nitrate reduction. However, pathogenic strains of *S. aureus* can cause health issues including skin infections, respiratory infections, endocarditis, pneumonia and osteomyelitis.[64] *S. aureus* and *S. epidermidis* are the leading causes of sepsis and

nosocomial bacteremia. These bacteria can enter the bloodstream through injuries to the skin and can also adhere to plastic surfaces, contaminating abiotic objects such as catheters in clinical environments. Pathogenic strains promote infections by producing protein toxins and by inactivating antibodies.[66] This has led to the formation of antibiotic resistant strains such as methicillin-resistant *S. aureus* (MRSA), which pose worldwide medical problems with no vaccines and very limited treatment options. Using LIBS for early detection and identification of pathogens would reduce the emergence of new genetic properties such as antibiotic resistant bacterial strains.

P. aeruginosa is a Gram-negative rod-shaped motile bacterium that is present in soil, water, skin flora and many other natural and artificial environments. It is known as an opportunistic, nosocomial pathogen and can cause serious infections in people with reduced immunity, existing conditions, and diseases. This means that it will invade the body through breaches such as wounds and burns as well as the urinary tract. It is especially dangerous to immunocompromised individuals and in hospital or clinical settings. *P. aeruginosa* thrives on moist surfaces and approximately 1 in 10 hospital acquired infections is from this bacterium.[64] Patients with cystic fibrosis and impaired lung defenses, contact lenses and scratched corneas as well as septic shock from burns are at high risk. After infecting damaged tissues, colonization in critical body organs such as the lungs and kidneys can cause inflammation, sepsis and fatality. *P. aeruginosa* is highly versatile multidrug resistant pathogen with advanced antibiotic resistance mechanisms.[67]

M. smegmatis is an acid-fast group member, with a rod shape and is considered a non-pathogenic organism. It can be found in water, soil and plants. This bacterium is tested commonly in laboratory settings because it colonizes and grows quickly. Even with a fast doubling time, visible colonies still take days to form, another reason why an identification technique that can be used on minute samples such as LIBS is important to save growth and preparation time. It is easy to work with and requires only biosafety 1 level facilities. *M. smegmatis* is capable of transformation, in which it uptakes DNA released by other cells in a medium and incorporates that DNA into its own genome. They also have efficient DNA repair machinery making them more

resistant to damaging agents such as ultraviolet (UV) light.[68] *M. smegmatis* is a common surrogate organism used to study important diseases such as tuberculosis (TB).[69] This type of bacteria was regularly tested by our group to compare the LIBS spectra of acid-fast bacteria with Gram-positive and Gram-negative bacterial species.

E. cloacae is another Gram-negative, rod shaped, motile bacterium that commonly exists in the normal gut flora of humans and on skin, fruits and vegetables. Certain strains are pathogenic and can cause respiratory or urinary tract infections in immunocompromised patients, especially the elderly and young. Reported cases have been treated with certain antibiotics but *E. cloacae* produce enzymes responsible for antibiotic resistance during treatment and can lead to bacteremia, endocarditis, septic arthritis, osteomyelitis and ophthalmic infections.[70] Fei et al. were able to study *E. cloacae* in mice and identified a link between the presence of these bacteria in the gut with obesity in the tested mice. *E. cloacae* has become a very common nosocomial pathogen in neonatal units, transported easily through intravenous fluids and by surgical equipment such as stethoscopes and dialysis. *E. cloacae* have the highest mortality rate among other *Enterobacter* infections and are particularly difficult to distinguish from other bacterial infections. Testing with LIBS was conducted to identify and distinguish this type of bacteria from other similar Gram-negative species of bacteria to avoid this identification problem.

2.3 Growth and Sample Preparation

The bacteria samples studied in this work were provided by Ms. Ingrid Churchill of the Department Integrative Biology of the University of Windsor. These initial stock samples were colonized by our Physics department lab group on agar plates and used to produce all other colonies and samples for the bacterial LIBS experiments. These mother cultures were scraped off carefully and suspended in labelled, refrigerated microcentrifuge tubes. During this period, the suspended cells are metabolically dormant. In this section, I will discuss the procedures used to grow, maintain, and prepare the bacteria samples, along with the devices used to concentrate and mount the samples for LIBS testing.

All bacterial specimens were grown on plates containing tryptic soy agar (TSA) nutrient media. TSA is a commonly used general purpose culture medium consisting of casein, soybean meal, NaCl, dextrose and dipotassium phosphate.[71] This media provides all of the nutrients that the previously mentioned bacterial species require to grow and colonize. In order to prepare the plates, 4 g of TSA powder was dissolved in a flask containing 100 mL of deionized water. The solution was autoclaved for a 40-minute period at a temperature of 121 °C in order to sterilize the mixture. After a period of cooling, the solution was safely and slowly poured into empty petri dishes to avoid bubbles and to achieve a uniform surface layer. The TSA was given 2 hours to set after which new colonies could be grown from the stored stock samples. This procedure was carried out for each bacterial species whenever new colonies were required in order to maintain genetically identical, reproducible test samples.

Bacteria harvested from the mother culture were deposited on the surface of TSA nutrient media with a disposable L-shaped spreader bar. The plates were incubated at 37 °C for 24-72 hour periods after streaking to allow the bacteria to form visible colonies. After incubation, a repeatable quantity of bacteria was harvested from the growth plates and suspended in labelled microcentrifuge tubes containing 1.5 mL of deionized water and stored in the fridge until required. The initial concentration in units of colony forming units (CFU)/mL for each bacterial suspension was determined through optical densitometry (absorbance) measurements on different fractional volumes of the initial suspension using optical quality cuvettes. The microcentrifuge tube suspensions were thoroughly vortexed to agitate and resuspend any bacteria that had collected into pellet formations at the bottom of the tubes, in order to create as uniform a suspension as possible when target samples were ready to be mounted.

Target bacteria were deposited onto disposable Millipore nitrocellulose filters with pore size 0.45 μm. The filters were modified using a sterilized punch and die set to reduce the size from a standard 13 mm diameter to a custom 9.5 mm diameter in order to fit within the diameter of a custom-built centrifuge tube insert. The deposition area was concentrated to a circular central spot of 1 mm diameter using a custom-built metal cone device. Deposition with both the centrifuge insert and metal

cone device utilize materials, equipment and methods that are commonly and easily implemented within clinical settings. The following section will describe how both devices are combined in order to achieve a simple and rapid concentration of bacterial cells for LIBS testing.

The centrifuge tube insert shown in Figure 2.1 was designed and 3-D printed by a previous student in our group.

Figure 2.1: Custom fabricated centrifuge insert (a) disassembled (b) assembled.

Figure 2.2 shows a schematic representation of the centrifuge insert components.

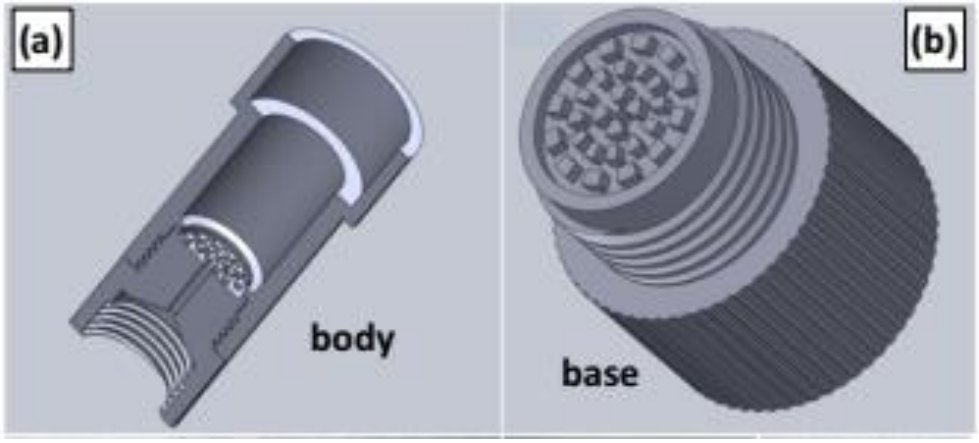

Figure 2.2: CAD drawing of custom centrifuge insert (a) body of insert (b) base of insert.

The insert is similar to commercially available models and fits into a standard 10 mL capacity centrifuge tube with a hinged plastic cap that is capable of closing the insert inside.[72] The insert is built out of lightweight composite material and consists of a cylindrical body with an outer diameter of 14 mm. The base of the insert detaches by unscrewing it and seals securely by screwing it back on, which allows for filter papers to be placed and removed from the insert. This can be seen in Figure 2.3.

Figure 2.3: Insert unscrewed with filter paper placed on the base.

This accessibility is important for transferring filters with bacterial depositions to be mounted and tested. Most market inserts are designed to remove the filtrate without needing the filtration media. The base contains threading so that additional bases can be attached in order to place multiple filters of different pore sizes into the insert simultaneously. This feature will be described in more detail in Chapter 5. The base also contains a central hole that allows the solution to be drawn through the filter, and during centrifugation, pass to the bottom of the tube where it can be discarded. The upper portion of the insert has a wider 17 mm diameter that allows it to rest on the lip of the centrifuge tube without sliding down or becoming dislodged. The entire insert totals 40 mm in height and during operation allows 1.5 mL of liquid suspension to travel through it.

This inexpensive filtration device assists with the concentration of bacterial cells in a liquid suspension onto disposable filter media and provides a convenient method for sample preparation. The resulting bacterial concentration was found to be uniform within 20% of the mean LIBS intensity along the surface of the 9.5 mm diameter filters with the use of the centrifuge insert as shown in Figure 2.4.

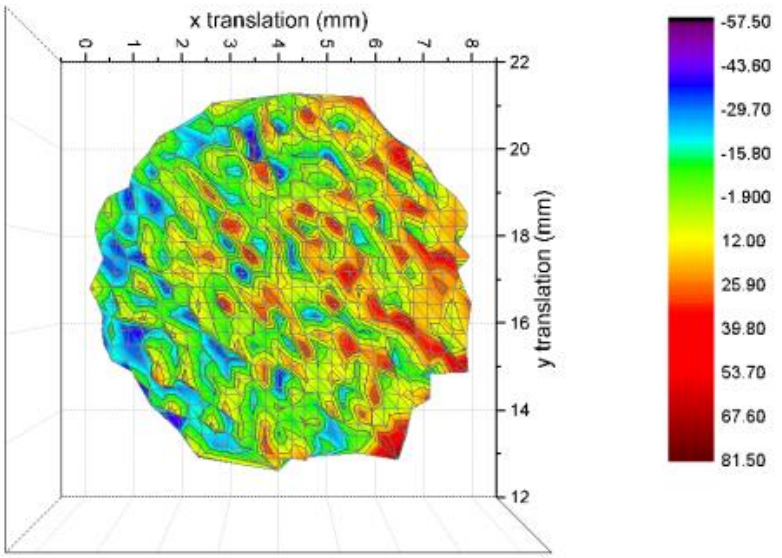

Figure 2.4: Color map indicating total measured LIBS intensity for single-shot LIBS spectra based on surface position along a nitrocellulose filter after centrifugation with the insert.

The insert allows for reproducible uniformity with some loss of bacteria cells that could be improved with a newer prototype containing a stronger base seal. With the addition of the centrifuge insert to our LIBS procedure, the limit of detection (LOD) was calculated to be approximately 90,000 cells per laser shot.[73] This LOD was determined with the construction of a calibration curve from multiple concentrations of bacterial suspensions.

A light-weight hollow aluminum cone was designed and crafted by another previous student to fit within the top of the custom centrifuge insert.[74] The cone is depicted in Figure 2.5 (a). When in place, the apex of the metal cone presses slightly into the surface of the filter media as shown in Figure 2.5 (b).

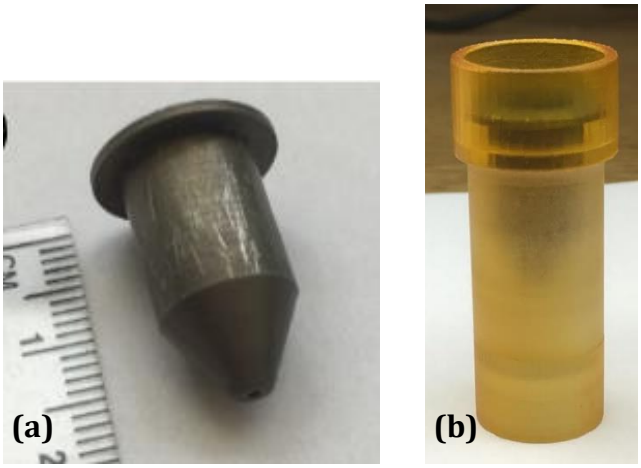

Figure 2.5: Aluminum cone (a) cone with scale showing bottom hole and (b) cone pressed into filter inside centrifuge insert showing top hole.

The cone forces the liquid through a small 1 mm diameter opening onto a central region of the nitrocellulose filter. The bacterial suspension is vortexed and pipetted directly into the metal cone where it passes through the filter during centrifugation without spilling. Figure 2.6 illustrates the combination of the cone and centrifuge insert resting in a centrifuge tube.

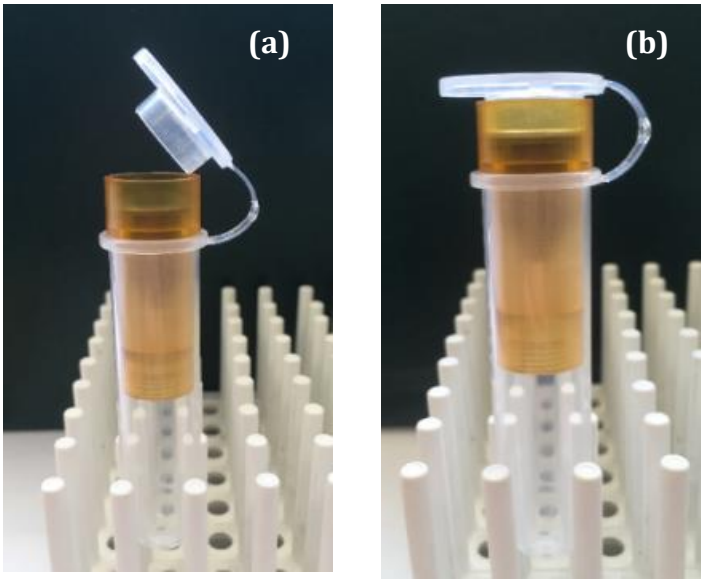

Figure 2.6: Metal cone positioned inside the insert resting inside a standard 10 mL centrifuge tube (a) with centrifuge tube cap open (b) with centrifuge tube cap closed pressing cone firmly into filter paper on the base of the insert.

During these experiments, a Unico PowerSpin BX centrifuge provides 5000 rpm and 2500g's of force during 5 minutes in order to pull the liquid suspension through the filter. The filter can then be removed by unscrewing the base of the insert and left to dry, after which the filter can be mounted onto any surface using a small piece of double-sided tape. When testing with LIBS, a slightly visible circular impression left by the cone helps outline where the laser ablations should be positioned on the nitrocellulose filter. The concentrated bacterial deposition on the central zone of the nitrocellulose filter as a result of the cone is depicted in Figure 2.7.

Figure 2.7: Bacterial deposition concentrated on center of filtration media surrounded by imprints formed by the base of the insert resulting from the pressure of the cone tip.

Used in conjunction with the centrifuge insert, the metal cone rapidly concentrates bacterial cells towards the center of the filtration media with minimal leakage. The limit of detection with the addition of the metal cone was calculated to be approximately 10,865 cells per laser shot, an improvement by almost a factor of 10 from the use of the insert alone.[74] This LOD was determined with the construction of a calibration curve from multiple concentrations of bacterial suspensions. Figure 2.8 illustrates the concentrated region of bacteria upon the filter and the total LIBS intensity measured across the entire surface of the filter. The laser shot spacing can be reduced to increase the number of sampling points per filter in the concentrated region to increase the total number of spectra in the library. The increased number of shots on a filter for clinical applications may not be necessary as a single representative measurement may be preferred for diagnosis. In theory cones of similar design could be fabricated using other materials, including different metals or 3-D composites, and be constructed to hold greater volumes in order to scale with larger centrifuges.

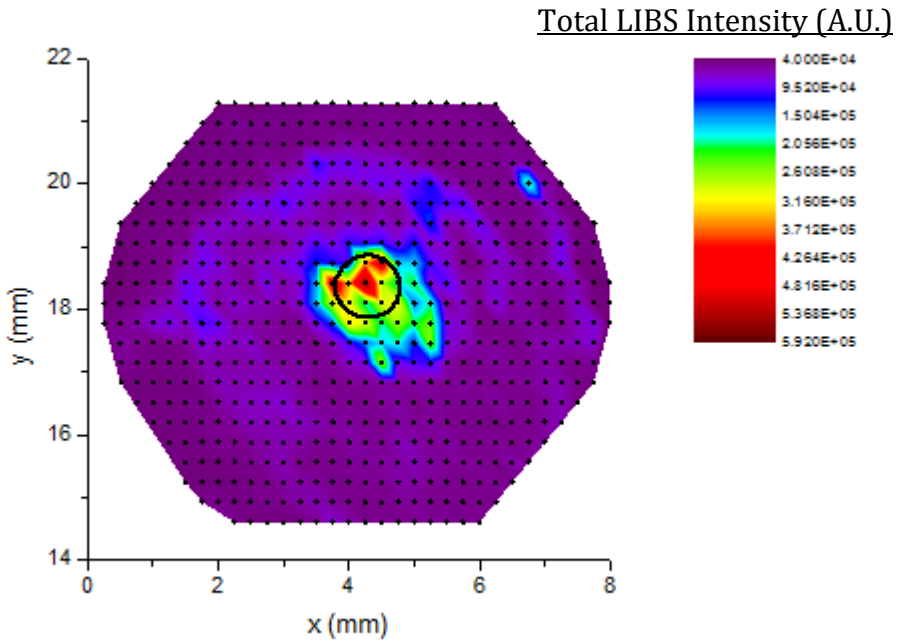

Figure 2.8: Color map indicating total measured LIBS intensity for single-shot LIBS spectra based on surface position along a nitrocellulose filter after centrifugation with the insert combined with the metal cone.

2.4 Mounting Procedure of Swabbed Samples

Our procedure allows for the collection of bacterial samples swabbed from surfaces or present in liquid solutions to represent samples collected from patients. The latter sample collection method simulates bacteria that would be present in blood, urine or cerebral spinal fluid samples and requires the use of multiple bases on the centrifuge insert and multiple filter papers of different pore sizes to separate out concentrated bacterial cells. This method will be discussed more in detail in Chapter 5. This section will describe the procedure for preparing and testing swabbed bacterial specimens. Swab samples of the nose, throat, eyes, and ears are regularly taken to collect clinical specimens in order to diagnose bacterial infections. Our current procedure includes LIBS analysis of bacteria that have been collected in this manner to support the capability of our technique in a more realistic clinical setting.

When a bacterial sample was ready to be tested with LIBS, the microcentrifuge tube was removed from the refrigerator and vortexed for 15 seconds to distribute the

cells evenly throughout the suspension. All components were cleaned thoroughly with a 1:10 bleach water solution and rinsed with deionized water prior to experimentation. 100 µL of liquid contaminant containing bacteria suspension was pipetted onto the surface of a steel plate. The steel plate was then heated using a hot plate at 200°C for 2 minutes and 20 seconds to remove excess moisture. The plate was used to simulate a surface that could be swabbed to acquire test samples. 10 µL of deionized water was deposited onto the head of a sterile flocked swab tip to make it moist and this was used to swab bacteria off the metal plate. The swab was transferred to a centrifuge tube along with 1 mL of deionized water. This is all shown in Figure 2.9. The tube was sealed and vortexed for 15 seconds to release bacterial cells from the swab into suspension.

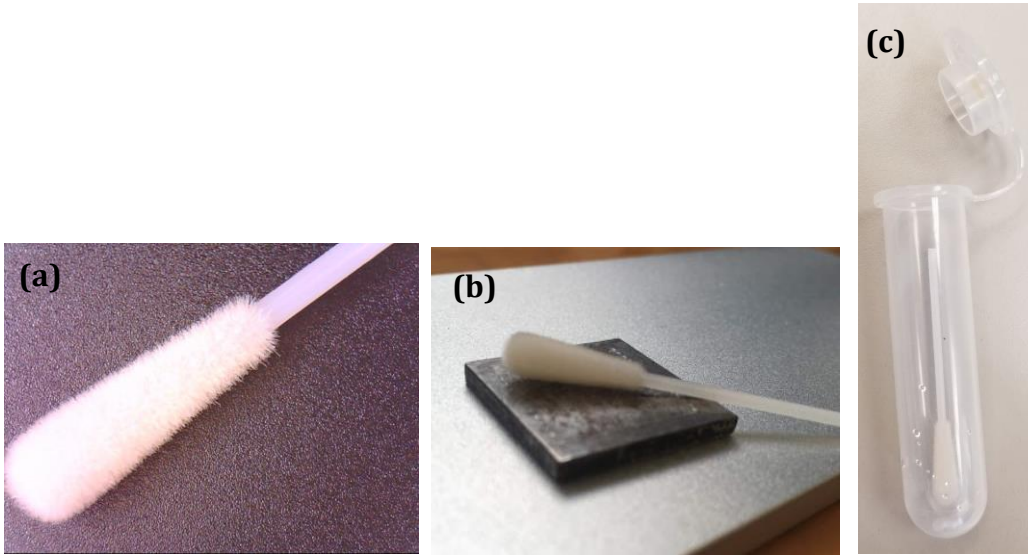

Figure 2.9: Flocked swab. (a) Zoomed in view of swab head. (b) Simulated swabbing of specimens from steel surface. (c) Swab sample placed in centrifuge tube.

A 9.5 mm diameter nitrocellulose filter of 0.45 µm pore size was placed onto the base of the custom centrifuge insert. The base was screwed securely into the body of the insert, and the custom metal cone was placed into the top of the insert. The insert was then placed into another centrifuge tube. 1 mL of sample suspension was pipetted and deposited into the metal cone. The cap of the centrifuge tube was closed to seal the tube for centrifugation and to press the metal cone into the surface of the filter paper. The tube was centrifuged for 5 minutes before the insert was removed.

The bacteria containing nitrocellulose filter was left to dry for approximately 5 minutes and then mounted onto another steel plate that measures 25mm by 25mm using double sided tape and tested with LIBS. This is shown in Figure 2.10.

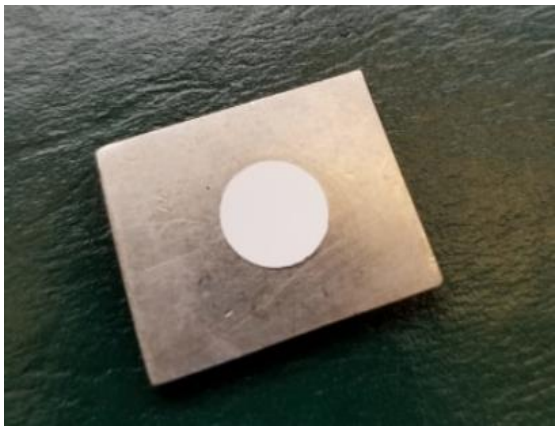

Figure 2.10: Nitrocellulose filter mounted on steel plate ready for LIBS.

The choice of filtration medium utilized during the bacterial deposition process was investigated in order to achieve more optimal LIBS spectra, along with the type of swab used for specimen collection by previous group members. The brand, pore size and membrane material of the filtration media are listed below.

MF-Millipore 0.45 μm MCE Nitrocellulose membrane filters (REF. HAWP01300) were tested against Durapore 0.22 μm PVDF membrane filters (REF. GVWP01300) and Whatman 0.7 μm glass microfiber filters (CAT No. 1825-090) to compare physical limitations, properties and characteristic elemental emission intensities. All three types of filtration media after laser ablation are displayed in Figure 2.11. Although uniform in surface, the Durapore filtration media developed significant scorching after laser ablation and resulted in increased carbon emission that limited overall detector amplification and hindered the limit of detection (LOD) of our LIBS technique. The glass microfiber filter displayed spectra with reduced carbon emission but significantly increased peak intensities of all other elements of interest in the absence of bacterial cells. This filter type becomes untestable after initial ablation, with complete destruction of the filter surface. Nitrocellulose filters were concluded to be the best of the filtration media tested, providing the most convenient, stable, and reproducible mounting substrate.

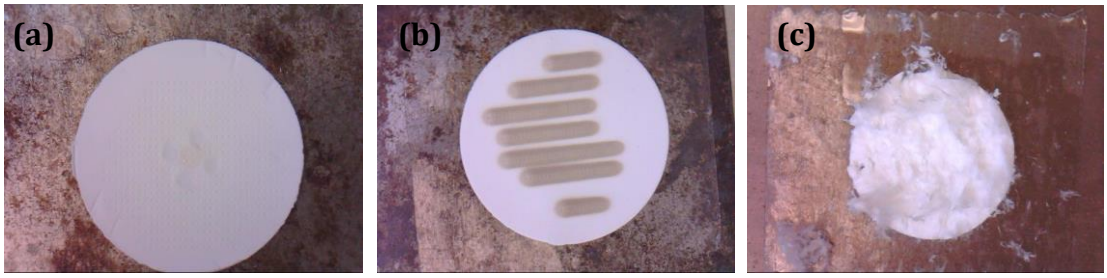

Figure 2.11: Ablated filtration media (a) Millipore Nitrocellulose membrane filter (b) Durapore PVDF membrane filter (c) Whatman glass microfiber filter.

Previous experiments were conducted in order to study the effectiveness of different swabbing media at collecting and releasing bacterial cells. Flocked swabs (Puritan PurFlock Ultra) are regularly used for specimen collection in clinical settings and were chosen as the most efficient collection type when tested against other swab media including cotton tipped swabs. In the flocked swabs, short nylon fiber strands draw in particles and liquids with capillary action. These flocked swabs hold sample materials close to the outer surface and release them when submerged in a liquid medium, or when agitated in the case of vortexing. LIBS testing was conducted directly on the surface of flocked swabs as well as cotton swabs. The ability to align or focus the laser on these uneven surfaces was found to be extremely difficult and that sampling methodology was abandoned. Vortexing the swab in deionized water to shake off bacterial cells was studied to quantify the fraction of bacteria that were released. It was determined experimentally that approximately 80 % of the bacteria picked up by the swab was released by vortexing and that 15 seconds was sufficient time for maximum release of cells. A reduction in the fraction of cells transferred from collection to the test sample is not ideal in the overall effort to lower the limit of identification (LOI) of the LIBS test. As the reduction of this background and water-contamination signal was a significant effort of this work, this will be detailed later in Chapter 6.

References

[50] Tacconelli, E. (2009). Antimicrobial use: risk driver of multidrug resistant microorganisms in healthcare settings. *Current opinion in infectious diseases*, *22*(4), 352-358. https://doi.org/10.1097/QCO.0b013e32832d52e0

[51] The World Health Organization, The World Health Report 1996: fighting disease, fostering development, (Geneva, Switzerland, 1996)

[52] Gast, R. J., Sanders, R. W., & Caron, D. A. (2009). Ecological strategies of protists and their symbiotic relationships with prokaryotic microbes. *Trends in microbiology*, *17*(12), 563-569. https://doi.org/10.1016/j.tim.2009.09.001

[53] Goel, A. (2014). Microbes in Agriculture and Medicine. Bioevolution, 1, 5-8

[54] Deurenberg, R. H., Bathoorn, E., Chlebowicz, M. A., Couto, N., Ferdous, M., García-Cobos, S., ... & Zhou, K. (2017). Application of next generation sequencing in clinical microbiology and infection prevention. *Journal of Biotechnology*, *243*, 16-24. https://doi.org/10.1016/j.jbiotec.2016.12.022

[55] Busse, H. J., Denner, E. B., & Lubitz, W. (1996). Classification and identification of bacteria: current approaches to an old problem. Overview of methods used in bacterial systematics. *Journal of biotechnology*, *47*(1), 3-38. https://doi.org/10.1016/0168-1656(96)01379-X

[56] Salyers, A. A., & Whitt, D. D. (2002). Salmonella species. *Bacterial pathogenesis: a molecular approach, 2nd ed. American Society for Microbiology, Washington, DC*, 381-397.

[57] Dudek, N. K., Sun, C. L., Burstein, D., Kantor, R. S., Goltsman, D. S. A., Bik, E. M., ... & Relman, D. A. (2017). Novel microbial diversity and functional potential in the marine mammal oral microbiome. *Current Biology*, *27*(24), 3752-3762. https://doi.org/10.1016/j.cub.2017.10.040

[58] Murat, D., Byrne, M., & Komeili, A. (2010). Cell biology of prokaryotic organelles. *Cold Spring Harbor perspectives in biology*, *2*(10), a000422. https://doi.org/10.1101/cshperspect.a000422

[59] Yang, D. C., Blair, K. M., & Salama, N. R. (2016). Staying in shape: the impact of cell shape on bacterial survival in diverse environments. *Microbiology and Molecular Biology Reviews*, *80*(1), 187-203. DOI: 10.1128/MMBR.00031-15

[60] Schaechter, M., Medoff, G., & Eisenstein, B. I. (Eds.). (1993). *Mechanisms of microbial disease*. Lippincott Williams & Wilkins.

[61] Rehse, S. J., Jeyasingham, N., Diedrich, J., & Palchaudhuri, S. (2009). A membrane basis for bacterial identification and discrimination using laser-induced breakdown spectroscopy. *Journal of Applied Physics*, *105*(10), 102034. https://doi.org/10.1063/1.3116141

[62] Korf, J. E. (2005). *The modulating properties of mycobacterial mycolic acids on murine macrophage function* (Doctoral dissertation, University of Pretoria). http://hdl.handle.net/2263/28500

[63] Ray, C. G., & Ryan, K. J. (2010). *Sherris medical microbiology* (Vol. 6). McGraw-Hill.

[64] Salyers, A. A., Whitt, D. D., & Whitt, D. D. (1994). *Bacterial pathogenesis: a molecular approach* (Vol. 1). Washington, DC: ASM press.

[65] Lyhs, U., Ikonen, I., Pohjanvirta, T., Raninen, K., Perko-Mäkelä, P., & Pelkonen, S. (2012). Extraintestinal pathogenic Escherichia coli in poultry meat products on the Finnish retail market. *Acta Veterinaria Scandinavica*, *54*(1), 1-6. https://doi.org/10.1186/1751-0147-54-64

[66] Lazcka, O., Del Campo, F. J., & Munoz, F. X. (2007). Pathogen detection: a perspective of traditional methods and biosensors. *Biosensors and bioelectronics*, *22*(7), 1205-1217. https://doi.org/10.1016/j.bios.2006.06.036

[67] Zavascki, A. P., Carvalhaes, C. G., Picao, R. C., & Gales, A. C. (2010). Multidrug-resistant Pseudomonas aeruginosa and Acinetobacter baumannii: resistance mechanisms and implications for therapy. *Expert review of anti-infective therapy*, *8*(1), 71-93. https://doi.org/10.1586/eri.09.108

[68] Norgard, M. V., & Imaeda, T. (1978). Physiological factors involved in the transformation of Mycobacterium smegmatis. *Journal of Bacteriology*, *133*(3), 1254-1262.

[69] Agrawal, P., Miryala, S., & Varshney, U. (2015). Use of Mycobacterium smegmatis deficient in ADP-ribosyltransferase as surrogate for Mycobacterium tuberculosis in drug testing and mutation analysis. *PLoS One*, *10*(4), e0122076. https://doi.org/10.3390/microorganisms7080237

[70] John Jr, J. F., Sharbaugh, R. J., & Bannister, E. R. (1982). Enterobacter cloacae: bacteremia, epidemiology, and antibiotic resistance. *Reviews of infectious diseases*, *4*(1), 13-28. https://doi.org/10.1093/clinids/4.1.13

[71] Ahn, Y., Lee, U. J., Lee, Y. J., LiPuma, J. J., Hussong, D., Marasa, B., & Cerniglia, C. E. (2019). Oligotrophic Media Compared with a Tryptic Soy Agar or Broth for the Recovery of Burkholderia cepacia Complex from Different Storage Temperatures and Culture Conditions. *Journal of microbiology and biotechnology*, *29*(10), 1495-1505. https://doi.org/10.4014/jmb.1906.06024

[72]https://www.thermofisher.com/search/browse/featured/ca/en/80012565/Conical+Tubes

[73] Malenfant, D. J. (2016). *Influences on the Emissions of Bacterial Plasmas Generated through Nanosecond Laser-Induced Breakdown Spectroscopy*, Master's thesis, University of Windsor. https://scholar.uwindsor.ca/etd/5843

[74] Paulick, A. E. (2018). *Development of Laser-Induced Breakdown Spectroscopy as a Rapid Diagnostic Tool for Bacterial Infection*, Master's thesis, University of Windsor. https://scholar.uwindsor.ca/etd/7653

Chapter 3: Laser-Induced Breakdown Spectroscopy

3.1 LIBS Theory

Experiments involving the ablation of materials began after the development of the solid-state ruby laser in 1960 by Theodore Maiman. Laser-induced breakdown spectroscopy emerged shortly after in 1963 with the first elemental analysis conducted on surfaces using plasmas generated through the utilization of lasers.[75] In 1964 the neodymium-doped ytterbium-aluminum-garnet laser (Nd:YAG) was built by Geusic, Marcos and van Uitert. This Nd:YAG laser is one of many types of pulsed lasers used to perform LIBS and is the current laser used throughout my own experimental research. The LIBS technique obtains the spectral fingerprint of a target material, whether it be a solid, liquid or gas sample, based on the light emitted from a laser-induced plasma (LIP). Figure 3.1 depicts a LIP. The plasma contains a collection of ions, atoms and electrons that distinctly emit light at wavelengths characteristic of the elemental composition of the ablated material in the sample. Laser-induced plasmas may be generated using a wide variety of laser wavelengths and pulse durations.

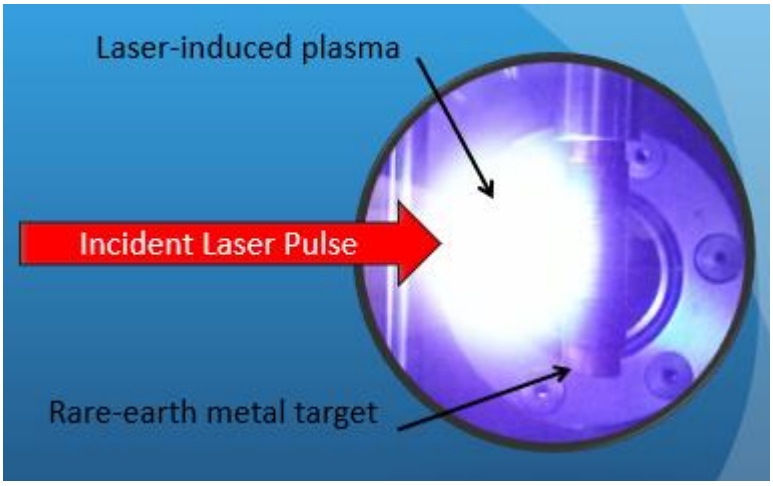

Figure 3.1: Laser-induced plasma formed by laser ablation of a metal target. The laser, though invisible, is incident from the left as illustrated in the figure.

Emitted light from the plasmas is collected and analyzed using high-resolution spectrometers that can disperse specific wavelength ranges, the choice of spectrometer used corresponding to the desired wavelength range of the experiment being carried out. The following sections of this chapter will discuss the theory of laser-induced plasmas, including plasma formation, optical emission and the collection of light emitted from such plasmas. This chapter will also describe the experimental apparatus used to deliver the laser pulse to the target material and the collection of light that is analyzed to determine the elements present in our bacterial specimens.

In order to understand laser-induced breakdown spectroscopy it is important to understand the atomic transitions that occur that produce the optical elemental emission peaks present in all LIBS spectra. For an isolated atom or ion there are three radiative processes that involve the emission or absorption of a photon: stimulated emission, absorption (sometimes called stimulated absorption) and spontaneous emission. The last of these, spontaneous emission, is the radiative process that is responsible for the majority of optical emission from a laser-induced plasma during LIBS ablation.

The bound electrons of an atom or ion occupy specific quantized energy levels. A valence electron can transition between energy levels as the atom becomes excited or de-excited by absorbing or emitting a photon. There are other mechanisms that can cause an electron to transition, such as collisions, but these will not be considered here. Electrons can also freely exist in a continuum beyond these discrete states, and this is important as in our laser-induced plasmas there are a significant number of free electrons which is what makes it a plasma.

A spontaneous emission occurs when an excited atom de-excites or decays from an upper state energy level to an energy level with a lower energy by emitting a photon. Denoting the upper energy level as j with an energy E_j, and the lower energy level as i with an energy E_i, the spontaneous emission of a photon with energy $\Delta E = E_j - E_i = h\nu_{ji}$ describes the transition of an electron spontaneously decaying between the two energy levels E_j and E_i. The chance of this spontaneous emission

occurring is represented by the Einstein A coefficient A_{ji} which describes the transition probability, or the probability per unit time in which the electron will decay to the lower energy level.

Detection and analysis of spectral lines in the collected LIBS spectra is vital for correctly identifying the elemental composition of a target material. These spectral lines represent distinct wavelength emissions that are characteristic of the photons emitted during the transition of electrons between different energy levels as previously described. The energy difference between discrete energy levels that these electrons can occupy in a specific atom correspond to discrete energies, which through the equation $E = \frac{hc}{\lambda}$ are indicative of the wavelengths that can be visually observed in resulting LIBS spectra. The abundance of observed spectral lines for some elements can be attributed to more complex electron configurations. For example, transition metals such as iron and silver in the d-block have a much larger number of electronic energy levels, leading to a much larger number of transitions that can occur during the generation of laser-induced plasmas. The number of observed emission lines in LIBS spectra from such elements is correspondingly much greater. Correspondingly, LIBS spectra from Group I and Group II elements are much more sparse, due the relative simplicity of their electron configurations. This is shown clearly in Figure 3.2 which provides LIBS spectra acquired in our laboratory from steel targets (mostly iron) and bacterial targets (emission dominated by calcium and magnesium). A periodic table is provided for reference.

Steel LIBS Spectra

(a)

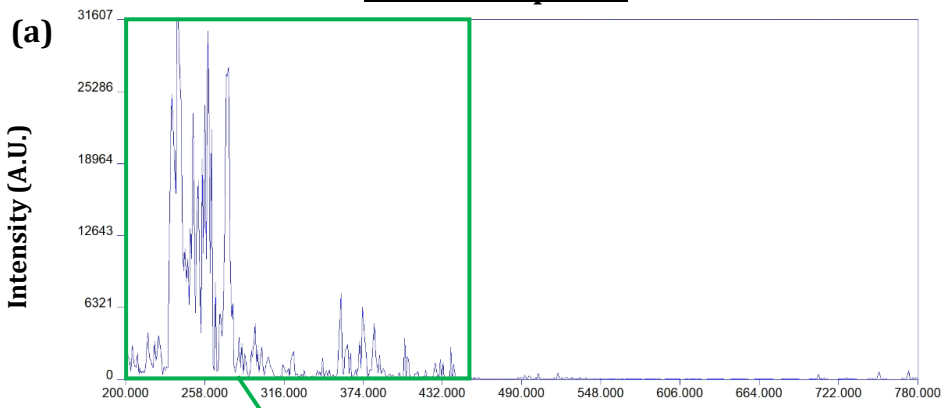

(b)

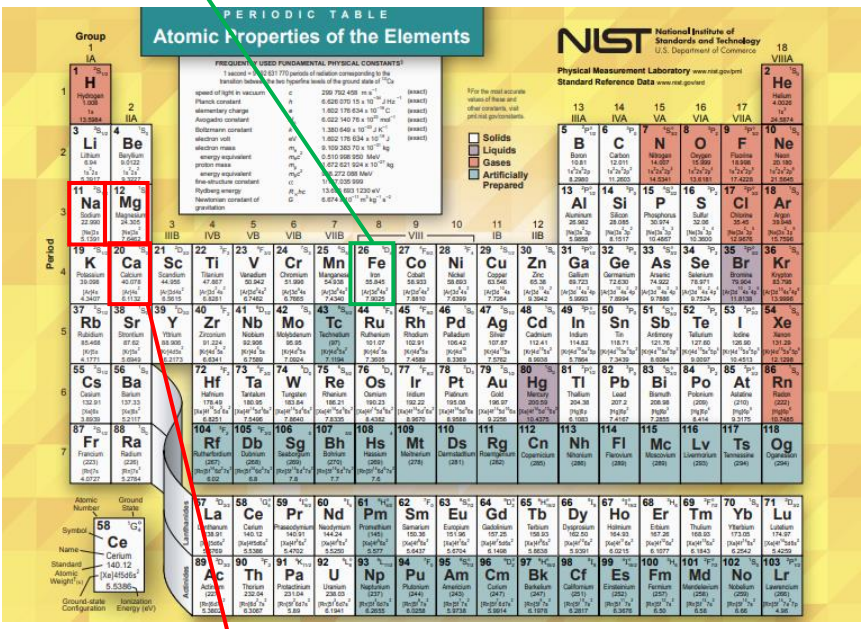

Bacteria LIBS Spectra

(c)

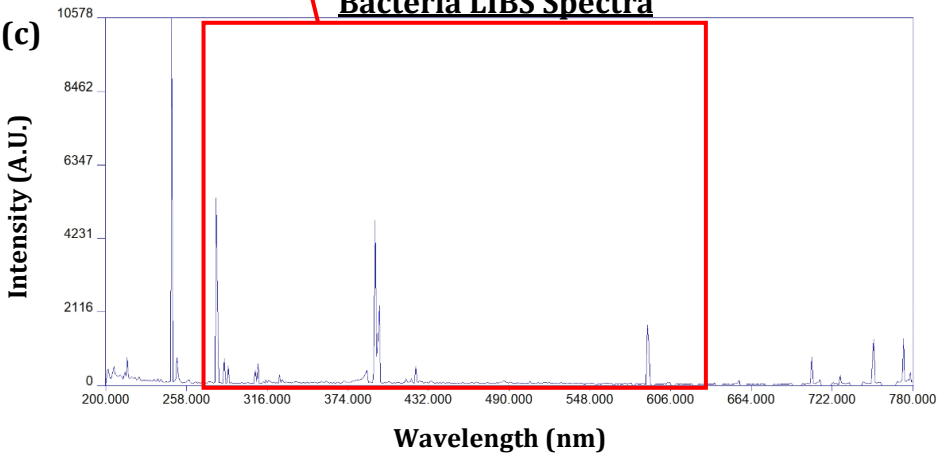

Figure 3.2: (a) Steel LIBS spectra with highlighted Fe emission lines. Iron is located in the d-block of the periodic table and has many allowed energy states that produce hundreds of emission lines when transitions occur between energy levels. Not all of the Fe lines are resolved at this level of display. (b) Periodic table highlighting key elements in each spectrum (adapted from https://www.nist.gov/pml/periodic-table-elements) (c) Bacteria LIBS spectra with highlighted Ca, Mg and Na emission lines. Bacteria spectra are mostly composed of elements from Groups I and II of the periodic table which have fewer electronic configurations to produce multiple spectral lines.

In a typical LIBS experiment a pulse of laser light, usually a nanosecond, picosecond or femtosecond duration pulse, is used. In the nanosecond regime, the LIP undergoes an isothermal expansion during the laser pulse and an adiabatic expansion after the termination of the pulse.[76] My research and discussion on LIBS are focused on the nanosecond regime, although experiments are performed with delay times in the microsecond range in order to minimize or eliminate early-time non-specific continuum emissions. Continuum emission of the plasma dominates the LIP emission at very short delay times (within nanoseconds of the plasma formation), is not wavelength specific, and does not provide information allowing the elemental analysis of sample materials. This continuum emission consists of bremsstrahlung radiation that results from transitions in the continuum during which a free electron loses energy and emits a photon in the presence of a charged particle, as well as photons emitted during the recombination process that occurs between the continuum and discrete energy levels as free electrons are captured into a bound level of an ion.[77]

In general, LIBS experiments depend on the properties of the target material, the properties of the incident laser light and the ambient gas environment in which the material is ablated. The physics of LIPs is complex and involves multiple physical processes including heat transfer, phase transitions, laser-plasma interactions, condensation, radiation and gas dynamics.[78] In some cases, a plasma does not generate after laser ablation. This is because the ablation rate and characteristic elemental emission intensity can vary on a pulse to pulse basis due to variations in laser energy, the availability of free seed electrons, the temporal pulse shape and the laser beam's spatial profile on the irradiated material.[79] The target material possesses

many properties that play a role in the generation of LIPs including the homogeneity and chemical composition of the ablated volume. Physical properties such as phase, temperature and pressure along with mechanical properties such as crystal orientation and smoothness are also factors.[80] The laser focusing conditions, the angle of the laser beam incidence, the sub volume of plasma being observed and the angle of light collection all have a significant impact on the resulting LIBS spectra. The presence of previously ablated particulates in the breakdown volume can also lead to memory effects for subsequent laser shots.

3.2 LIBS Apparatus and Experimental Setup

Laser-induced breakdown spectroscopy requires a high energy pulsed laser, beam focusing optics, an ablation chamber and a system to observe the plasma light. This light collection system consists of a dispersion device, in our case a spectrometer, along with a computer to control the detector and display the resulting spectra. The experimental setup used in my research utilizes a 1064 nm Nd:YAG pulsed laser (Quanta Ray LAB-150-10, Spectra Physics) to generate laser-induced plasmas. The Nd:YAG laser operates with a beam diameter of 9 mm, a 10 Hz repetition rate and has a 10 ns pulse duration. The maximum initial pulse energy was reduced from 650 mJ per pulse to 180 mJ per pulse by combining a half-wave plate to rotate the polarization of the beam along with a Glan-Taylor calcite polarizing beam splitter to direct a portion of the laser into a beam dump to be discarded. The energy of the beam was adjusted through the remaining optical system before being directed and focused on a target sample with a final incident energy of 8 mJ per pulse. The optical system contains two high-reflectivity dielectric coated mirrors to direct the laser into a 3x telescope beam expander that triples the beam diameter, consisting of a antireflection coated plano-concave lens (f = -5 cm, ϕ = 2.54 cm) followed by a plano-convex lens (f = 18.5 cm, ϕ = 7.62 cm) separated by a distance of 13.5 cm. The central and primarily Gaussian portion of the beam was then directed through an iris of 9 mm to reduce the beam diameter to its initial size. In this way the telescope performs as a laser beam "spatial mode cleaner" and it also reduces the pulse energy to approximately 20 mJ

per pulse. A final high reflection dielectric coated mirror was used to direct the laser pulse downwards towards target samples where it is focused by a long working-distance 5x antireflection coated microscope objective. A beam splitter was positioned before the objective to allow a CCD camera to view the target through the objective in order to display the ablation area and monitor the positioning and sampling during data acquisition. The final laser energy at the surface of the target was approximately 8 mJ.

A helium-neon (He-Ne) laser was positioned in close proximity to the optical train and directed by aluminum mirrors in order to visually adjust the height of the pedestal. The visible red dot distinctly identifies the position of the surface area of the target to be ablated. The entire schematic of the laser, optical train and ablation chamber for delivery of the laser pulse is shown in Figure 3.3.

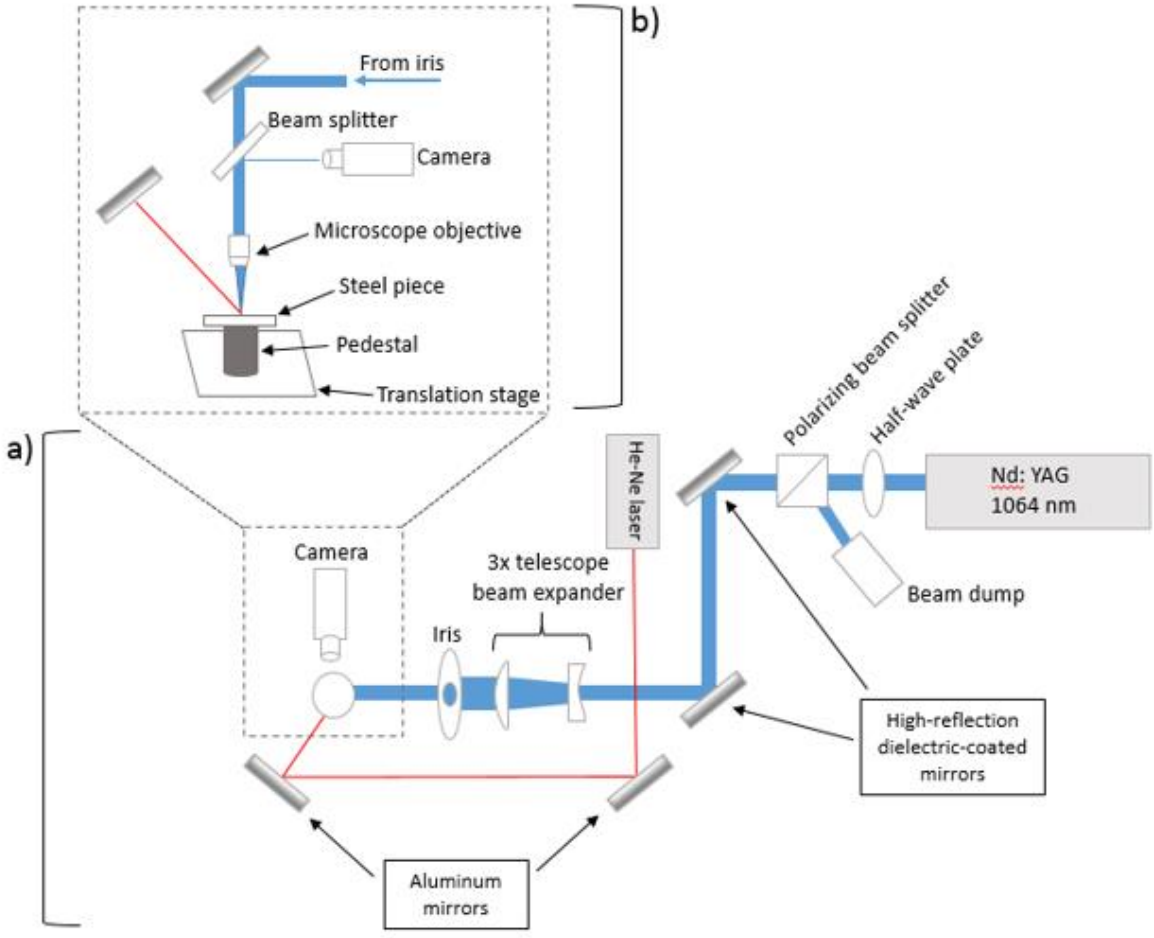

Figure 3.3: Experimental setup used to conduct LIBS on target samples. (a) Overhead view of optical laser pathway. (b) Side view pathway of laser pulse incident on mounted sample.

LIBS studies have been conducted on numerous target materials in a wide variety of ambient gas environments. Greater emission intensities can be achieved by increasing the number of electrons in higher energy states and in turn increasing the number of emissions as these excited electrons transition to lower energy levels. Plasmas with higher electron densities and higher temperatures result in increased populations of these excited state electrons and it has been shown that argon gas environments produce plasmas with both hotter temperatures and greater electron densities compared to that of air, helium, nitrogen and neon gas environments.[81] This is because argon has the greatest mass and a higher ionizing capability compared to that of the other gases. Argon exerts a force on the plasma, confining it to a smaller area, which results in more collisions between the species present in the plasma plume. Emission peaks and bands from elements and molecules formed by the other gaseous species are eliminated when using pure argon, as it does not react to form new species in the chamber. Previous LIBS studies determined atmospheric pressure conditions result in the greatest emission intensities.[82] It has also been shown that argon gas improves signal to noise ratios of emission lines compared to the other gas environments making it the most suitable choice for LIBS analysis.[83] In this research, all experiments were carried out in an argon environment conducted under atmospheric pressure.

The target samples prepared on nitrocellulose filtration media were mounted on steel pieces which are positioned and held in place on a magnetized pedestal located inside a chamber constructed of Plexiglas. The sealed chamber is purged and flushed with argon at a flow rate of 20 SCFH. The chamber itself is mounted on a xyz-translation stage to control the position and movement of the chamber and the target samples in all directions. The HeNe laser can be visually traced along the surface of the steel and nitrocellulose filter surfaces through the walls of the chamber as well as on a tv monitor display. Adjusting the stage in the z direction upwards or downwards allows for proper alignment with the focal spot of the laser beam by changing the height of the target relative to the microscope objective. Alignment markings on the monitor screen displaying the CCD camera image of the target corresponded with the position of the viewed HeNe laser spot when the height of the target was such that

the highest intensity of lines of interest in our spectra could be reproducibly obtained after optimization and numerous LIBS spectra. The focal spot of the laser is unmoving. The stage position is adjusted to ablate the target at multiple chosen locations. Translations in the x and y directions, forward, backward and to the left or right, guide the mounted sample surface to collect additional data for the construction of a more robust spectral library.

The plasma light is directed into a 1 m steel-encased multimodal optical fiber (NA = 0.22, core ϕ = 600 μm) using two matching off-axis parabolic aluminum mirrors (f = 5.08 cm, ϕ = 3.81 cm) placed in proximity to the plasma. The mirrors increase the amount of light being collected and ensure the light is being collected from the same location of the plasma during each laser pulse. Light emitted from the plasma is dispersed and detected using an intensified charge-coupled device (ICCD) camera (Kodak KAF 1001) connected to an echelle spectrometer (ESA 3000, LLA Instruments, Inc.). The operation of the laser, echelle spectrometer and gating of the ICCD were controlled with a computer equipped with ESAWIN v3.20 software (provided by the manufacturer).

The echelle spectrometer schematically displayed in Figure 3.4 contains a step-like diffraction grating and a cross-dispersing prism. The echelle grating has grooves that are spread apart to spatially disperse the plasma light by wavelength. Each wavelength is diffracted at a different angle by the grating according to the equation

$$m\lambda = d(sin\alpha + sin\beta) \qquad (1)$$

Where the angular spacing for an incident wavelength λ decreases as the diffraction order m increases. The value d refers to the width of the groove spacing, α is the angle of incidence and β is the angle of diffraction. For a given angle of incidence and groove spacing, it can be proven with the above equation that different wavelengths of varied order will overlap in certain locations. A first order line of wavelength λ will be diffracted at the same angle as a second order line of wavelength $\lambda/2$ and third order line of wavelength $\lambda/3$ and continues for higher orders. The echelle spectrometer is optimized for very high diffraction order efficiency such that with our grating we observe orders m = 29 up to m = 119. Integrated into the light imaging system is a prism mounted perpendicularly to cross-disperse the light in the

highly overlapping orders into a two-dimensional array. The components and internal optics of the ESA 3000 spectrometer are depicted in Figure 3.4. The orders are separated vertically while the wavelength is separated horizontally within an order, which maintains spectral bandwidth and results in a very high level of resolution.[84] The formation of this two-dimensional pattern imaged onto a CCD chip is known as an echellogram, and this is shown in Figure 3.6.

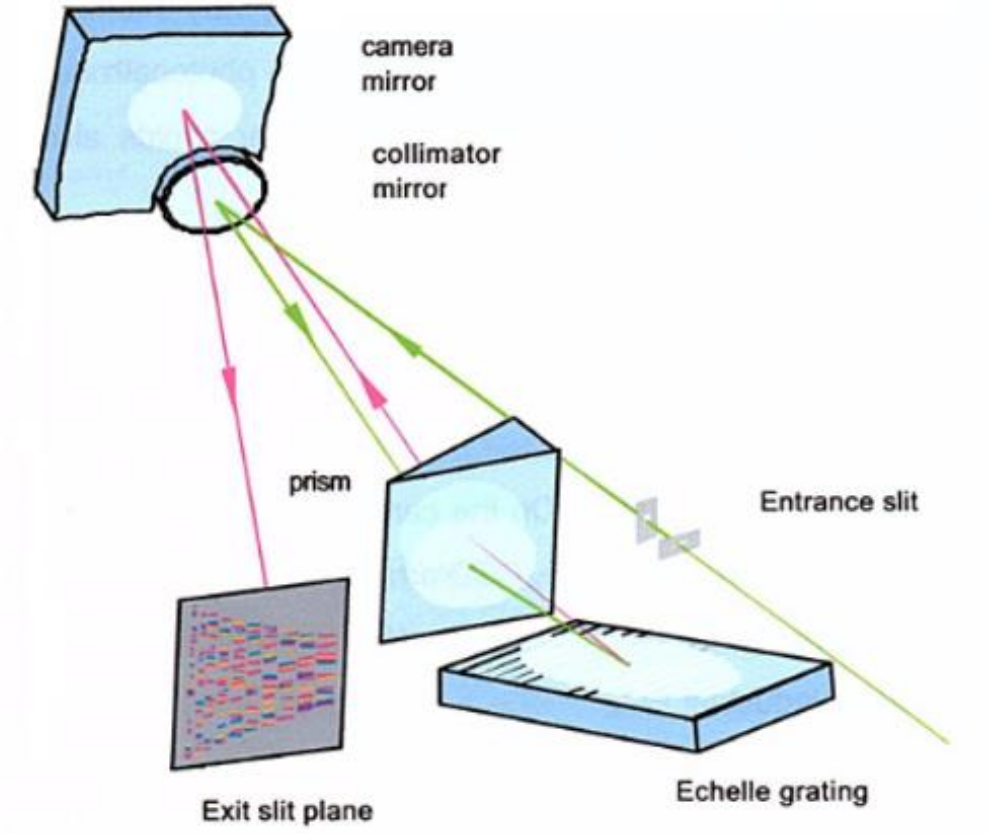

Figure 3.4: Schematic diagram of an echelle spectrometer and components. Figure adapted from Installation Guidelines Echelle Spectra Analyzer ESA 3000, LLA Instruments GmbH, Berlin, Germany, 2005. [85]

The diffraction pattern of the echellogram is detected and recorded by an intensified CCD camera. The CCD is a 1 inch by 1 inch chip (1064 pixels by 1064 pixels, 24 μm^2 pixel size) that images the dispersed light using a grid of potential well capacitors. The incoming photons produce electron-hole pairs and the number of holes is linearly proportional to the intensity of light that a specific pixel in the array is exposed to. The intensity values of the charge in each pixel of the CCD are measured simultaneously by the computer and displayed immediately afterwards. The ICCD

camera also consists of a microchannel plate (MCP) image intensifier that acts as a gating mechanism (essentially a very fast electronic shutter) that also amplifies the signal from a very low number of initial incident photons. Incoming photons from the laser-induced plasma are converted to photoelectrons by the MCP and a voltage produces a cascade of electrons, which are then converted back to photons by a phosphor screen and detected by the CCD. This amplifies the signal enough that the photons of all wavelength emissions present can be distinguished. When no voltage is applied, there is no signal generated or received by the CCD chip. Adjusting the voltage allows for nanosecond timing control of the incoming plasma light. The time between the laser pulse and the collection of light is known as the delay time or τ_d. The length of time used to collect the light that produces the echellogram is known as the gate window or τ_w. Both the gate delay and gate window are illustrated with respect to the incident laser pulse in Figure 3.5.

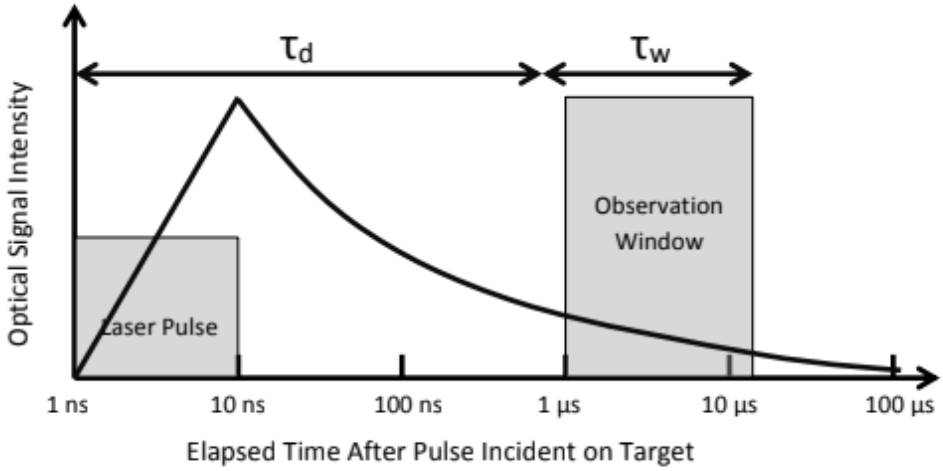

Figure 3.5: Timing diagram of laser-induced plasma evolution and plasma observation characterized by gate delay and the gate window adapted from R. A. Putnam, Recent Advances in the Measurement of Rare-Earth Metal Transition Probabilities Using Laser-Induced Plasmas (2014) [86]

An echellogram is shown in Figure 3.6 and depicts the two-dimensional plot of the spectral lines as a function of both diffraction order and wavelength. The diffraction orders are indicated by green lines. This is a false color image. The yellow false color indicates areas where there is no light on the chip, while darker bands and spots represent areas where more light is detected as the photon wavelengths that are

being dispersed by the spectrometer are mapped to these locations on the CCD. The dispersion is not uniform along all wavelengths. In fact, the spectrometer is customized to maximize resolution in the region of the spectra where many of our elements of interest possess strong emission lines. The uppermost green line of the chip represents the highest order m = 119 which contains the shorter wavelengths in the ultraviolet region and spans a narrower range of 201.023 to 202.615 nm. The wavelength increases moving downwards on the chip, with the wavelength at the end of a line continued on the start of the following line below. The lowest green line on the chip represents the lowest order m = 29 which contains the longer wavelengths in the infrared region and spans a wider range of 816.875 to 838.393 nm. The linear dispersion per pixel in the UV region is approximately 5 pm per pixel with a stated resolution of 0.005 nm at 200 nm and the linear dispersion per pixel in the IR region is approximately 20 pm per pixel with a stated resolution of 0.019 nm at 780 nm.[85] The location of the image intensifier in front of the CCD chip is illustrated by the green circle. Only light in this circular region is amplified and detected. All light outside of this circle which occurs for some of the lower orders is eliminated and ends up as gaps in the resulting spectra. Dark spots that appear within the green circle and outside the range of the horizontal green lines, either to the left or right, are attributed to diffraction into different orders outside the primary order centered on the CCD chip. These dark spots satisfy equation 1 but do not interfere or alter the light intensities measured within the green circle. The shape and size of the chip and intensifier are design choices made by the manufacturers and do not inhibit our ability to conduct LIBS analysis for our bacterial spectra, nor do they directly affect any of our elemental peaks of interest as a majority fall within the higher order UV region.

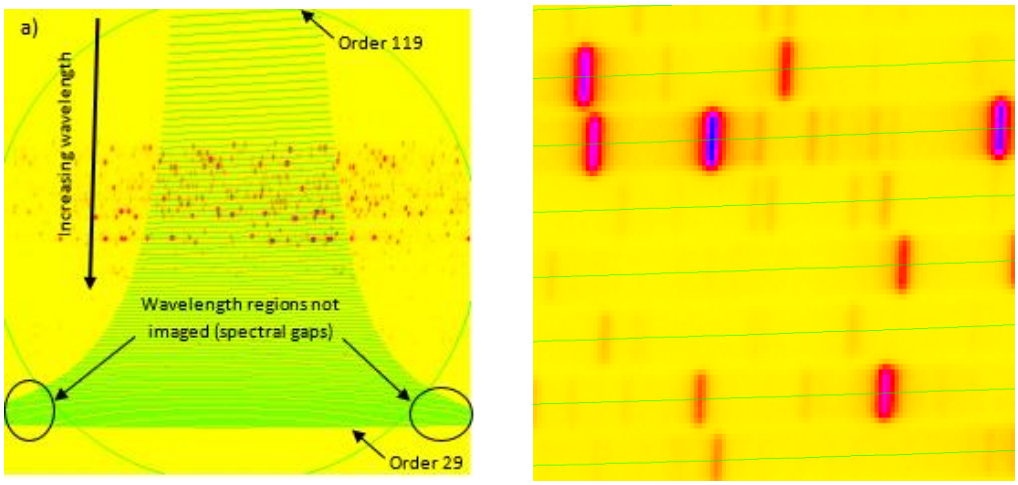

Figure 3.6: Echellogram. (a) CCD chip with mapping of incoming light. The green bands represent the orders of available wavelengths that can be recorded by the spectrometer while the green circle illustrates the detection region. (b) Zoomed in view of the CCD depicting regions exposed to light. On the CCD the position thus determines wavelength after appropriate calibration.

3.3 Plasma Formation and Measurements

To form a laser-induced plasma in the nanosecond regime, a laser pulse with an intensity between 10^8 – 10^{10} W/cm^2 must be focused onto a target material.[75] As the laser pulse reaches a target, the leading edge will be absorbed causing rapid thermal processes such as heating, melting and vaporization of the material. The vaporized material results in an ablation event which can occur within nanoseconds and up to tens of nanoseconds in duration. A crater forms in the target surface as ablated debris is ejected into the area above the surface forming a cloud of atoms. The cloud absorbs the remaining energy of the laser pulse forming a plasma plume and initiating the ignition of the LIP. Multi-photon ionization events occur as atoms absorb several photons simultaneously and become ionized. These ionizations generate free electrons that interact and absorb energy from the laser pulse through inverse bremsstrahlung interactions. The electrons interact with photons and transition to alternate free states which result in a cascade ionization as the accelerated electrons collide and ionize other atoms, producing more free electrons. Once a critical electron density is achieved (roughly 10^{16} cm^{-3}), the plasma acts as a shield for the substrate,

a process known as plasma shielding, which ends the ablation process. The plasma formation via LIBS is shown schematically in Figure 3.7.

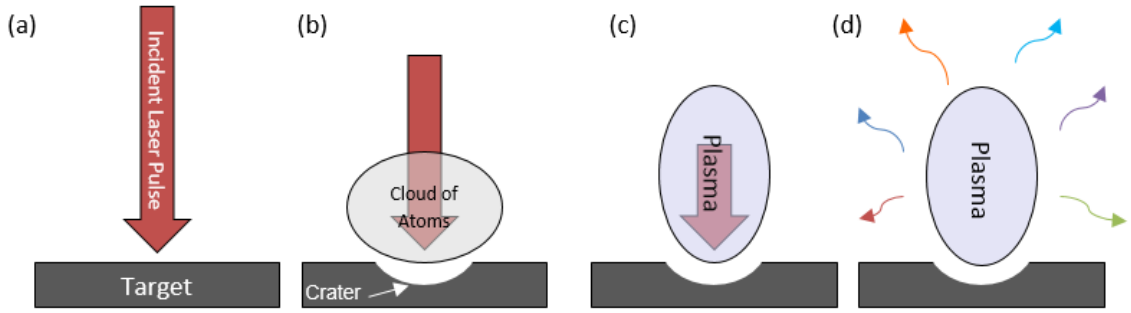

Figure 3.7: Formation of a LIBS plasma (a) incident laser pulse energy is absorbed by target (b) heating vaporizes the target material, forming a crater and ejecting a cloud of atoms above the target surface (c) ejected atoms are ionized forming a LIP (d) photons representative of the vaporized elements are emitted as the plasma cools.

As the plasma expands into the surrounding atmosphere, the external ambient argon gas environment increases the temperature and electron density in correlation with the mass of the argon particles.[82] Although the spectra contain relatively strong argon emission lines, the argon gas does not react, produce molecules or interfere with the ability to measure resulting bacterial spectra.[87] The expansion of the plasma continues until a pressure equilibrium is met between the plasma and argon gas, usually within a time of microseconds after ignition. LIBS plasmas are weakly ionized plasmas that contain both atomic and ion species.[75] When the plasma first becomes observable during maximum ionization, the ratio of electrons in the LIBS plasma to atoms and ions is less than 10 %. The multiply ionized species occur near the surface and reduce in number as the plasma expands and begins to cool. Lower ionized species and neutral atoms and molecules are more abundant towards the outer regions of the plasma. As the lifetime of the plasma increases, recombination forms more neutral species and electrons transition to lower energy levels through spontaneous emission, releasing photons as they decay.

Temperature and electron density are the two parameters used to quantitatively characterize plasmas, however these values are difficult to calculate directly from

spectra that lack a large number of observed spectral emission lines. To calculate the plasma temperature, the plasma system must be in local thermodynamic equilibrium (LTE), where the temperature of the free electrons, ions and atoms are equal.[88] If a sufficient number of emission lines can be observed, the temperature of the laser-induced plasma can be determined experimentally using a Boltzmann plot which is based on the following relationship. The emissivity I_{ji} of a spectral line as an electron transitions from an upper energy level j to lower energy level i is

$$I_{ji} = \frac{hc}{4\pi\lambda_{ji}} A_{ji} L \frac{N}{Z} g_j e^{-\frac{E_j}{k_B T}} \qquad (2)$$

where λ_{ji} is the wavelength of the photon emitted by the electron decay and $A_{ji}$is the transition probability between the two energy levels. The length of the plasma is indicated by L and the value N refers to the total number density of species in the plasma. In this equation E_j is the energy of the upper level, Z is the partition function of the species, and g_j is the multiplicity of the upper energy level, also known as the statistical weight. The value in the denominator of the exponential term is the Boltzmann constant term k_B. Lastly, T is the temperature of the plasma which can be determined by rearranging the equation and taking the natural logarithm of both sides, as shown by equation 3

$$\ln\left(\frac{I_{ji}\lambda_{ji}}{g_j A_{ji}}\right) = -\frac{1}{k_B T} E_j + \ln\left(\frac{hcLN}{4\pi Z}\right) \qquad (3)$$

Equation 3 is an equation of the form $y = mx + b$. Plotting equation 3 as a "modified intensity" $\ln\left(\frac{I_{ji}\lambda_{ji}}{g_j A_{ji}}\right)$ as a function of upper state energy E_j produces a Boltzmann plot with slope of $-\frac{1}{k_B T}$ and an intercept of $\ln\left(\frac{hcLN}{4\pi Z}\right)$. Such a plot requires a large number of points in order to perform a linear regression of the slope, but it does not require the value of the intercept term in this case to extract the temperature. The temperature is not directly calculated in our LIBS experiments because there are not enough line intensities detected in our bacterial spectra that originate from the upper energy levels. Any calculated slope would not include enough emission lines to provide any reliable information for our particular experiments.

With respect to electron density, the LIBS plasma must be considered optically thin, where the photons emitted are not being reabsorbed by the system.[88] There are two methods that can be used to determine the electron density of a plasma. The first method is to estimate this value by using the Saha-Boltzmann equation

$$n_e = \frac{2(2\pi m_e k_B T)^{\frac{3}{2}}}{h^3}\left(\frac{I^I_{nm} A_{ji} g^{II}_j \lambda_{nm}}{I^{II}_{ji} A_{nm} g^I_n \lambda_{ji}}\right) e^{-\frac{E_{ion}+E^{II}_j - E^I_n}{k_B T}} \qquad (4)$$

if the plasma is in LTE, in which the plasma temperature must be known. The electron density n_e, can be determined by taking different line intensities given by the ionization states of an element and calculating the ratio of a measured intensity from a line in the lower ionization state I to a measured intensity from a line in the higher ionization state II. In this case, m_e is the rest mass of an electron and E_{ion} is the ionization potential of the elemental species.[89] The energies E_j and E_n represent two different upper energy levels j and n, while the lower energy values energies E_i and E_m are not included, they represent two different lower energy levels i and m.

The alternative method involves estimating the electron density by analyzing Stark-broadened emission lines. The broadening of observed emission linewidths due to the Stark effect is caused by the perturbation of the energy levels by the electric fields caused by charged particles in the plasma. Stark-broadened lines can be several nanometers wide, many times larger than the elemental peaks observed in the LIBS spectra that span fractions of a nanometer in linewidth. These broadening effects are most commonly used to determine electron densities in LIBS plasmas using emission lines from hydrogen, singly ionized metals similar to hydrogen as well as heavy metal species.[77] To extract Stark broadening from the line shape, other forms of broadening such as pressure, Doppler, instrumental and natural broadening must be taken into account and removed.

The full width at half maximum (FWHM) of a Stark broadened emission line is described by the following equation

$$\Delta\lambda_{1/2} = \frac{2wn_e}{10^{16}}\left(1 + 1.75A\left(\frac{n_e}{10^{16}}\right)^{1/4}\right)\left(1 - \frac{3}{4}N_D^{-1/3}\right) \qquad (5)$$

where $\Delta\lambda_{1/2}$ represents the FWHM. The literature value w refers to the electron impact parameter and the literature value A refers to the ion broadening parameter. The

other constant can be substituted into the final term of the equation as $N_D = 1.72\text{x}10^9 \left(\frac{T_e^{3/2}}{n_e^{1/2}}\right)$ and represents the number of particles in the Debye sphere. The Debye sphere describes the electrostatic effects that charged particles exhibit, which become screened at increasing distance in terms of Debye length. T_e is the temperature of the electron and the terms involving ion temperature T_i are insubstantial and are usually dropped. Equation 5 simplifies when the ion broadening and Debye terms are taken to be equivalent to zero and gives

$$\Delta\lambda_{1/2} = \frac{2wn_e}{10^{16}} \qquad (6)$$

where the FWHM can be used directly to estimate the electron density. For this method, equation 6 requires the presence of a neutral and ion emission line from a single atomic species. However, in the case of our LIBS plasmas, the bacterial emission lines of interest to us do not contain any Stark broadening and the neutral lines contain too much natural variation to be used to calculate electron density or plasma temperature.

References

[75] Cremers, D. A., & Radziemski, L. J. (2013). *Handbook of laser-induced breakdown spectroscopy*. John Wiley & Sons.

[76] Gornushkin, I. B., Shabanov, S. V., Omenetto, N., & Winefordner, J. D. (2006). Nonisothermal asymmetric expansion of laser induced plasmas into vacuum. *Journal of applied physics*, *100*(7), 073304. https://doi.org/10.1063/1.2345460

[77] Singh, J. P., & Thakur, S. N. (Eds.). (2020). *Laser-induced breakdown spectroscopy*. Elsevier.

[78] De Giacomo, A., Dell'Aglio, M., Gaudiuso, R., Amoruso, S., & De Pascale, O. (2012). Effects of the background environment on formation, evolution and emission spectra of laser-induced plasmas. *Spectrochimica Acta Part B: Atomic Spectroscopy*, *78*, 1-19. https://doi.org/10.1016/j.sab.2012.10.003

[79] S. Musazzi, U. Perini (Eds.), Laser-Induced Breakdown Spectroscopy: Theory and Applications, Springer, Berlin, 2014, , https://doi.org/10.1007/978-3-642-45085-3_17.

[80] Ciucci, A., Corsi, M., Palleschi, V., Rastelli, S., Salvetti, A., & Tognoni, E. (1999). New procedure for quantitative elemental analysis by laser-induced plasma spectroscopy. *Applied spectroscopy*, *53*(8), 960-964.

[81] Son, J. G., Choi, S. C., Oh, M. K., Kang, H., Suk, H., & Lee, Y. (2010). Application of pulsed buffer gas jets for the signal enhancement of laser-induced breakdown spectroscopy. *Applied spectroscopy*, *64*(11), 1289-1297.

[82] Dawood, M. (2015). Space and time characterization of laser-induced plasmas for applications in chemical analysis and thin film deposition. http://hdl.handle.net/1866/12347

[83] Ko, J. B., Sdorra, W., & Niemax, K. (1992). Basic investigations for laser microanalysis: III Application of different buffer gases for laser-produced sample planes. *Mikrochim. Acta*, *107*, 319.

[84] Porter, M. J. (2000). Spectroscopy on small telescopes: the echelle spectrograph. *Astrophysics and Space Science*, *273*(1-4), 217-224. https://doi.org/10.1023/A:1002737017056

[85] Installation Guidelines Echelle Spectra Analyzer ESA 3000, LLA Instruments GmbH, Berlin, Germany, 2005

[86] R. A. Putnam, (2014). *Recent Advances in the Measurement of Rare-Earth Metal Transition Probabilities Using Laser-Induced Plasmas*, Master's thesis, University of Windsor. https://scholar.uwindsor.ca/etd

[87] Rehse, S. J., Jeyasingham, N., Diedrich, J., & Palchaudhuri, S. (2009). A membrane basis for bacterial identification and discrimination using laser-induced breakdown spectroscopy. *Journal of Applied Physics*, *105*(10), 102034. https://doi.org/10.1063/1.3116141

[88] Unnikrishnan, V. K., Alti, K., Kartha, V. B., Santhosh, C., Gupta, G. P., & Suri, B. M. (2010). Measurements of plasma temperature and electron density in laser-induced copper plasma by time-resolved spectroscopy of neutral atom and ion emissions. *Pramana*, *74*(6), 983-993. https://doi.org/10.1007/s12043-010-0089-5

[89] Miziolek, A. W., Palleschi, V., & Schechter, I. (Eds.). (2006). *Laser induced breakdown spectroscopy*. Cambridge university press.

Chapter 4: Chemometric Analysis

4.1 Overview of Chemometric Techniques

Initial work for the identification and discrimination of bacterial targets with laser-induced breakdown spectroscopy began in 2003 and has explored numerous approaches with respect to preparing samples, mounting targets, and collecting data. One of the most important areas of interest related to LIBS that is under investigation and currently evolving is the analysis of spectral data. Early methods began with varying mathematical models and by comparing elements of interest in the LIBS spectrum.[90] Linear correlation techniques comparing relative emission intensities and univariate analysis of ratios between emission line intensities were tested by groups to determine how much information was required and sufficient to discriminate bacteria.[91] More advanced mathematical and multivariate techniques including linear regression models, chemometric algorithms and neural network designs have been quickly adapted in LIBS research.[92,93] This section will compare some of these chemometric routines chosen for identification of bacteria specimens.

Chemometric algorithms greatly reduce the amount of data required for reliable discrimination. One such example is the traditional multivariate technique known as Principal Component Analysis (PCA). A multivariate statistical method refers to a method that emphasizes correlations with regards to multiple variables as opposed to a univariate approach that examines the description and analysis of a single variable. With the use of a few or even one principal component there are enough reliable variables to discriminate different species of bacteria based on the variance in the spectral data. LIBS spectral data generally contains information from many different elements and by choosing LIBS emission lines from elements pertinent to bacteria, a lot of unnecessary information from background materials may be eliminated. The utilization of multivariate analysis techniques also provides the ability to compare relative intensities. Rather than relying on absolute intensity values of single emission lines or channels, the ratios of different combinations of line intensities can be computed. These ratios serve to reduce the complexity of the analysis by lowering the overall background noise inherent in the shot-to-shot

variations of LIBS data acquisition. Comparing relative intensities also eliminates variations due to external effects that are present in every spectrum. PCA has been combined with other techniques for preprocessing and tested against many as well.

Another option that was explored using PCA was carried out by comparing variable down-selection against a full spectrum analysis to test if regions with little or no relevant information were required for discrimination. The selection of specific spectral lines to serve as independent variables in the multivariate analysis is known as variable down-selection and uses a sub-set of the acquired data. For example, Merdes et al. performed a PCA on bacterial species with LIBS which reduced 2048 elements contained in the full spectral analysis down to a sub-set of 11 principal components.[94] LIBS spectral data frequently contain thousands of data elements and are routinely composed of 1024 elements at a minimum, which makes data reduction a significant benefit of chemometric algorithms. As will be shown in our data, LIBS spectra obtained by our spectrometer contain over 22,000 pixel elements of information. Prior to performing chemometric analysis we discard most of this spectral data by utilizing only the measured intensities of nineteen lines and a number of ratios made from these lines. In this way, the data size is reduced from over 22,000 channels to 164 channels, making calculations much faster and eliminating extraneous, non-specific information from the analysis. This is discussed in more detail in 4.2 below.

Artificial support vector machines (SVM) such as Neural Networks have also been investigated in LIBS research. NN models are based on multilayer perception and rely on a supervised network built up of several information processing units. These units act as neurons and can receive all the information from other neuron layers. Both input and output data are used in this supervised method to optimize the system's ability to detect similarities between the new spectrum and all reference spectra during training. Neural network analysis models highlight the ability of LIBS as a sensitive technique for discrimination between *E. coli* and *S. aureus.*[95] This technique was also applied to data sets that had been preprocessed using PCA in order to remove outliers and classify unknown spectra. Neural networks provided rapid identification and discrimination of different species and strains of bacteria that

contain multidrug resistance, single gene variations and that commonly cause hospital acquired infections.[96]

In this chapter I will discuss the chemometric techniques used to discriminate bacteria in my work along with our data model and the variables chosen to represent our acquired spectral fingerprints in order to enhance our sensitivity and specificity of our spectral identification method.

4.2 Data Model

Previous LIBS experiments performed by our group at the University of Windsor began with the chemometric analysis of 13 intense emission lines that were resolvable and commonly found in the bacteria spectra. This initial model was labeled the 'Lines Model' and utilized the intensity of the peaks of interest normalized to the sum of those particular intensities. The model was refined to include multiple complex ratios consisting of 5 elements of interest, namely phosphorus, calcium, magnesium, sodium and carbon summed intensities. This model was named the 'Ratio Model 1' (RM1) and contained a total of 24 variables. RM1 was adapted to form 'Ratio Model 2' (RM2) which was comprised of the 13 emission lines from the Lines Model along with 67 additional ratio combinations of those lines of interest for a total of 80 variables in RM2. The creation and evolution of these models are discussed in more detail elsewhere.[97]

For all of my LIBS analysis, I worked with the newest constructed variable basis, 'Ratio Model 3' (RM3) which uses 19 commonly observed normalized peak intensities of the previously mentioned 5 elements of interest along with 145 simple ratio combinations of those normalized peak intensities for a total of 164 independent variables in RM3. This model allows for a more robust and accurate classification of bacteria compared to the previous models and is used throughout the entirety of my thesis research. Table 4.1 and Table 4.2 are located in section 4.6 and include the initial results of the discrimination between 5 genera of bacteria mounted on nitrocellulose filters using two different chemometric algorithms.

The variations in chemical composition of bacterial cells with respect to these chosen elements which are present throughout cell walls, membranes and cytoplasm allow for indirectly observed detection of genetic differences during LIBS analysis. Table 4.3 can be found at the end of chapter 4 and contains the regularly observed spectral lines of interest chosen from the bacterial LIBS spectra along with variable designations. Table B can be found in **Appendix B** and contains a complete list of RM3 ratios used in this research.

4.3 Sensitivity and Specificity

There are numerous clinical techniques that can be used to detect the presence of infections, viruses, and disease in order to accurately diagnose patients. Not only is it ideal to correctly identify all patients that are infected and carrying a disease (known as a "true positive" detection), it is just as vital to correctly determine which patients are free of infection or disease (known as a "true negative" detection.). There are far less clinical techniques that accomplish both without some level of misdiagnosis. A patient or sample that is misidentified could fall under the category of a false positive where they test positive but do not contain the disease or bacteria. Another possibility is that a patient is carrying the disease and the test is not sensitive enough to detect the presence of the underlying pathology resulting in a false negative. False negatives can be detrimental to the contained spread of infectious organisms and viral outbreaks. To quantify the rates of such true or false test results, sensitivity and specificity are two important values that can be calculated and used to quantitatively evaluate a medical test used to diagnose patients.

Sensitivity is the ability of a particular test to identify all patients that do have the disease or in our case the ability to detect if a species of bacteria is present in a sample. This is a measure that represents the levels of true positives and false negative cases. The sensitivity can be given by the following equation:

$$\textbf{Sensitivity} = \frac{\text{True positives}}{\text{True positives} + \text{False negatives}}$$

A level of 75% sensitivity would mean that 25% of the positive cases would not be detected by the test. Higher sensitivity levels improve the diagnostic process and are

desirable for treatable infections that can kill within short periods of time. A value of 100% sensitivity correctly identifies all patients with a disease as positive disease carriers, or all bacteria-containing samples as having bacterial cells present. In our case higher sensitivity allows us to detect bacteria present in prepared samples with very high dilutions or clinical samples with extremely low concentrations (which is referred to as the bacterial titer or just titer.) Although a level of 100% seems optimal, a test method that is constructed to be extremely sensitive to the point where all of the population tests positive regardless of whether or not they carry the disease is the reason why another value related to negative cases is also important. This value is the specificity.

High numbers of false positive cases can lead to serious and invasive procedures, unnecessary operations, as well as preventable mental, physical, and financial stress on patients. True negatives and false positive cases are best represented by the specificity value. A high specificity is vital to correctly identifying all patients that do not have an illness or infection. The specificity can be measured by the following equation:

$$\textbf{Specificity} = \frac{\text{True negatives}}{\text{True negatives} + \text{False positives}}$$

A level of 75% specificity would mean that 25% of the population would test positive for a condition that they do not have. In our case a sample of sterile water could be identified as a bacterial organism if the specificity of our test is too low, or a species of bacteria could be misclassified as a completely different species. A value of 100% specificity correctly identifies all patients without a disease as negative disease carriers, or all samples without bacteria as having no bacterial cells present. A level of 100% specificity also seems optimal, however a test method that is constructed to be extremely specific to the point where all of the population tests negative regardless of whether or not they carry the disease is not helpful for determining the presence in any positive cases.

Combinations in which the sensitivity or specificity are too low are not ideal and the case in which either value is made too high at the expense of the other can be equally as harmful to the overall diagnosis. The ideal scenario is to achieve an optimal

combination with both values at maximum levels. The sensitivity and specificity generally have a trade off that is inherent to the cut off values chosen by the test to form a threshold of positive indication. In order to achieve 100% accuracy both the sensitivity and specificity levels would be perfect at 100%. This level of accuracy is not a currently obtainable standard for any clinical diagnostic test of any disease, but the addition and combination of newer more advanced testing procedures is always improving the accuracy of medical diagnoses. Chemometric algorithms are one such improvement that can help to increase the overall sensitivity and specificity of a diagnostic test.

As the previous discussion shows, the idea of a diagnostic "accuracy" is complicated and there is not one standard definition for it. In our work we always attempt to report the sensitivity and specificity values along with the limit of detection, which details the lowest titer for which those numbers are valid, in order to express overall "accuracy" of the diagnosis. The dependence of this accuracy on the number of bacteria cells present is ongoing in this work, as a specimen from a pre-symptomatic patient would contain a much lower titer than a specimen collected from a diagnosed infection. It is worthy to note that the classification accuracy has been observed to increase with the addition of sample data to the overall bacterial spectral library.

While a single test may not be able to achieve both a high sensitivity and high specificity simultaneously, there is no limit to the number of tests that could be combined to improve the ability to detect and discriminate bacteria or properly diagnose a population – assuming those tests could all be performed using one obtained clinical specimen. Combining a test (which in our case would be a numerical analysis of the spectral data) with very high sensitivity and a lower specificity identifies the true positive cases. Once these have been identified only false positives and true negatives remain, there should not be any false negatives if 100% of the true positives are accounted for. A second test can then be conducted on the true positive cases utilizing a lower sensitivity and high specificity to subsequently identify the false positives among the subpopulation that initially tested positive. The

combination of the results would then provide 100% of all the true negative cases as well.

My work has been conducted using the combination of two chemometric algorithms: Discriminant Function Analysis (DFA) and Partial Least-Squares Discriminant Analysis (PLS-DA) to analyze LIBS bacterial spectra. Both analysis techniques are based on the ability to identify LIBS data using a pre-compiled library of many samples collected over time. This allows for the detection, identification and discrimination of different known and unknown bacterial strains and species. The collected spectral data are organized in a table of values that form a matrix as shown in Figure 4.1. The data include the file names labeled to include species, laser shot number and the respective date the data were acquired. The data also include the normalized emission intensity values of the 164 independent elemental or ratio combination variables.

Label	Class	C247 (c)	P213 (p1)	P214 (p2)	P253.3 (p3)	P253.5 (p4)	P255.3(p5)	P255.4 (p6)	Mg279 (mgii1)	Mg279.5 (mgii2)	Mg279.8 (mgii3)	Mg280 (mgii4)	Mg277 (mgi1)	Mg285 (mgi)	Ca317 (caii2)	Ca393 (caii3)	Ca396 (caii4)	Ca422 (caii1)	Na588 (na1)	Na589 (na2)	*p1/c*
5922ecoliFifth_00	1	0.2918	0.0063	0.0032	0.0007	0.0018	0	0.0004	0.0059	0.16575	0.0099	0.0874	9E-04	0.0108	0.0182	0.2503	0.134	0.0138	0.0124	0.0056	0.0217
5922ecoliFifth_00	1	0.3353	0.0101	0.0026	0.0005	0.002	0	0.0005	0.0048	0.15715	0.0086	0.0805	0.001	0.0109	0.0182	0.2322	0.1279	0.0096	0.0097	0.0069	0.0301
5922ecoliFifth_00	1	0.281	0.0086	0.0051	0.0004	0.0015	0	0.0004	0.0054	0.17597	0.0086	0.0985	9E-04	0.0146	0.0177	0.2253	0.1189	0.0143	0.0134	0.01	0.0307
5922ecoliFifth_00	1	0.1449	0.0059	0.0026	0.0003	0.0012	0	0.0004	0.0077	0.21285	0.0146	0.1262	0.001	0.009	0.0182	0.3241	0.1354	0.0048	0.0053	0.0037	0.0407
5922ecoliFifth_00	1	0.3933	0.0087	0.0049	0.0011	0.002	0	0.0004	0.0031	0.13527	0.0065	0.074	1E-03	0.0062	0.0186	0.2113	0.111	0.0068	0.0102	0.0062	0.0222

Figure 4.1: Example of collected spectral data from the bacteria LIBS library. The first column contains the file name for the spectrum, the second column contains a numerical species label for the known or unknown class. The remaining columns show a portion of the RM3 model including the 19 elements of interest along with the first of the 145 ratios used to represent the spectral data.

The data are then used to form a model to illustrate the internal validation of the test along with the ability of the test to accurately classify unknown groups of data through external validation. External validation is conducted by removing subgroups of the library data and then recreating the model to classify the removed group based on all of the remaining sample data, which can include several other species of bacteria, dilutions of the removed group, sterile water samples or different strains of the same species. There are variations in data sets based on the growth, handling,

preparation, mounting procedure, shot conditions, temperature and much more. These variations between each filter group of data are minimized as the data library is increased. It is expected that each group of shots should contain similar characteristics and that with enough samples of each type of bacteria that overall trends improve classification accuracy. External validation uses chemometric algorithms to graphically illustrate the variations in the data groups to ensure that the spectral data acquired over longer periods of time are reproducible on a day-to-day and a shot-to-shot basis.

After classification with DFA and PLS-DA has been conducted using external validation, the sensitivity and specificity values of each test can be calculated and displayed using a truth table. Truth tables contain the weighted true positive, false positive, true negative and false negative values for each data group externally validated against the entire bacteria spectral library. In order to develop LIBS as a rapid point of care diagnostic tool, the goal is to optimize our procedure, preprocessing and chemometric analysis to achieve an overall test with a high level of sensitivity and specificity. It is important to correctly identify all patients that are infected with pathogenic bacteria and to discriminate the bacteria accurately to allow for proper treatment while minimizing any false positive cases. The following sections will describe our classification algorithms in more detail.

4.4 Discriminant Function Analysis (DFA)

DFA is a multivariate analysis of variance between sample data. Multiple groups of data are classified using a set of independently chosen variables. This can be done for a very large number of different groups or with just two groups. Based on an initial library of collected spectral data, the DFA creates a discriminant function to maximize variance between an unknown row of data and all of the classified spectral data. The DFA then calculates a discriminant function score by comparing how closely the unknown data resembles any of the other known groups contained in the library using that function. This is done by projecting the unknown data onto lines connecting the midpoint of each group contained in the precompiled library. Take the

simplest case, for example in a classification between two groups A and B, the discriminant score can be given by the following equation:

$$D_{AB} = (\bar{X}_A - \bar{X}_B) \cdot S^{-1} \cdot X^T - 1/2\ (\bar{X}_A - \bar{X}_B) \cdot S^{-1} \cdot (\bar{X}_A + \bar{X}_B) \qquad \text{(Equation 1)}$$

Where X is the unknown group being classified and $\bar{X}_A$ and $\bar{X}_B$ are the average vectors for the independent variables in group A and B respectively. S represents the pooled variance-covariance matrix for the groups A and B. The first term of the equation determines a score value while the second term scales the value to determine whether the overall score is positive or negative. A positive indicates that the unknown group most closely resembles group A, while a negative score most closely resembles group B. The S matrix accounts for outlier data more effectively and considers points in group A or B that are more spread from the majority of data as opposed to a well clustered data group.

For a model containing N groups, a total of N – 1 discriminant scores are required to classify an unknown group. The DFA generates an N – 1 dimensional space in which an unknown group lies between all of the other known groups. The minimum distance formed between the unknown group and any of the other groups indicates which group the unknown data resembles with the highest certainty. An unknown data set will be classified to one of the other groups regardless if any of the other groups are the same, in this case the algorithm will choose the group with the least variation from the unknown data. For example, a filter of sterile DI water may classify as *E. coli* when tested with DFA against 5 different types of bacteria because it must be classified as one of the groups in the analysis. The discriminant functions are ordered numerically based on the weightings they attribute to the overall variance between data groups. Discriminant function 1 (DF1) accounts for the largest fraction of the variance between the groups, while DF2 and each subsequent function represents lower degrees of variance between the groups. In some cases, the first couple of discriminant functions contain almost the entirety of the variation between groups and including the remaining functions does not contribute to the classification accuracy of the DFA. If there is a significant difference between groups, the discriminant functions will assign discriminant scores to calculate the correlations between the data points. Figure 4.2 shows a discriminant function analysis plot

between 5 genera of bacteria and DI water samples. In this plot, discriminant function score one (DF1) accounted for 87.0% of the variance in the data of the six groups, and DF2 accounted for 11.3% of the variance. All N-1 DF scores are always calculated, but we often choose to only display the first two in a two-dimensional plot for clarity. Obviously, data with more than three scores cannot be plotted in any physical way.

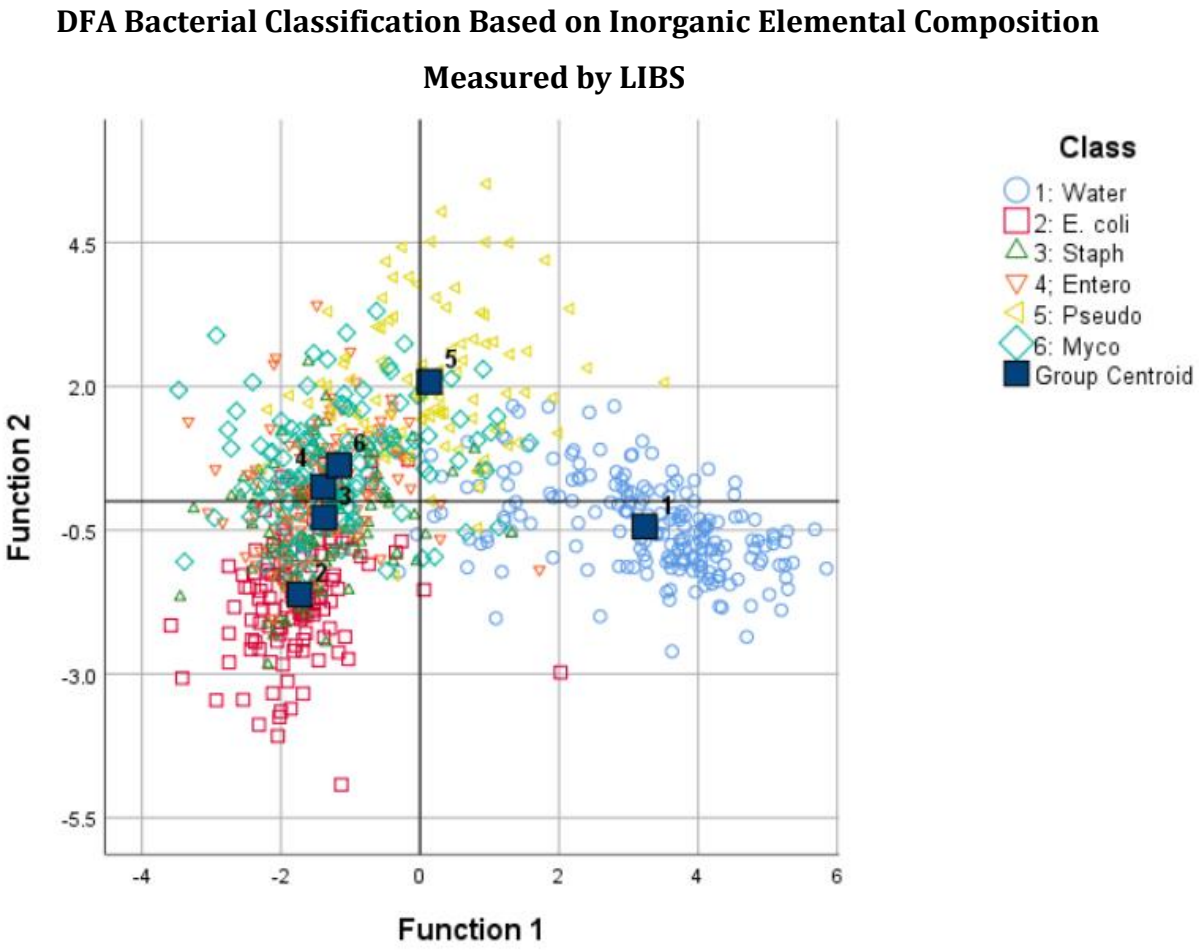

Figure 4.2: A plot showing the first two discriminant function scores in an analysis made on LIBS spectra obtained from sterile deionized water, Escherichia coli, Staphylococcus epidermidis, Enterobacter cloacae, Pseudomonas aeruginosa, and Mycobacterium smegmatis. DF scores three through five are not shown.

In order to conduct a DFA on a data library there must be a minimum number of data sets equal to the number of independent variables. For a more accurate classification it is optimal for the system to contain more data samples than variables. This means that for our RM3 model of 164 independent variables that a minimum of

164 sample points should be included in any DFA model. Best practice would include at least 10 times as many sample points as variables. Because the statistical DFA approach always assumes a Gaussian probability distribution of data, in order for discriminant function analysis to work properly the data must also be normally distributed. The presence of extremely random data or outliers in our bacteria samples lower the effectiveness of the functions to identify variance in groups of data. Because DFA is highly sensitive to points that are not well contained, an entire function could be wasted to account for one or two bad data points such as laser ablation of a contaminant on a filter or a blank shot. It is also important that the variables are independent from one another. There cannot be multicollinearity between variables and none of our 164 chosen emission lines or ratios could be sums or multiples of one another. Due to these factors DFA performed superior to PLS-DA when identifying unknown organisms at the genus-level and acts as a potential means of classification and discrimination of LIBS spectral data. All DFA was performed using SPSS Statistics v.25 (IBM, Inc.).

4.5 Partial Least-Squares Discriminant Analysis (PLS-DA)

Partial least squares is a multivariate linear regression analysis of spectral data. PLS-DA uses latent variables (LVs) that act as predictor values, in order to construct calibration curves. The number of latent variables used to express the variance between data sets can be suggested by the algorithm or chosen manually using our current software. PLS-DA was performed using PLS_toolbox v.8.7.1 combined with Matlab 2016b v.9.1 (Eigenvector Research, Inc.). Several data models can be generated with different numbers of LVs to produce a range of test results in order to verify classification results. Latent variables act by maximizing the variance between inter-class differences rather than variance between each individual sample. Rather than comparing variations between multiple groups and determining which group an unknown data set resembles, this chemometric technique statistically calculates a single predictor score for each member of the unknown data set during discrimination. These scores provide a ‘yes’ or ‘no’ prediction classification by PLS-

DA with a number score such as 0 and 1 or +1 and -1 to indicate which class the unknown member belonged to. This gives an advantage over DFA when trying to identify whether an unknown bacterium belongs to a specific class.

The linear regression of the PLS is combined with Bayesian statistics in order to construct a threshold to divide the two groups, and this is really the key to PLS-DA. The unknown group is tested once against each class individually to identify which groups the data corresponds to. If the unknown data point is assigned a predictor value above the selected threshold it tests positive, while a value below the threshold gives a negative result. The additional advantage of this type of regression is that the unknown group might produce a null result as opposed to DFA having to commit to at least one of the available classes. This is a unique feature that allows the PLS-DA to highlight sample data that does not classify as a member of any of the groups contained in the spectral library. This is particularly useful in the event that a bacterial sample has become contaminated or another variation in the preparation or mounting procedure has occurred, or if the bacterial species in the test has never before been encountered and is not contained in the pre-compiled library. The unclassified data can then be studied further to give a more in-depth analysis into potential anomalies. This is crucial towards maintaining a robust library that represents each species correctly in order to accurately classify newly tested specimens. Figure 4.3 shows a partial least squares analysis plot between 4 genera of bacteria.

PLS-DA Bacterial Classification Based on Inorganic Elemental Composition Measured by LIBS

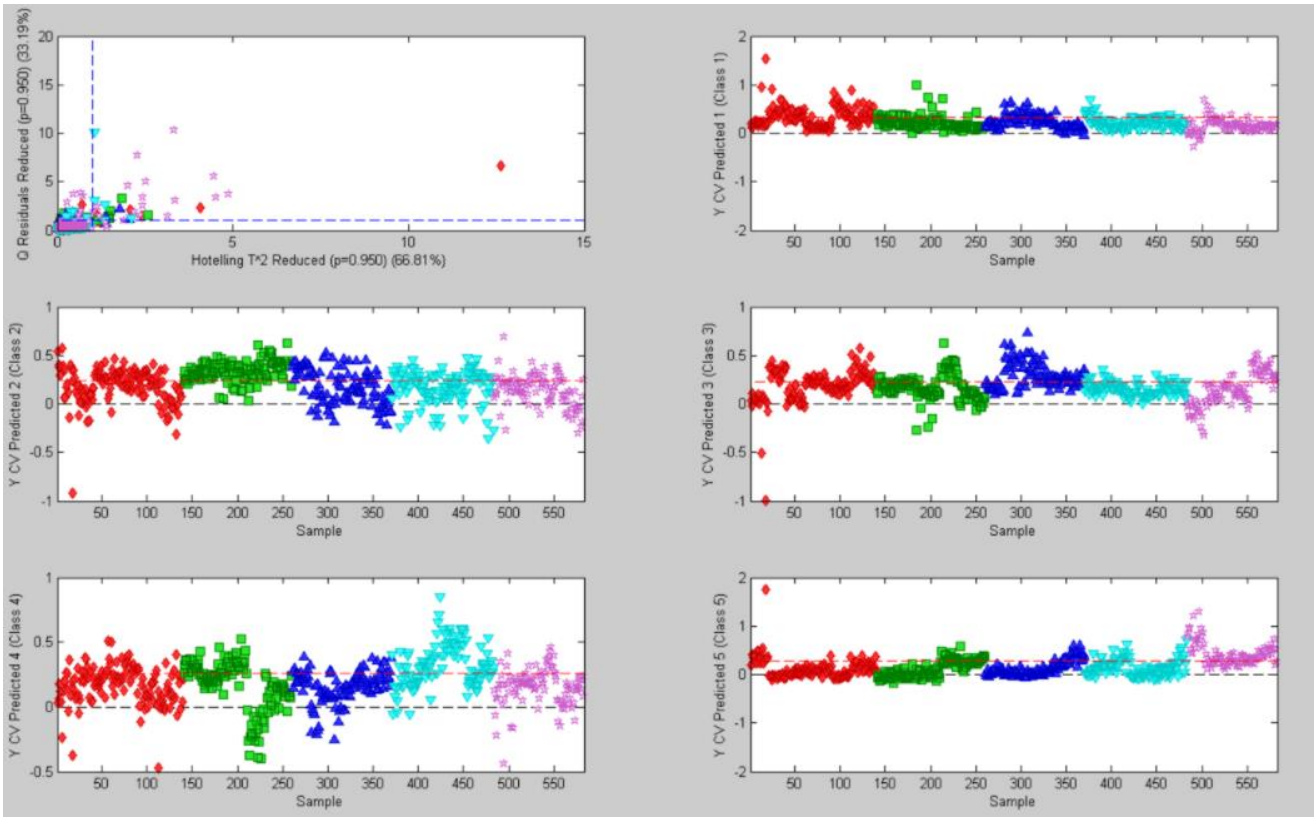

Figure 4.3: Example of PLS-DA discrimination of LIBS spectral data obtained from Escherichia coli (red-class 1), Staphylococcus epidermidis (green-class 2), Pseudomonas aeruginosa (blue-class 3), Enterobacter cloacae (aqua-class 4), and Mycobacterium smegmatis (pink-class 5). In this test, each individual class is classified with a Predictor score of "1" and all other types of bacteria are classified with a Predictor score of zero. The Bayesian threshold for classification is indicated by the dashed red line. All data points subsequently tested that possessed a predictor score greater than the value of the Bayesian threshold were classified as that class of bacteria.

Similar to DFA in order to conduct a PLS-DA on a data library there must be a minimum number of data sets equal to the number of independent variables. Again, for a more accurate classification it is optimal for the system to contain many more data samples than variables to avoid overfitting when constructing the discrimination model. This overfitting of data can cause latent variables to assign higher rates of false positives during classification. Adjusting the number of LVs to an optimal value can reduce the number of unclassified and misclassified spectra. Overall PLS-DA performed better for highly similar spectra and was superior to DFA when identifying unknown organisms at the species or strain level. Our results support PLS-DA as a

potential model that captures enough spectral information during LIBS in order to provide robust classification and discrimination based on elements of interest and ratios of emission lines. An in-depth comparison of the two techniques as performed in our lab but done with data obtained with a different experimental method than is described in this thesis has previously been published.[98]

4.6 Truth Tables and Initial Discrimination Results

Spectra of each bacterial species were collected during LIBS ablation on nitrocellulose filtration media using a swabbing collection technique combined with a mounting protocol that utilized the centrifuge insert and custom fabricated cone for concentrating dilute samples, to build a spectral library database. The data sets were collected over 3 semesters, approximately 12 months, to account for slight variations in sample preparation. This precompiled library of approximately 1665 spectra, were classified using discriminant function analysis and partial least-squares discriminant analysis combined with external validation. The library was analyzed to determine the quality of each classification technique and to determine whether a single algorithm was the optimal choice or if combining the techniques provided more of an advantage in discrimination of the bacteria. The chemometric algorithms resulted in a sensitivity of 66.37% and a specificity of 81.82% using DFA and a sensitivity of 65.78% and a specificity of 79.70% using PLS-DA when classifying a five-genus library comprised of *Escherichia, Pseudomonas, Staphylococcus, Mycobacterium* and *Enterococcus.* These initial discrimination results did not provide a measurable difference in the classification or discrimination ability of DFA and PLS-DA. The results recorded in truth tables can be shown in Table 4.1 and Table 4.2 below.

Table 4.1: Truth Table from a DFA 5 class test with overall sensitivity and specificity values

Escherichia	Cal	CV	***Staphylococcus***	Cal	CV
Sensitivity	0.78	0.73	Sensitivity	0.76	0.63
Specificity	0.85	0.85	Specificity	0.79	0.79
Mycobacterium	Cal	CV	***Pseudomonas***	Cal	CV
Sensitivity	0.54	0.53	Sensitivity	0.81	0.60
Specificity	0.83	0.82	Specificity	0.86	0.85
Enterobacter	Cal	CV	**DFA Results**		
Sensitivity	0.79	0.67	**Sensitivity: 63 ± 7%**		
Specificity	0.78	0.78	**Specificity: 82 ± 3%**		

Table 4.2: Truth Table from a PLS-DA 5 class test with overall sensitivity and specificity values

Escherichia	Cal	CV	***Staphylococcus***	Cal	CV
Sensitivity	0.50	0.49	Sensitivity	0.89	0.86
Specificity	0.85	0.85	Specificity	0.63	0.62
Mycobacterium	Cal	CV	***Pseudomonas***	Cal	CV
Sensitivity	0.67	0.66	Sensitivity	0.66	0.61
Specificity	0.84	0.83	Specificity	0.74	0.73
Enterobacter	Cal	CV	**PLS-DA Results**		
Sensitivity	0.65	0.62	**Sensitivity: 65 ± 8 %**		
Specificity	0.76	0.76	**Specificity: 76 ± 12%**		

Combining DFA followed by PLS-DA could be the next step to improve classification as the spectral library was efficacious in both chemometric techniques. Performing both techniques simultaneously would allow for two independent forms of discrimination to verify the classification of unknown bacteria spectra. The accuracy of an external validation can be improved by training the data library using objective data rejection techniques. These techniques are used to remove outliers such as spectra with unacceptably low or high intensity values, ones that contain contaminant materials or spectra that do not classify correctly. These preprocessing methods and data rejection methods will be discussed in more detail in Chapter 6.

Table 4.3: Regularly observed spectral lines of interest present in bacterial LIBS spectra

Elemental Symbol	Emission Line Wavelength (nm)	Variable Name
C	247.856	c
P	213.618	p1
P	214.914	p2
P	253.398	p3
P	253.56	p4
P	255.326	p5
P	255.491	p6
Mg	279.079	mgii1
Mg	279.553	mgii2
Mg	279.806	mgii3
Mg	280.271	mgii4
Mg	277.983	mgi1
Mg	285.213	mgi2
Ca	317.933	caii2
Ca	393.366	caii1
Ca	396.847	caii3
Ca	422.673	cai1
Na	588.995	na1
Na	589.593	na2

References

[90] Samuels, A. C., DeLucia, F. C., McNesby, K. L., & Miziolek, A. W. (2003). Laser-induced breakdown spectroscopy of bacterial spores, molds, pollens, and protein: initial studies of discrimination potential. *Applied optics*, *42*(30), 6205-6209. https://doi.org/10.1364/AO.42.006205

[91] Baudelet, M., Yu, J., Bossu, M., Jovelet, J., Wolf, J. P., Amodeo, T., ... & Laloi, P. (2006). Discrimination of microbiological samples using femtosecond laser-induced breakdown spectroscopy. *Applied physics letters*, *89*(16), 163903. https://doi.org/10.1063/1.2361270

[92] Lewis, D. E., Martinez, J., Akpovo, C. A., Johnson, L., Chauhan, A., & Edington, M. D. (2011). Discrimination of bacteria from Jamaican bauxite soils using laser-induced breakdown spectroscopy. *Analytical and bioanalytical chemistry*, *401*(7), 2225. https://doi.org/10.1007/s00216-011-5274-y

[93] Diedrich, J., Rehse, S. J., & Palchaudhuri, S. (2007). Escherichia coli identification and strain discrimination using nanosecond laser-induced breakdown spectroscopy. *Applied Physics Letters*, *90*(16), 163901. https://doi.org/10.1063/1.2723659

[94] Merdes, D. W., Suhan, J. M., Keay, J. M., Hadka, D. M., & Bradley, W. R. (2007). The investigation of laser-induced breakdown spectroscopy for detection of biological contaminants on surfaces. *Spectroscopy-Springfield then Eugene then Duluth-*, *22*(4), 28.

[95] Marcos-Martinez, D., Ayala, J. A., Izquierdo-Hornillos, R. C., de Villena, F. M., & Caceres, J. O. (2011). Identification and discrimination of bacterial strains by laser induced breakdown spectroscopy and neural networks. *Talanta*, *84*(3), 730-737. https://doi.org/10.1016/j.talanta.2011.01.069

[96] Manzoor, S., Moncayo, S., Navarro-Villoslada, F., Ayala, J. A., Izquierdo-Hornillos, R., de Villena, F. M., & Caceres, J. O. (2014). Rapid identification and discrimination of bacterial strains by laser induced breakdown spectroscopy and neural networks. *Talanta*, *121*, 65-70. https://doi.org/10.1016/j.talanta.2013.12.057

[97] Putnam, R. A., Mohaidat, Q. I., Daabous, A., & Rehse, S. J. (2013). A comparison of multivariate analysis techniques and variable selection strategies in a laser-induced breakdown spectroscopy bacterial classification. *Spectrochimica Acta Part B: Atomic Spectroscopy*, *87*, 161-167. https://doi.org/10.1016/j.sab.2013.05.014

[98] Malenfant, D. J. (2016). *Influences on the Emissions of Bacterial Plasmas Generated through Nanosecond Laser-Induced Breakdown Spectroscopy*, Master's thesis, University of Windsor. https://scholar.uwindsor.ca/etd/5843

Chapter 5: LIBS Detection

5.1 Bacteria Spectral Library

The use of the current preparation, deposition, and testing methods described in previous chapters for the construction of a bacterial LIBS spectral library is ongoing. The goal of building a robust data library is that any bacterial pathogen contained in the library could be collected and tested with LIBS by comparing it to all the spectra in the library using chemometric analysis. To date, the library contains a total of 1665 bacteria LIBS spectra consisting of serial dilutions of *Escherichia coli, Staphylococcus aureus, Pseudomonas aeruginosa, Mycobacterium smegmatis* and *Enterobacter cloacae.* The number of each species tested thus far are outlined in Table 5.1. The library also contains 260 DI water LIBS spectra and 250 blank nitrocellulose filter LIBS spectra. These bacteria and water samples were tested over a span of 2 years of data acquisition. The concentration of our initially collected stock samples is unknown and cannot be determined without comparing the intensities of different relative concentrations.

Because the true concentration of our initial cultured samples is unknown, we produce dilutions of the stock sample in terms of titer for testing. Titer is a standard method used to measure dilutions of a biological sample expressed as a ratio of the dilutant to that of the total suspension volume. The initial suspensions were defined to be a concentration of 1 (A.U.) and used to produce five titers. Serial dilutions in DI water were performed to generate suspensions of concentrations of c = {1/5, 1/10, 1/50, 1/100 and 1/500} to test with LIBS and to add to the library. Any sample with a concentration above a 1/5 titer contained too many bacterial cells and physically clogged the metal cone used to deposit the cells onto the nitrocellulose filters. Even after multiple centrifugations, the large number of cells clumped together, and the water could not be filtered through the insert to isolate the cells.

Table 5.1: Current bacterial LIBS spectra included in data library

	LIBS Spectral Data Library	
Bacteria Species	Number of Acquired Bacteria Spectra	**Total**
Escherichia coli	797	**1665**
Mycobacterium smegmatis	430	
Staphylococcus aureus	148	
Pseudomonas aeruginosa	160	
Enterobacter cloacae	130	
Blank	Number of Acquired Bacteria Spectra	
Deionized water	260	**510**
Nitrocellulose Filter	250	

A majority of the bacteria LIBS spectra contained in the library are *E. coli.* This species was the most commonly tested pathogen in past research and is the least challenging to vortex back into solution when producing various serial dilutions. Other species of bacteria such as the *M. smegmatis* are harder to separate in solution. *E. coli* cells were also prepared in a large number of samples to produce a bacterial curve of growth, detailed in Chapter 6. A majority of the concentrations contained in the bacterial spectral library are 1/5 dilutions, and lower titers of *Pseudomonas, Enterococcus and Staphylococcus* cells are required to evenly distribute the spectra in order to improve classification accuracy and determine the limit of detection and the limit of identification of our current technique. If these results are promising, LIBS spectra from a variety of medically relevant pathogens can be collected to create a more extensive bacterial spectral library.

5.2 Limit of Detection and Limit of Identification

The limit of detection and the limit of identification are two important values related to the LIBS technique that need to be investigated in the next stage of developing LIBS as a realistic diagnostic tool for bacterial discrimination. The LOD and LOI are very difficult to determine quantitatively because the cell concentrations of the serial dilutions are not known. For the purposes of determining the limit of detection, only *E. coli* is being explored, as other bacteria are of similar volumes to

within the same order of magnitude. The limit of detection will be calculated by constructing calibration curves for many serial dilutions of *E. coli.*

A calibration curve measures the analytic signal plotted as a function of the amount of analyte present in a sample, where the amount of analyte is represented as a bacterial concentration. Bacteria cells are not dissolved in DI water solutions, they are dispersed to form bacterial suspensions. The concentration of these bacterial suspensions is characterized by the number of cells in colony forming units (CFU) suspended in a 1 mL volume of water. Therefore, a quantity such as 5×10^7 CFU/mL is an example of an appropriate bacterial concentration. In this work the samples are prepared by centrifuging the suspension and passing it through a nitrocellulose filter to deposit the suspended bacterial cells. In these cases, the volume of water is immaterial. 5×10^7 CFU suspended in 1 mL or in 10 mL would yield identical signals after being passed through the filter and being tested with LIBS. It is therefore our standard practice as a group to report the "concentration" merely as the quantity of bacteria, in CFU.

In LIBS, a calibration curve typically has a linear dynamic range, wherein the signal from a line of interest has a simple linear relationship to the amount of material ablated, typically measured as a mass or a concentration. This is the regime in which the LOD can be calculated. A calibration curve can be formed by plotting the total spectral intensity of the *E. coli* samples, defined as the sum of the area under the curve of the intensities of the emission lines used in bacterial classification against the relative concentrations. The values must then be scaled to true concentrations in terms of CFU/mL by performing optical densitometry measurements on the dilutions of the initial stock suspension. By observing the uniformity of the bacterial depositions for each dilution, the true concentrations could be converted to a value for the number of CFU ablated per laser pulse.

The bacterial LOD with LIBS can be improved by maximizing the number of bacterial cells that are ablated in a single laser shot. The LOD in terms of bacterial detection with LIBS would be defined as the minimum number of CFU ablated per laser pulse required to produce a LIBS spectrum with a 99.7% (3σ) confidence that the measured signal was due to bacteria and not random signal noise of a sample with

no bacteria, known as a blank spectrum.[99] This does not mean that the species will remain differentiable at this concentration. The smallest number of bacteria cells required to accurately discriminate different species is known as the limit of identification, which is expected to be a higher concentration of CFU than the limit of detection.

The sensitivity and specificity of this technique for classifying and identifying bacteria must be determined to calculate the LOI. Bacterial dilutions can be analyzed via chemometric algorithms to determine the sensitivity and specificity for each corresponding concentration. Preliminary results for the cross validation of serial dilutions of *E. coli* are shown in Table 5.2. PLS-DA discriminations were carried out for filters of 1/5, 1/10, 1/50, 1/100 and 1/500 dilutions of *E. coli* and while the external validation results are still required, the initial results are very promising. The cross validated sensitivity and specificity values suggest titers below 1/500 are required to determine the current LOI of our detection technique. Weaker dilutions of bacteria suspensions are to be tested next in order to identify the value of CFU required to maintain a sensitivity and specificity value above 50%. At a value of 50%, the bacteria are no longer discernable from other species or blank filtration media.

Table 5.2: Cross validated results for PLS-DA discriminations of serial E. coli dilutions

E. coli Dilution	**Sens (CV)**	**Spec (CV)**
1/5	0.96	0.98
1/10	0.89	0.94
1/50	0.88	0.92
1/100	0.92	0.87
1/500	0.91	0.93

Several methods to improve the measured LIBS signals and improve the sensitivity and specificity values are detailed in the following sections and later in Chapter 6.

5.3 Latent Variable Study

As described in Chapter 4, partial least squares is a multivariate linear regression analysis of spectral data that uses latent variables as predictor values, in order to construct calibration curves. The latent variables are used maximize the variance between classes rather than the variance between each individual sample. The 1/5 dilutions of *Escherichia coli, Staphylococcus aureus, Pseudomonas aeruginosa, Mycobacterium smegmatis* and *Enterobacter cloacae* were tested using PLS-DA one set at a time against a library of DI water spectra and the remaining bacteria spectra. The sensitivities and specificities were then recorded for each classification. Typically, the number of LVs is chosen by the program when performing an external validation of a data set using PLSDA, usually on the order of 3 to 5. In this study, the effect of controlling the number of LVs was investigated to determine if using a larger number would improve the classification or cause overfitting of the differences in spectral data. Several classifications were conducted using PLS-DA for each case between 1 and 20 latent variables. It is important to note that this external validation is strictly for a true two class test and only two classes can be tested using this technique at a time.

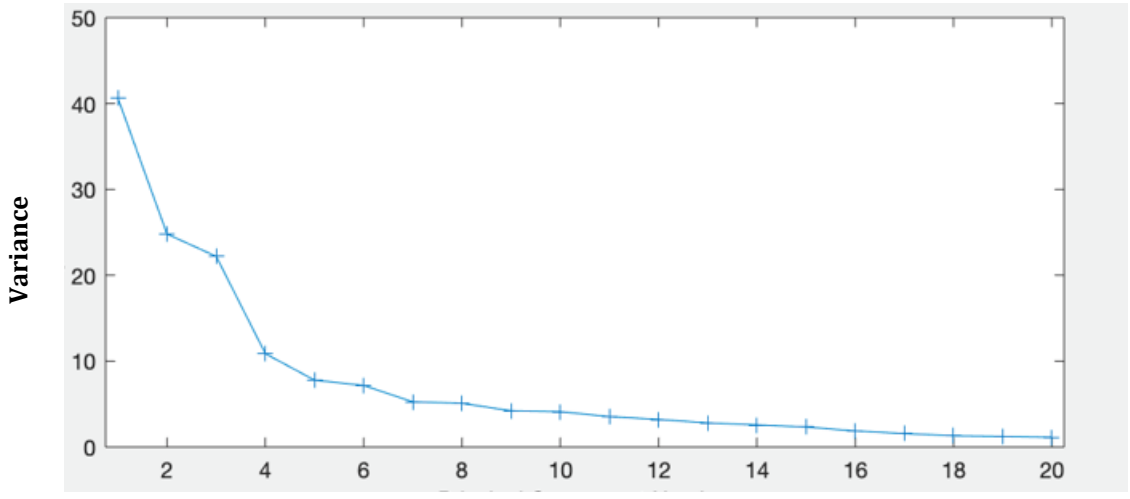

Figure 5.1: The variance per latent variable. In this case the first four latent variables account for a large majority of the variance between 2 classes.

The ideal number of latent variables is subjective. The optimal number of LVs was chosen as the number at which the sensitivity values began to level out. An example of the variance for each latent variable in a classification using 20 LVs is shown in Figure 5.1. Class 1 was defined as one type of bacteria, chosen as the test subject. Class 2 was defined as all the other types of bacteria and/or water. The sensitivity for Class 1 can be directly inferred by the ratio between the number of true positives and the total number of test data points in Class 1. The sensitivity as a function of LVs fluctuated a great deal and did not provide consistent conclusions between different species of bacteria. After averaging the results, 15 was the chosen number of latent variables to use moving forward, however several other pre-processing techniques were explored before pursuing the study of latent variables further. These pre-processing techniques and studies are described in Chapter 6.

5.4 Dual Stage Centrifugation – Separation of Larger Components

In our research, dual centrifugation refers to a two-tiered filtration technique during a single centrifugation process. The bottom of the custom centrifuge insert described in Chapter 2 was designed to have threads so that additional bases could be screwed and connected. The insert with base along with the second base fit within the centrifuge tube and can be easily combined to perform tiered filtration. Filters of different pore sizes can be directly inserted onto each bottom for the separation of cells and larger particulate matter. In the case of pure bacterial cultures, the bacteria are all of similar sizes and ideally do not contain other material or contaminants to be removed using this additional base piece. Both bases contain a central hole for the removal of excess liquid when centrifuging a suspension. Previous work was conducted by our group to remove a contaminant from bacterial samples using dual centrifugation with nitrocellulose filter papers of different pore sizes.

Bacteria are on the scale of approximately 1 μm in size, while larger cells such as red blood cells are typically between 6-8 μm in size and entire eukaryotic cells can be up to 100 μm in size.[100, 101] These larger cells and other materials are present in biological samples that would be collected from patients used for clinical LIBS testing.

The relative difference in size can be used to isolate bacteria based on their smaller size. A larger pore size filter can be strategically placed in the upper base piece to remove unwanted material while a small pore size filter can be placed on the lower base piece to capture the bacteria as the solution drains through to the bottom of the centrifuge tube.

Preliminary testing of dual centrifugation with the centrifuge insert device was conducted by a previous graduate student on bacterial suspensions that were combined with tungsten powder (10401, Alfa Aesar) that were of an average particle size of 12 μm.[102] Tungsten powder was chosen and tested by A.E. Paulick because of its biologically relevant size, while being substantially larger than bacteria cells and because tungsten lines are not observed in LIBS bacterial spectra, which makes it easily distinguishable from the elemental peaks typically observed in bacterial LIBS spectra. The tungsten peaks are contained in a group to the far left of the LIBS spectra, between 200 nm and 250 nm, which allows for easy identification to when any tungsten powder is present in ablated sample filters. Suspensions of *E. coli* with added tungsten powder were vortexed and pipetted directly into the insert device. A nitrocellulose filter with a pore size of 5 μm was positioned on the upper base piece, while a nitrocellulose filter with a pore size of 0.45 μm was positioned on the lower base piece. The entire insert device was centrifuged at 5000 rpm with 2500 g's of force for a duration of 3 minutes. After centrifugation, the filter papers were carefully removed and tested with LIBS. The tungsten powder was visually observed to be deposited upon the 5 μm filter. When tested with LIBS, tungsten emission lines were observed in the 5 μm spectra with the presence of weak bacterial emission lines. No tungsten emission lines were present in the spectra of the 0.45 μm filter.

These results indicated that the larger tungsten powder used to simulate a contaminant material was entirely removed and separated from the bacterial cells and that a majority of the bacterial cells passed through the larger pores to be captured on the second filter. After multiple trials it was also determined that approximately 10% of the bacteria cells are caught on the first filter and that a small fraction of the remaining cells also pass through the second filter. These cells that are caught on the first filter are inherent to the natural clumping of bacterial organisms.

The amount of bacteria that pass through the second filter does depend on the concentration of the initial suspension and further investigation into the approximate amount of bacteria that are not captured using a 0.45 μm pore size would have to be conducted. Different pore sizes could be strategically employed for the separation of different mixtures and the capture of various unwanted matter. One drawback of this technique is that it is not capable of separating a mixture containing different species of bacteria. The bacterial cells are too similar in size and additional methods would have to be used as this dual centrifugation technique is designed for size-based separation.

Further dual centrifugation experiments were conducted by our group on bacterial suspensions that were combined with yeast cells (*S. cerevisiae).* The yeast was grown with the goal to simulate red blood cells of 8 μm in size and assess the efficacy of the insert device to separate bacterial cells from unwanted matter that more closely resembles that of a clinical sample. This was an important proof of concept preliminary experiment to simulate collected bacteria present in the bloodstream, while blood samples could not be currently obtained to test directly. The yeast was ordered through chemical control from VWR and grown from an initial gel slant. A Sabauroud Dextrose broth powder was mixed with distilled water and heated to the point at which the broth completely dissolved in a boiling mixture. The mixture was autoclaved for 15 minutes and allowed to cool to room temperature in a sterile enclose biohood. The yeast was collected from the gel slant using sterilized inoculating loops and slowly transferred to the broth. The yeast cells were gently placed onto the broth and the broth was then transferred via glass test tubes to an incubator. The incubator was kept at 37 °C and the yeast was grown for a period of 48 hours, at which point in time the yeast would have grown to an approximate size similar to red blood cells based on yeast curves of growth from external literature sources.

The yeast cells were visibly observed on the broth medium after the growth period of 48 hours. The broth was washed, vortexed and centrifuged multiple times to remove a pellet of yeast from the rest of the material in the tube. The yeast pellet was collected and suspended in a centrifuge tube of DI water and stored within a

fridge. After preparing the yeast, samples were pipetted onto a metal plate and collected via swab in the same routine outlined for bacteria collection and deposition in Chapter 2. Yeast cells were transferred onto a nitrocellulose filter of 8 µm pore size and a nitrocellulose filter of 5 µm pore size to test the deposition effectiveness of the metal cone procedure. The filters were tested via LIBS, with 20 single accumulations (laser ablations) taken from each. Each set of 20 accumulations were added together to produce an averaged total spectrum known as an 'add all' spectrum. The two add all spectra were compared with blank filter spectra to observe the presence or absence of yeast cells. The 8 µm filter add all spectra appeared identical to the blank spectra while the yeast LIBS emission peaks that resemble bacteria LIBS emission peaks were visible in the 5 µm filter. The add all spectra of the yeast cells deposited on 8 µm filter and 8 µm filter are shown in Figure 5.2. These results suggest that some of the yeast cells were caught by the 5 µm filter and that they all passed through the 8 µm filter.

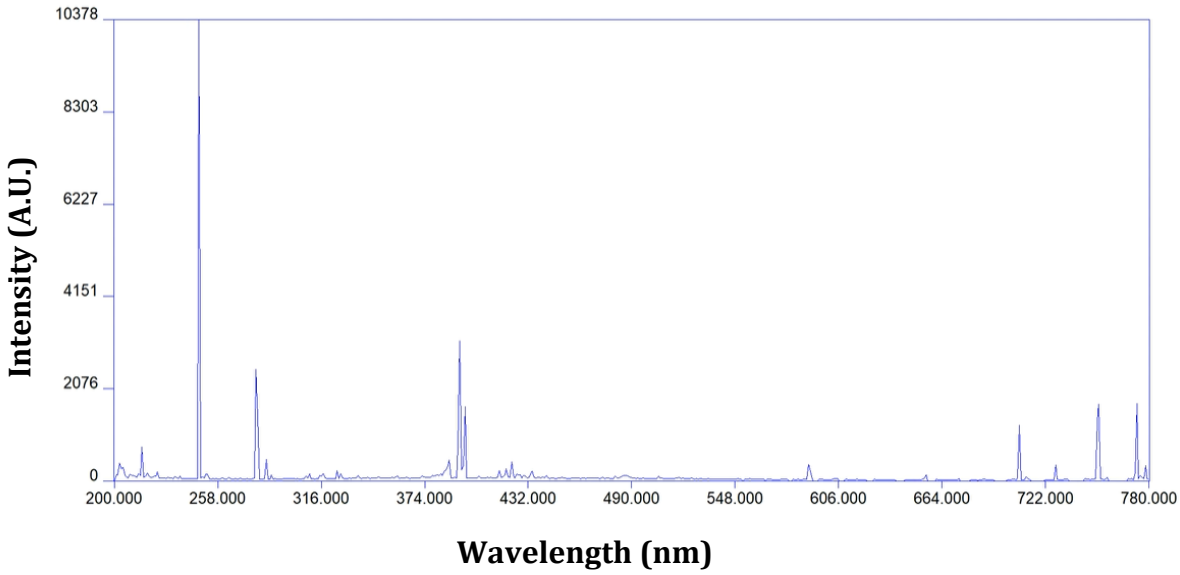

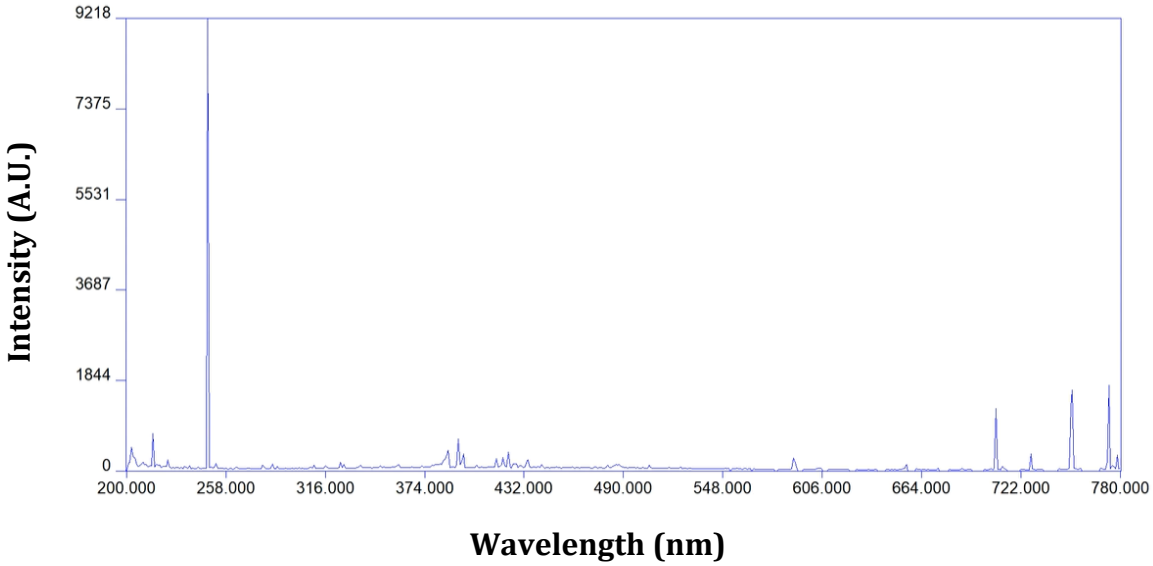

Figure 5.2: LIBS spectra of a) Yeast cells caught by the 5 µm pore size nitrocellulose filter vs b) absence of yeast cells on the 8 µm pore size nitrocellulose filter. b) Closely resembles blank spectra with no bacteria.

The yeast cells were theorized to be approximately 5 µm in size and an additional test was conducted using dual centrifugation. The yeast cells were centrifuged using a nitrocellulose filter of 5 µm pore size positioned in the upper base insert, with a nitrocellulose filter of 0.45 µm pore size positioned on the second base insert. The filters were tested via LIBS to determine whether all of the yeast cells were captured by the 5 µm filter or if some of the yeast cells passed through to the 0.45 µm filter. 10 single accumulation spectra from each were filter were taken and used to produce two totaled spectra. Less shots were taken than the previous case in order to leave an undisturbed area in the center of the filter (close to the laser ablation craters) to image with an SEM. The two add all spectrums were compared with blank filter spectra to detect bacteria signal and then imaged using the SEM. Both the 5 µm and the 0.45 µm filter spectra contained LIBS emission peaks evident of the presence of yeast cells. These results suggest that some of the yeast cells were caught by the 5 µm filter and that smaller yeast cells also passed through to be caught on the 0.45 µm filter. The SEM images are shown below in Figure 5.3 and showcase yeast cell in clumps of 5 – 7 µm in size deposited within the 5 µm nitrocellulose filter and individual yeast cells of approximately 2 µm deposited within the 0.45 µm nitrocellulose filter.

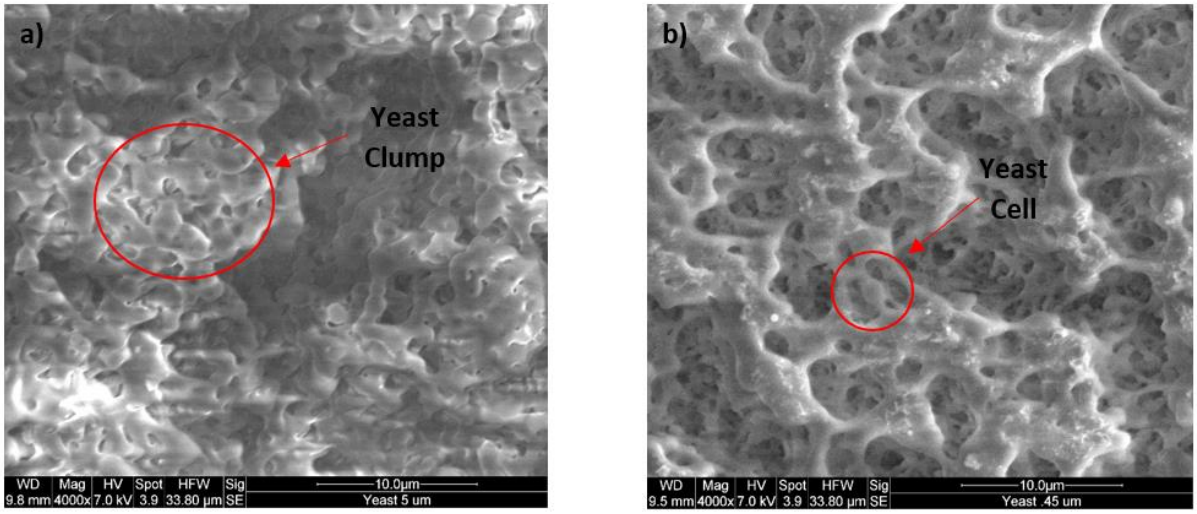

Figure 5.3: SEM images acquired of a) Budding yeast cells clustered together, caught in nitrocellulose filter with 5 µm pore size 4000x magnification. b) Individual yeast cells caught in nitrocellulose filter with 0.45 µm pore size 4000x magnification.

These results suggest that the yeast were not grown to the expected size of RBCs in the 6 – 8 µm range and after 48 hours of growth reached sizes of approximately 2 µm, however yeast cells do develop clumped formations as they bud and multiply. The size of the yeast cells is unpredictable as the size range varies greatly depending on the extent of budding, they undergo before being tested. Further testing with the technique of dual centrifugation and tiered filtration needs to be carried out for yeast cells in the presence of bacteria after the yeast cells are successfully grown to the size of RBCs and for other similarly sized biological contaminants.

References

[99] Committee, A. M. (1987). Recommendations for the definition, estimation and use of the detection limit. *Analyst*, *112*(2), 199-204.

[100] Turgeon, M. L. (2005). *Clinical hematology: theory and procedures*. Lippincott Williams & Wilkins.

[101] Size Scales of Cell Biology, Moosmosis. https://moosmosis.org/2015/09/17/size-scales-of-cell-biology/ (2015)

[102] Paulick, A. E. (2018). *Development of Laser-Induced Breakdown Spectroscopy as a Rapid Diagnostic Tool for Bacterial Infection*, Master's thesis, University of Windsor. https://scholar.uwindsor.ca/etd/7653

Chapter 6: Improved LIBS Technique

6.1 Preprocessing Motivation

The detection and identification of bacteria with LIBS are proven using more concentrated samples of bacterial cells grown in a laboratory setting, but a limit of detection that is clinically relevant must be achieved to demonstrate LIBS as a rapid diagnostic tool for patient infections. The overlying goals to accomplish this are to accurately identify and classify as small a number of bacterial cells as possible in order to improve the LOD and to also maximize the rates of true positives while minimizing the rates of false positives during classification. The bacterial LOD with LIBS has been improved by concentrating the collected cells in a smaller area on the filtration media in order to maximize the number of bacteria ablated in each laser pulse by using the custom centrifuge insert and metal cone. Another method to improve the LOD that is currently being investigated will be discussed in Chapter 7.

Figure 6.1 includes a blank sample spectrum with sterile DI water and a bacteria LIBS spectrum both deposited on a nitrocellulose filters for comparison of LIBS emission lines.

a)

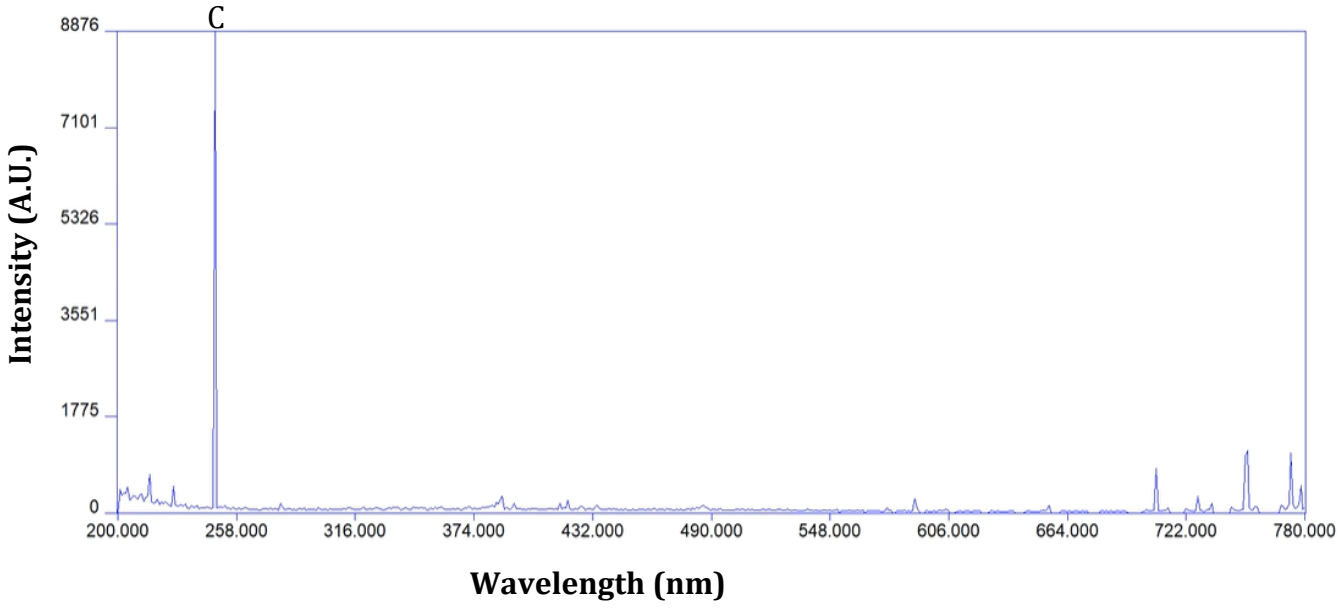

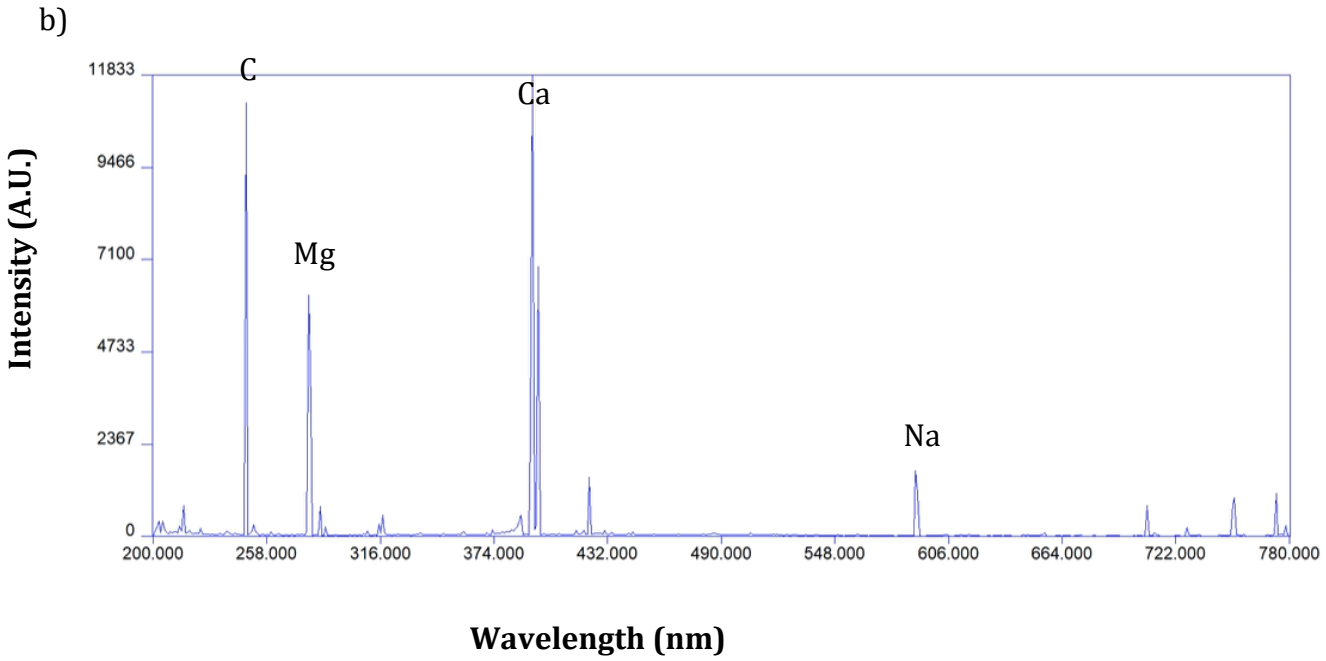

Figure 6.1: a) Blank sterile deionized water LIBS spectrum vs. b) E. coli bacteria LIBS spectrum. Key elemental emission peaks labeled.

In terms of improving classification accuracy, several pathways were explored by conducting experiments that focused on reducing background signal in the spectrum, investigating data pre-processing of samples with small amounts of bacteria, and separating contaminants or unwanted cellular material from the bacteria themselves. All the attempts to improve classification accuracy will be discussed in the sections of this chapter.

6.2 Blank Spectra Study

Laser ablation of the filter medium and other elemental contaminants yielded a non - zero background signal when a control experiment was performed on swabbed water samples in the absence of any bacterial cells. The purpose of this research was to optimize the bacterial sample preparation protocol by identifying the source of this background signal and introducing new cleaning procedures that could reduce this background signal that would mask the smaller signal from a small number of bacterial cells. Considering each step of the sample collection and mounting

procedure, potential sources of background signal that could be the result of contaminant material present on surfaces were investigated. The areas of concern were: the swab itself used for collecting the bacteria from a sterile surface, the surface of the metal plate that diluted samples of bacteria were pipetted directly onto before swabbing, and the aluminum cone used to concentrate the bacteria.

All of the sample collection conducted in this work was conducted with flocked swabs (Puritan PurFlock Ultra) which are regularly employed in clinical settings to collect specimens. This process was conducted to simulate the common practice of screening for bacterial infections by swabbing the nose, ears or throat of a patient. Flocked swabs are built up of short nylon fiber strands that efficiently draw in particulate matter through capillary action and gently release the collected material when submerged in a liquid medium such as the deionized water contained in the centrifuge tubes. Flocked swabs used to collect bacterial cells were vortexed to maximize the release of the sample. The swab itself was not ablated during the LIBS process for several reasons. The surface of the swab head is not an ideal substrate for ablation because it is nonuniform and irregularly shaped which prevents alignment or adjustment of the swab in the focus of the laser beam. The bacterial cells themselves are not concentrated to a particular area upon the swab fibers and only a small portion would be ablated. The swabs are sealed before use and are sterile prior to swabbing, however the collected samples may contain unwanted biological material that would have to be separated with additional steps before testing with LIBS.

Multiple swabs were tested to ensure the sterility of the flocked swab and to ensure that nylon fibers did not contaminate the mounted bacteria samples. The swabs were vortexed in DI water to shake off contaminants and the swab water was then deposited onto a nitrocellulose filter and tested with LIBS. The resulting spectra were compared to DI water directly deposited onto nitrocellulose filters. The swab fallout after vortexing was minimal and within error of the DI water signals and it was concluded that the flocked swabs did not contribute to background emission. Similarly, blank nitrocellulose filters were previously tested with LIBS without the

presence of any samples or water to confirm that the filtration media does not contribute to this non-zero background signal.

A small steel piece measuring approximately 2.5 cm by 2.5 cm was used to simulate the surface that bacteria could be swabbed and collected from. The metal plate that bacteria cells were directly pipetted onto before being collected with a swab was cleaned using a 10% bleach solution, rinsed with DI water, and allowed to dry before and after each sample was prepared. This cleaning step is standard and has a significant impact on reducing background signal that would be caused by leftover bacterial cells from previous samples. However, cleaning the steel substrate with other methods including stronger bleach solutions, methanol, acetone, or soap as well as the use of an ultrasonic cleaner yielded similar LIBS spectra. The conclusion was that more intensive methods of cleaning the steel plate did not reduce the background signal present in the blank spectra.

Ruling out the swab, filter, and metal plate indicated that the potential contamination causing the non-zero background signal could be from the aluminum cone. This source of elemental contaminants could be caused by exposure, corrosion, extensive use and the wearing down of the metal cone over time. 20 LIBS filter spectra were acquired for two different cone cleaning procedures and for the case of an uncleaned cone when deionized water containing no bacteria was centrifuged through the cone to compare the elemental intensities of carbon, sodium, magnesium and calcium. The metal cone was cleaned with the standard of 10% bleach solution and DI water and in addition the metal cone was also cleaned by ultra-sonicating in acetone for 2 minutes followed by ultra-sonicating in methanol for 2 minutes. The comparison of the averaged LIBS spectra collected for both cleaning procedures along with the uncleaned cone and blank filter are shown in Figure 1 below.

a) Comparison of LIBS Spectra on Nitrocellulose Filtration Media

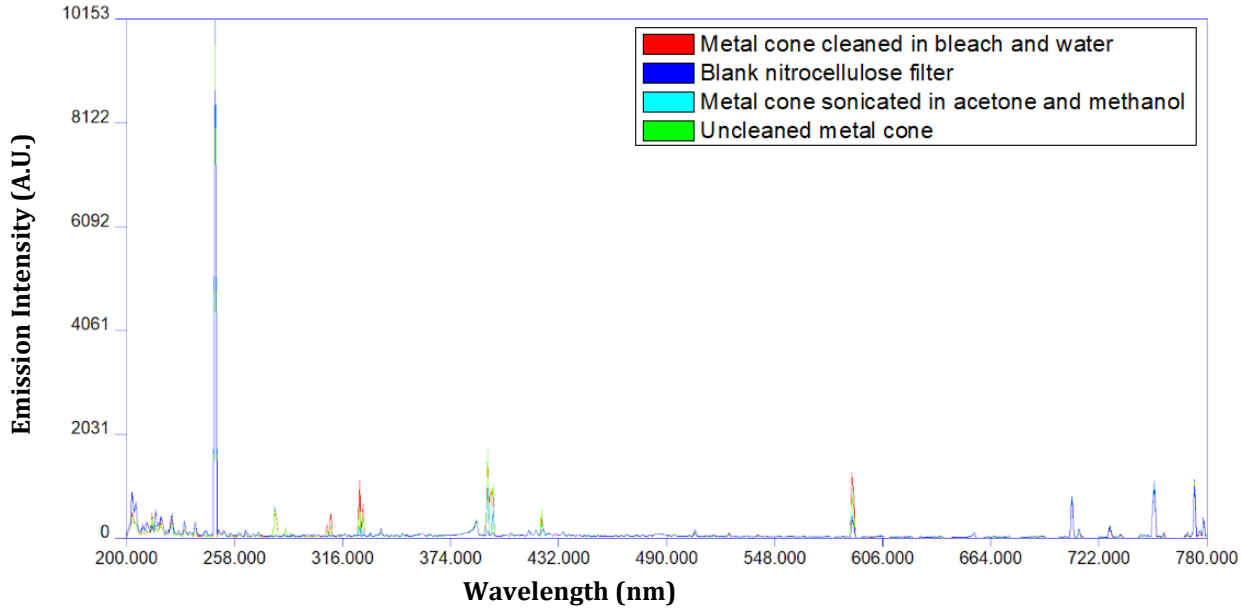

b) Mg

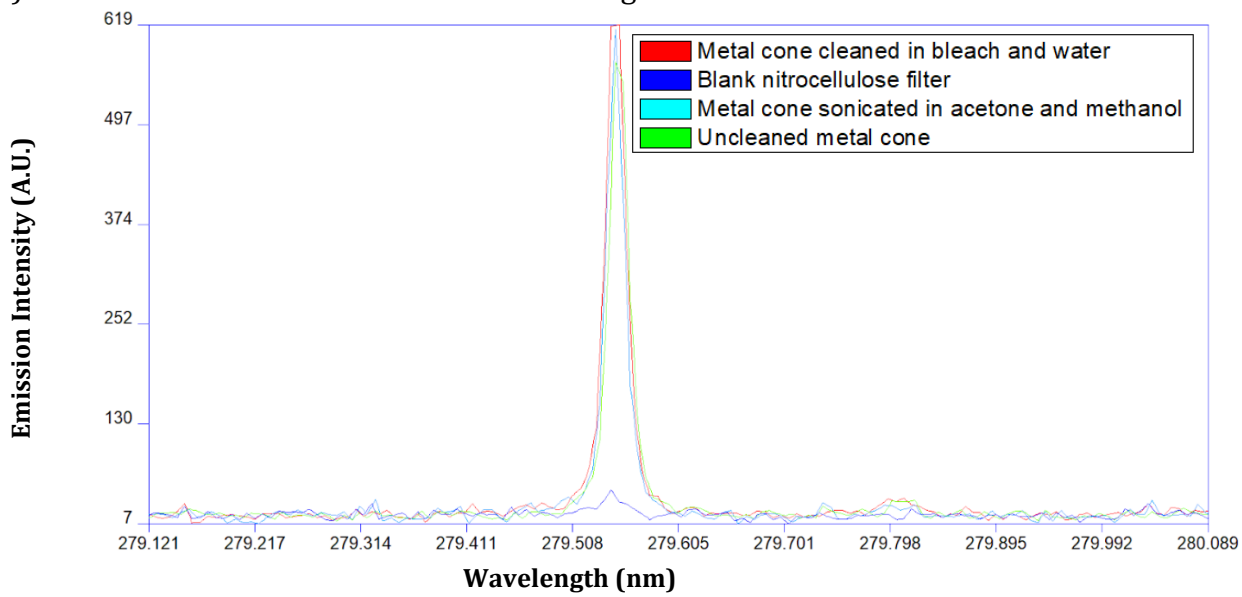

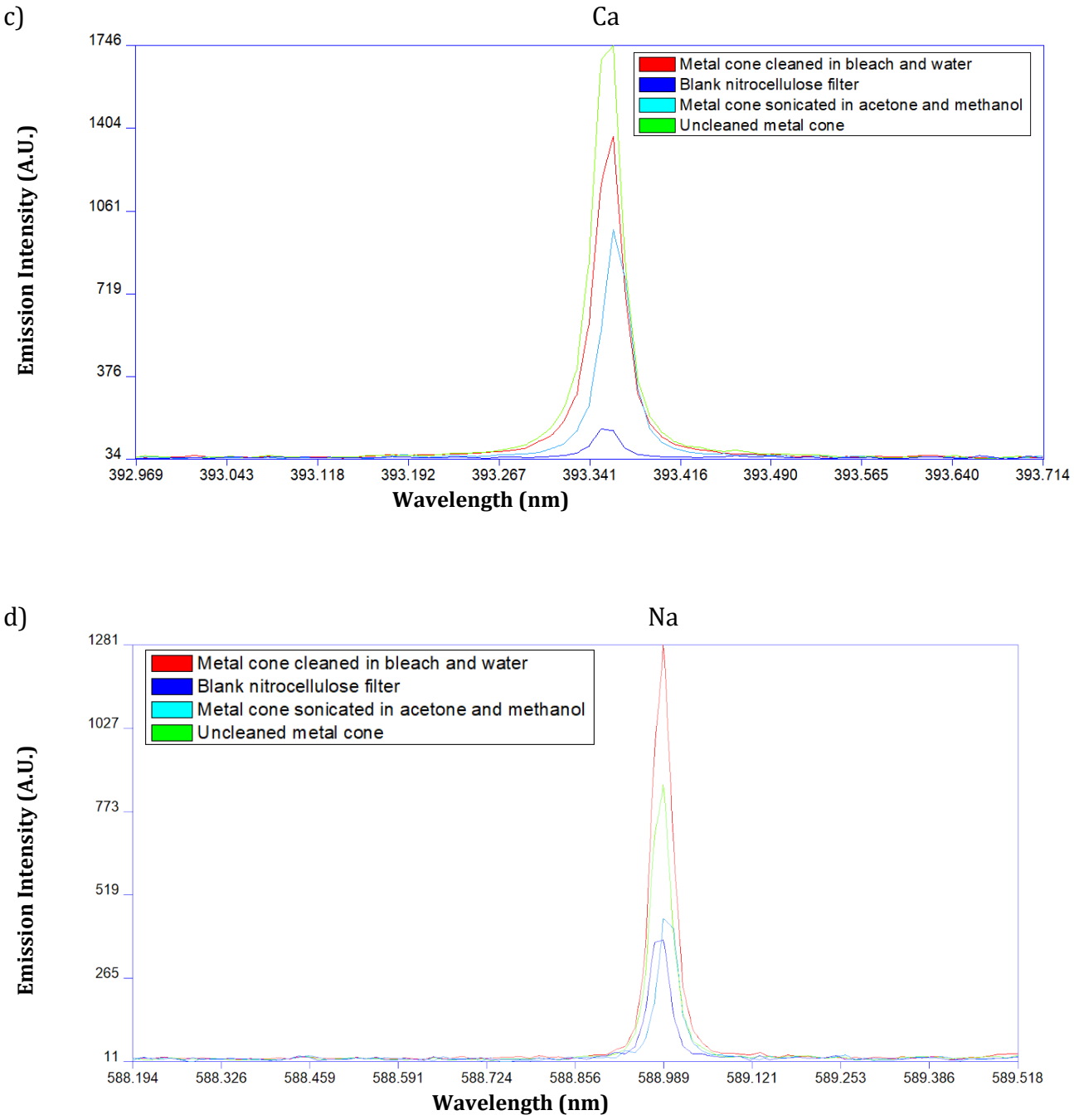

Figure 6.2: a) Cleaning the metal cone by ultrasonication in acetone and methanol shown in cyan reduced the LIBS emission intensities when compared to using an uncleaned cone shown in green or cleaning the cone in bleach water shown in red. Zoomed in view of b) magnesium peaks, c) calcium peaks and d) sodium peaks.

6.3 Water Study

In order to quantify a limit of detection for bacterial cells using LIBS, samples of *E. coli* were serially diluted and used to construct a calibration curve based on the strength of the LIBS signal intensity with respect to the various titer. A typical LIBS calibration curve exhibits a linear relationship between the signal intensity and the amount of target material ablated. Figure 6.3 depicts a cartoon version of an ideal calibration curve of growth for the LIBS spectra collected from serial dilutions of *E. coli* at 5 titers along with the LIBS spectra collected from deionized water and blank nitrocellulose filters. The spectra are averaged into a single point value and produce a simple linear relationship between the concentration and signal intensity. Blank filters and water should exhibit little to no signal while increasing the concentration of the samples should increase the signal as there is more bacteria present during ablation in higher titers. The linear dynamic range generally becomes saturated at higher concentrations because of self-absorption in the resulting laser induced plasmas. The outer shell of the LIP largely consists of cooler atoms and as photons are emitted from the plasma core, they become reabsorbed before reaching the light collection apparatus. This decrease in detected signal forms a saturation plateau for very concentrated samples in the calibration curve.

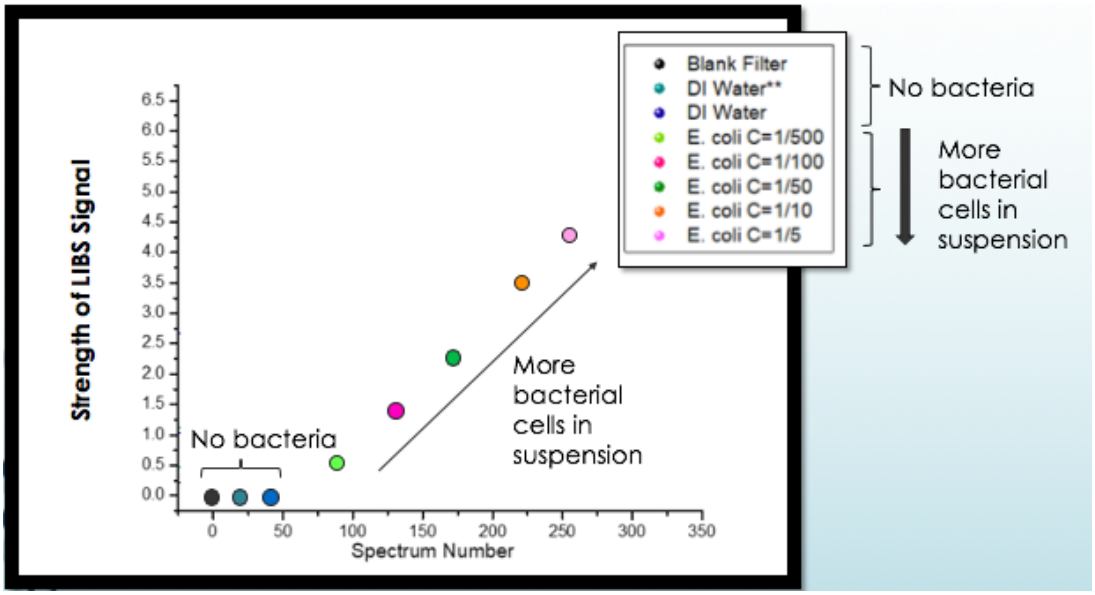

Figure 6.3: Idealized LIBS bacterial curve of growth.

Only *E. coli* was explored for the purpose of the calibration curve, as the other types of bacteria used in this work are of similar volumes to within the same order of magnitude. The various dilutions of 1/5, 1/10, 1/50, 1/100 and 1/500 were chosen to remain consistent with previous studies conducted by our lab group and to cover a large range of concentrations. Concentrations larger than the 1/5 dilution of our bacterial samples contain more cells than the number that would be retrieved via clinical samples and enough cells that they clump together during the centrifugation process and clog the apex hole of the metal cone, which prevents deposition on the filtration media.

The calibration curve we obtained is shown in Figure 6.4. Each point represents a single LIBS spectrum collected by our apparatus. The signal intensities for all elements were summed and divided by the carbon intensity and normalized. Carbon is the major signal present in the nitrocellulose filtration media. The large carbon signal is a physical limitation of our spectrometer which prevents us from increasing the signal amplification settings to boost all other elemental signal intensities. Increasing any particular signal such as the carbon peak too high will cause signal overflow and potentially damage the spectrometer itself.

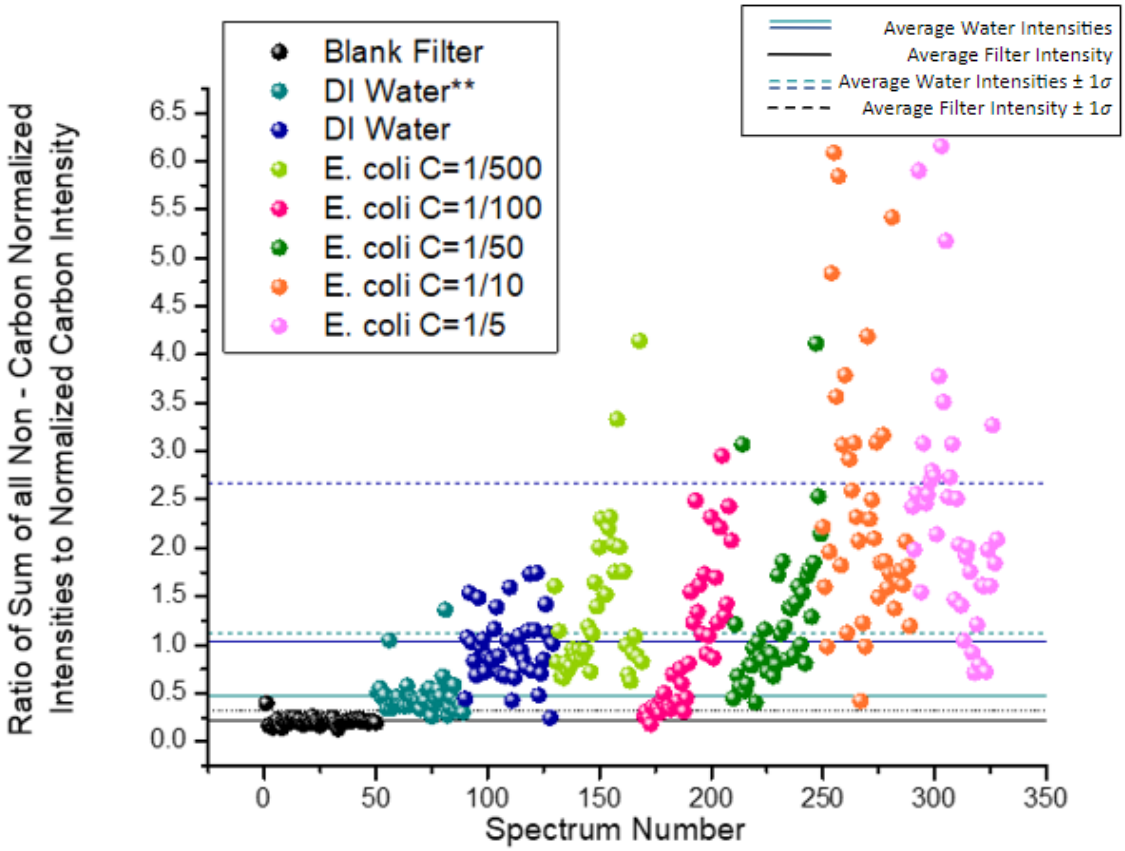

*Figure 6.4: Actual LIBS bacterial curve of growth constructed with serial dilutions of E. coli and sterile water samples (** refers to 24-hour filter drying period after deposition).*

The blank filters displayed in black have the lowest measured signals on the calibration curve however, since the blank filter always provides a strong carbon background at all concentrations, the measured signal never decays to zero. The light and dark blue points represent the pure deionized water samples that do not contain any bacteria. Increases in LIBS intensity above that measured for pure water indicate the presence of bacteria. Bacteria samples are suspended in deionized water, which contributes to bacterial LIBS spectrum. From the calibration curve we can still conclude that saturation of the LIBS emission intensities occurs as concentration increases and that the number of spectra indistinguishable from blank water spectra increases as concentration decreases.

Overall, the LIBS bacterial curve of growth still exhibits a linear relationship between concentration and measured signal however, two important questions arise. Firstly, why do sterile DI water specimens produce non-zero spectra significantly

higher than blank spectra? Secondly, why do some of the bacteria spectra appear as blank water spectra or "empty shots"? The calibration curve and the total LIBS bacterial spectral library were used to investigate these questions. Different approaches of outlier rejection methods to account for misclassified spectra along with library preprocessing were conducted to improve the curve of growth and the LIBS bacteria spectral library.

6.4 Background Reduction

An attempt to train the library to improve sensitivity by removing all spectra that did not classify correctly using a PLS-DA discrimination between bacteria and water was conducted first. The discrimination was done between *E. coli* and DI water using an unaltered spectral library labeled Library 1, containing all the past collected spectra of *E. coli* and DI water. One at a time, each spectrum of both *E. coli* and DI water were removed and externally classified against Library 1. The initial average sensitivity calculated from an external validation of Library 1 for DI water and *E. coli* were 78.4% and 72.5% respectively. Any spectra that were removed and classified incorrectly was subsequently removed from Library 1 in one of two ways.

The first method of removal sequentially eliminated each misclassified spectrum from Library 1 and a PLS-DA discrimination was performed after each removal to build Library 2. This method was to determine if removing a subset of data points improves the quality of the library. After each discrimination, a new sensitivity was calculated and compared to observe any improvement between Library 2 and Library 1. This resulted in an increased sensitivity for the external validation of *E. coli* of 88.8% however the sensitivity of the DI water did not change and remained 78.4%. The second method of removal eliminated all of the misclassified spectra simultaneously from Library 1 to build Library 3. This method was to determine if all misclassified spectra must be removed in order to improve the quality of the library. After removing all the misclassified spectra, a discrimination was performed on Library 3 and a decrease in the average sensitivity of DI water was observed. The average sensitivity of DI water was 75.9% while the average sensitivity of *E. coli* was

88.8%, comparable to Library 2. Although there was an increase in sensitivity for *E. coli* in both the construction of Library 2 and 3 during the preprocessing of Library 1, this resulted in removal of the *E. coli* spectra contained in Library 1. Removal of these spectra does not benefit the overall construction of a large and robust spectral library, instead it removes too many of the *E. coli* spectra collected from lower concentrations in order to improve the quality of the library. In addition, removal of these spectra does not work towards improving the limit of identification between bacteria and blank water samples.

While removing misclassified water spectra did not significantly improve the quality of the library, two additional tests were investigated to identify and potentially reject bacteria spectra that appeared as outliers. The first test was a water threshold analysis where any bacteria spectra that were within ± 1 standard deviation of the mean value of DI water were excluded. These lower intensity bacteria spectra possessed overall intensities consistent with DI water and could be the result of laser ablations outside of the concentrated areas of the centralized filter regions or dilutions that did not contain enough cells to be detected by our current level of identification. This analysis was carried out with multiple dilutions of *E. coli* and *M. smegmatis* to include high and low concentration comparisons with low intensity outliers removed. The sensitivity and specificity values for a PLS-DA discrimination of both *E. coli* and *M. smegmatis* are included in Table 6.1 for both the unprocessed and active water threshold cases. The left side of table includes 1/5 dilutions and the right side of table includes all serial dilutions. The result of the water analysis was that by implementing the water threshold intensity cut-off, the sensitivity and specificity values decreased during PLS-DA discrimination. The removal of a large number of bacteria samples using outlier rejection in this method did not improve the quality of the library or increase the accuracy of the classification between different species of bacteria.

Table 6.1: Outlier rejection - water threshold analysis using PLS-DA between E. coli and M. smegmatis

Only Concentrated Bacteria	Sensitivity	Specificity	All Concentrations of Bacteria	Sensitivity	Specificity
Unprocessed	97.5%	100.0%	**Unprocessed**	85.5%	87.2%
Water ± 1σ	94.4%	100.0%	**Water ± 1σ**	67.8%	79.0%

A second test for outlier rejection using histograms to retain more bacteria spectra while removing the lowest intensity spectra acquired from each tested filter was also investigated. Each filter was kept as either test data or library data and was not present in both sets of data simultaneously. The histograms were constructed for each data set based on the sum of all of the observed emission intensities known as the total spectral power (TSP). Histograms were also constructed for each data set using the total spectral power after subtracting the emission intensity of carbon (TSP-C). Each bacteria filter data set contained between 20 and 30 laser shots and were divided into approximately 6 histogram bins. The building of the histograms was done using Origin Pro 8 and the binning was chosen by the program automatically. All the spectra categorized in the bin containing the weakest intensities were taken to represent "empty shots" and were removed from the library before using a PLS-DA discrimination to calculate sensitivity and specificity values. These values for the TSP and TSP-C discrimination tests were compared to the PLS-DA results for the spectral library without any excluded filter data. An example of the histogram constructed for *E. coli* where the weakest emission intensities have been circled in red, is shown in Figure 6.5. The calculated and cross validated sensitivity and specificity values for the discrimination between the library containing *E. coli* and *M. smegmatis* bacteria samples using the unprocessed data along with the histogram altered data sets are shown in Table 6.2 below.

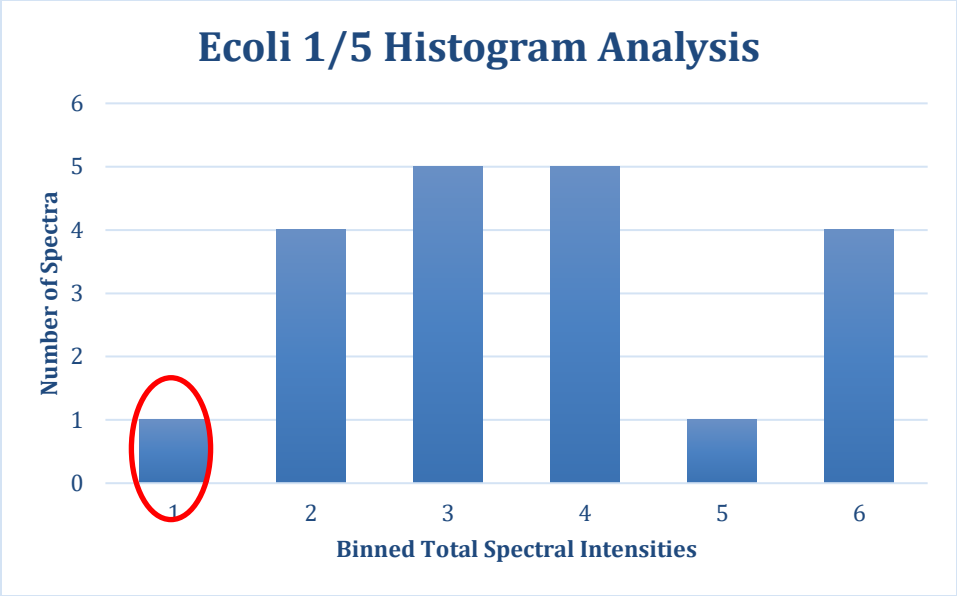

Figure 6.5: Histogram of intensities from spectra acquired from one filter deposition of E. coli 1/5 titer. The left most column circled in red represents the "empty shots" that do not follow a normal distribution. 1 of the 20 spectra were binned in the weakest emission intensity region by the histogram analysis and rejected from the total library.

Table 6.2: Calculated and cross validated sensitivity and specificity values

Tested Spectra	**Sensitivity (Cal)**	**Specificity (Cal)**	**Sensitivity (CV)**	**Specificity (CV)**
Ecoli 1/5 vs Myco 1/5 (w/o exclusion)	1.000	1.000	0.975	1.000
Ecoli 1/5 vs Myco 1/5 (TSP – C)	1.000	1.000	1.000	0.969
Ecoli 1/5 vs Myco 1/5 (TSP)	1.000	1.000	1.000	1.000

The method that provided the most accurate classification between library data groups containing *E. coli* 1/5 and *M. smegmatis* 1/5 was the exclusion of the TSP data based on histograms. This method of excluding data provided the highest sensitivity and specificity scores, as well as a highly visible divide between groups during the PLS-DA analysis. Further study into all other dilutions and combinations of bacteria along with discrimination between all bacteria and water are being conducted to verify the behaviour is consistent when performing the histogram data rejection method. A potential limit of identification could be obtained by studying the

behaviour of the remaining dilutions in this type of discrimination up to the point where the sensitivity and specificity drop to a value of or below 0.5. An additional method of verifying that a data set contains a large number of empty or misclassified spectra is to swap the test data and the library data and by conducting the reverse classification test. If the discrimination produces different results the test data could be removed altogether for inconsistencies.

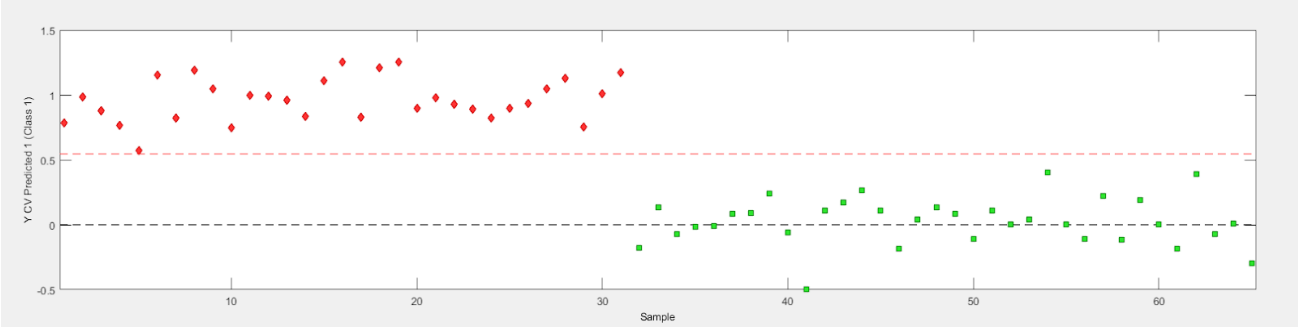

Figure 6.6: PLS discrimination between E. coli and M. smegmatis after removal of the weakest TSP spectra in which all remaining spectra classified correctly.

6.5 Tween Study

Bacteria cells are observed to aggregate in groups which could reduce the uniformity and exposed surface area during laser ablation of more dilute samples. As the bacteria cluster together, regions of the filter exhibit little to no bacterial signal and this contributes to shot-to-shot variations between adjacent spectra. The expected source of these low intensity spectra that resemble empty shots are expected to be the result of laser-matter interactions that do not generate bright plasmas during the LIBS ablation process because of non-uniform bacteria surface coverage. This idea is enforced by Figure 6.7, which shows scanning electron microscope (SEM) images of the deposition of clustered *Staphylococcus epidermidis* bacteria spread in the central region of the nitrocellulose filter contained where the apex of the metal cone presses into the media.

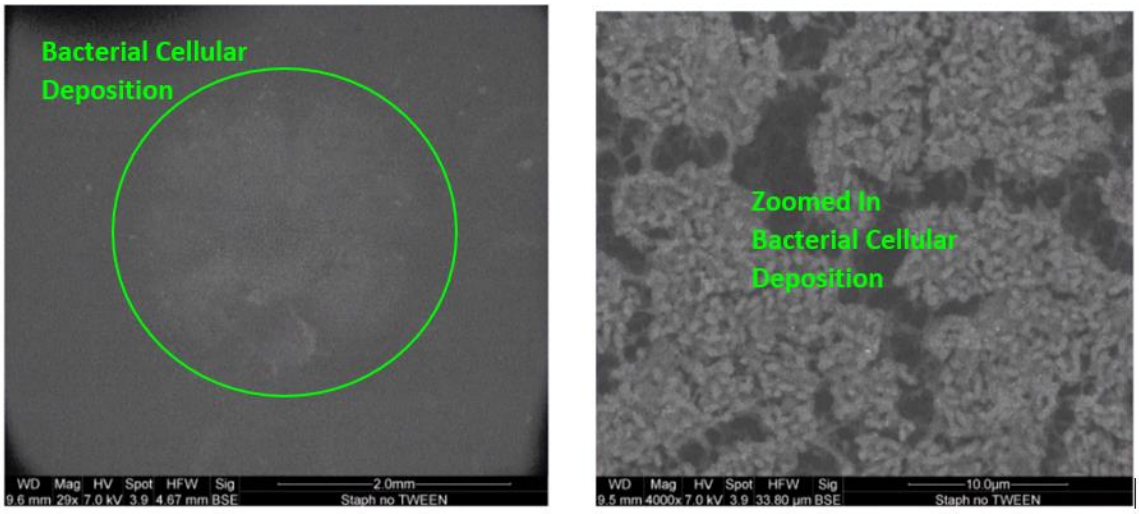

Figure 6.7: SEM micrographs of a) S. epidermidis bacteria deposition upon nitrocellulose filtration media and b) Magnified clustering of S. epidermidis bacteria calls.

There is a clear visible divide between the outer edge of the deposited bacterial cells and the blank filter. The clumping also results in the removal of bacteria that become filtered out with other contaminants and larger organic matter when different filter pore sizes are used or when additional filtration steps are included in the deposition process. This reduces the number of bacterial cells that make it through the deposition process to be identified with LIBS and presents a major issue with determining a limit of detection.

To prevent bacterial cells from clumping together and forming clusters in our samples a detergent known as Tween 20 was introduced to concentrated samples of *S. epidermidis*. Deposited samples of *S. epidermidis* were imaged using a SEM at multiple magnifications to compare bacteria with and without the Tween present to observe any differences in the bacteria cell's behaviour on the nitrocellulose filters. A detergent is a substance that makes hydrophobic compounds that are insoluble in water miscible in aqueous media. They act as emulsifiers and help to combine liquids that do not naturally mix together. Detergents generally disrupt the cell membranes of bacteria causing lysis which releases intracellular components. Tween 20 ($C_{58}H_{114}O_{26}$) is a non-ionic detergent that is non-denaturing and does not disrupt the structure of water-soluble proteins present in the bacteria cells.

A previous study was conducted by past students using Tween 20 to provide a more uniform laser ablation when combined with bacteria samples.[103] Two sets of dilutions of *E. coli* were prepared from the same initial suspension and tested with and without Tween 20 to evaluate the effectiveness of the detergent in preventing clumping of bacteria cells at multiple concentrations. It was concluded that the Tween had no effect on the *E. coli* samples and no significant difference was observed for the sets of dilutions. The expected reason was thought to be that there might be too many cells still present, however the more dilute samples still exhibited clumping in both cases.

Several SEM images were taken and the sample depositions with and without Tween exhibited clumping with no observable qualitative differences. When bacteria group together on the filtration media, gaps form between these clusters and expose the blank filter paper underneath. LIBS laser ablation is fundamentally a thermal process that requires absorption along a uniform surface in order for the flow of heat underneath the laser spot to remain consistent when forming LIPs. Our results spanning multiple years of ablating a test piece of steel prior to every LIBS experiment demonstrates the consistency of LIBS ablation upon a uniform surface.

A more in-depth investigation of Tween 20 concluded that the chemical is a neutral detergent and would be more effective when tested with Gram-positive bacteria species such as staphylococcus and streptococcus. Detergents can be cationic, anionic, zwitterionic or non-ionic depending on the organic compounds contained within the hydrophilic head group and hydrophobic hydrocarbon tail. *E. coli* is a Gram-negative bacterium that contains a membrane with a high concentration of lipids. This causes it to be resistant to non-ionic and anionic detergents such as Tween 20. Therefore, only cationic detergents would be effective in preventing clumping of *E. coli* cells.

The study was reproduced using *S. epidermidis* dilutions to determine if the Tween 20 was effective at producing a uniform deposition for a Gram-positive bacterium. Control samples of *S. epidermidis* were also prepared to compare using the SEM as shown in Figure 6.8. The detergent investigation was successful compared to previous attempts in the past. When using the Tween 20 with *E. coli*, the bacteria were

completely unaffected and there was no difference in the spread of the bacteria on the filter. Using Tween 20 with *S. epidermidis* produced a visible difference in the spread between the samples containing Tween and the samples without Tween present. The sample with Tween 20 had a more uniform spread on the area of the filter and between laser ablation craters while the sample with no Tween contained visible clumping and spaces between bacteria.

Although the non-ionic detergent prevented clumping of the Gram-positive *S. epidermidis*, the Tween formed a distinct layer on the surface that interfered with the visibility of the bacteria. Although the surface appears to be more uniform, we do not know what is happening to the cells that are trapped under the film of detergent. The new issue is that the cells are no longer visible on the surface and may not be receiving an effective dose of laser light. Further testing and research need to go into the procedure of using the detergent and possibly investigating a rinsing method that can remove the excess detergent from the surface of the treated bacteria.

The SEM micrographs in this work were taken with the environmental scanning electron microscope instrument located at the Great Lakes Institute for Environmental Research (GLIER). The regular or repeated use of such an instrument for imaging of a large number of our samples would be impractical, prohibitively expensive and time consuming. Timing the availability of such an instrument with many other research groups for use on samples that are best observed immediately after being tested with LIBS also poses a time constraint.

Tween vs. No Tween

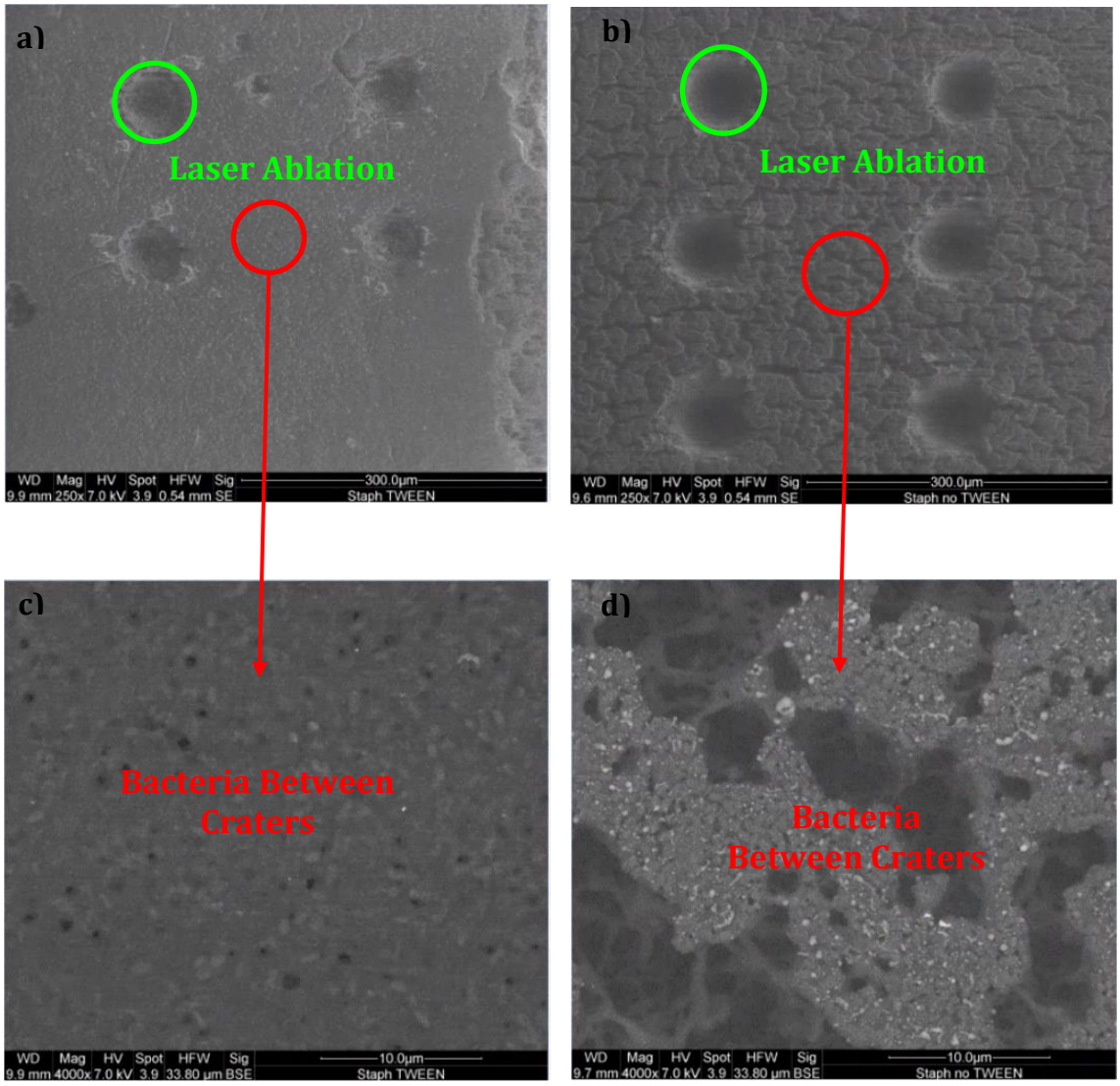

Figure 6.8: SEM images of S. epidermidis bacteria deposition upon nitrocellulose filtration media. Laser ablation results in uniform crater sizes with and without Tween. a) 250x magnification of laser ablation craters with Tween. The presence of Tween chemical resulted in a more uniform bacterial deposition upon the filter surface. b) 250x magnification of laser ablation craters without Tween. Cracks between clusters of bacterial cells were visible on surface in the absence of Tween chemical. c) 4000x magnification of bacterial cells with tween between laser craters show a solid film of Tween and bacteria. d) 4000x magnification shows the porous nitrocellulose filter substrate beneath the clusters of S. epidermidis cells.

References

[103] Paulick, A. E. (2018). *Development of Laser-Induced Breakdown Spectroscopy as a Rapid Diagnostic Tool for Bacterial Infection*, Master's thesis, University of Windsor. https://scholar.uwindsor.ca/etd/7653

Chapter 7: Metal Microparticle Enhanced LIBS

7.1 Nanoparticle Enhanced Laser - Induced Breakdown Spectroscopy - NELIBS

Recently, the use of metallic nanoparticles to enhance emission intensities in LIBS spectra has been demonstrated among various research groups, as detailed below. For an excellent review of this emerging area of research see Dell'Aglio et al.[104] This enhancement technique has been named nanoparticle enhanced laser-induced breakdown spectroscopy or by the acronym NELIBS. This section will discuss the achievements and advancements of NELIBS thus far.

Vinod et al. demonstrated that chemically pure colloidal suspensions of gold and silver nanoparticles (NPs) were synthesized using pulsed laser ablation.[105] These nanoparticles can be deposited and used directly for NELIBS to boost spectral emission intensities of target samples. Qayyum et al. also synthesized colloidal solutions of gold and silver NPs by nanosecond pulsed laser ablation of metal plates in ultrapure water. The absorption spectra of the colloidal solutions revealed strong plasmon resonance of the NPs. The silver NPs did have a wider size distribution and greater average size than the gold NPs. Significant enhancement of spectral lines in soda lime glass and copper targets were observed using deposited NPs. The spectral enhancement is attributed to an improved ablation efficiency caused by the coupling of the laser's electromagnetic field with the NPs plasmonic field.[106] Spectral enhancement via Au NPs was greater than the enhancement via Ag NPs, however the specific degree of enhancement of each enhanced elemental emission peak detected in a single spectrum was not consistent. This result will be consistent with the observations reported later in this chapter.

The phenomenon of plasmon resonance is created as the laser pulse induces coherent oscillation of the conduction electrons in small metallic particles, which in turn amplifies the incident electromagnetic field. This has the overall effect of increasing the electromagnetic field in the vicinity of the particle surface.[107] In the case of LIBS, the crucial process for plasma formation and ablation is the production

of seed electrons. The local enhancement of the electromagnetic field allows existing extracted electrons from the sample material by field electron emission to be used simultaneously at multiple ignition points. This effect of the NPs results in a more efficient ablation and greater plasma excitation which increase the LIBS emission signals.

Liao et al. prepared Au and Ag shell nanoparticle decorated silicon nanowires that were designed to capture bacterial adhesins. The bio interface promoted the binding of NPs to the bacteria in drinking water. LIBS and surface-enhanced Raman spectroscopy (SERS) were then used in combination to detect these bacteria.[108] Ag and Au NPs exhibit antibacterial rates towards both Gram-positive and Gram-negative types of bacteria. This group highlighted the ability of NELIBS to control and prevent microbial hazards in drinking water. Infectious diseases caused by pathogens are one of the most widespread health risks associated with natural sources of drinking water and cause millions of deaths each year.[109]

Work by Dell'Aglio et al. employed Au NPs to enhance LIBS of organic samples for quantitative trace metal detection at the sub-ppm level and even sub-ppb level for specific elements. The rapid quantification of these trace metals in liquid solutions is important for applications such as environmental, food, mechanics, forensics, archeometrics, and waste management. These results supported the detection and enhancement of metallic elements in protein and biological environments. The group also demonstrated NELIBS as a promising application with high sensitivity for cases where limitations in the sample amount are demanded.[110] This is very important for destructive processes such as LIBS that destroy specimens during laser ablation.

De Giacomo et al. have studied the underlying mechanisms responsible for NELIBS, the sample preparation for NELIBS to reach the optimal surface concentration of NPs and have tested a variety of samples including metals, transparent materials, fresh samples, and biological fluids.[1] Several issues arise during NELIBS including depositing the NPs on a target surface uniformly, focusing the laser spot and ablating regions where the NPs are homogeneously concentrated, avoiding impurities in colloidal solutions of NPs that could interfere with the measured analyte, and consistent particle size to allow for reproducibility in the

performance of an NELIBS measurement.[111] In another paper this research group detailed NELIBS enhancement over LIBS with respect to field enhancement, adsorption of analytes on a NP surface and an increase in the number density of particles in the LIBS plasma.[112] Further investigation of sample preparation and ablation procedures could improve the sensitivity and accuracy of NELIBS for use in medical and forensic science.

7.2 Microparticles

It is known that nanoparticles enhance LIBS emission, however the effects of metallic particles in the micron range have not been investigated by other research groups. Microparticles (MPs) fall between 1 and 100 μm in size and include typical particles that we encounter daily such as pollen, dust, sugar, flour and sand.[113] Tungsten powder on the micron scale had previously been used by our group to test the ability of our deposition process to separate larger contaminant particles from the bacterial specimens using dual centrifugation.[114] What if these metal powders were added to the bacteria or the surface of the filtration media directly? The addition of such powders to the bacteria samples for enhancement could introduce an entirely new field of LIBS.

Not only are we trying to quantify the enhancement we observe, but we are investigating ways to distribute these MPs easily on our nitrocellulose filters. MPs do not form colloidal suspensions like NPs, instead they aggregate and cluster together along the surface of a liquid solution. Agitating or vortexing the solution does not increase the miscibility of these particles either. Common practice with depositing NPs includes submerging surfaces in the colloidal NP suspensions or adding microdroplets of the NP solution to the surface.[115] Because the MPs clump together, neither of these aforementioned deposition techniques are viable for producing uniformly deposited microparticles to the surface of our nitrocellulose filters. Pipetting the MPs or mixing them with the bacteria samples and trying to execute our current mounting procedure will introduce several issues.

Firstly, the larger particles will clump together and clog the apex hole of the aluminum cone, also preventing the bacteria from passing through. Secondly, the MPs that do make it through will be concentrated in the center of the filter paper. While this is a benefit for the bacteria cells when ablating them with LIBS this is a detriment for the MPs. The metallic MPs will perform similar to our metal substrates during laser ablation and the LIP will be too intense. This will burn the nitrocellulose filter and damage the surface and deposited bacteria in close proximity, lowering the number of sample data that can be collected and overflowing our spectra with metal emission lines. Another issue is that the metal MPs come into contact with multiple pieces of equipment and the apparatus must be even more thoroughly cleaned to remove these contaminants when preparing bacteria and water samples where the MPs are not included. Alternate methods for depositing metal MPs to avoid these issues will be discussed in detail in section 7.4

7.3 Proof of Concept

In our lab we have various metallic powders, including tungsten, copper, and silver particles. With silver and gold being general choices for nanoparticles used in biomedical applications and LIBS research, the high purity 0.5 – 1 micron spherical silver powder was chosen as a possible MP candidate for LIBS enhancement. Ag NPs are well-known antibacterial agents and their antibacterial potential increases with a decrease in the bacteria particle size. This is an additional benefit of using silver powder when conducting LIBS research. The silver powder was deposited directly onto a nitrocellulose filter paper and tested with LIBS to compare the resulting spectrum with the NIST database. NIST is the National Institute of Standards and Technology and this Institute compiles and maintains a database of all atomic properties, including an entire spectral library for elemental LIBS emission spectra. Figure 7.1 shows our experimentally obtained silver LIBS spectrum compared to the calculated NIST LIBS silver spectrum. The emission peaks of both spectra aligned without the appearance of contaminant elements in our silver LIBS spectrum, aside from the carbon peak inherent to the nitrocellulose filter. Note that in these spectra,

as always, the spectroscopic notation is used where Ag I denotes emission from neutral silver atoms and Ag II denotes emission from singly-ionized silver.

a) **NIST LIBS Spectrum for Ag**

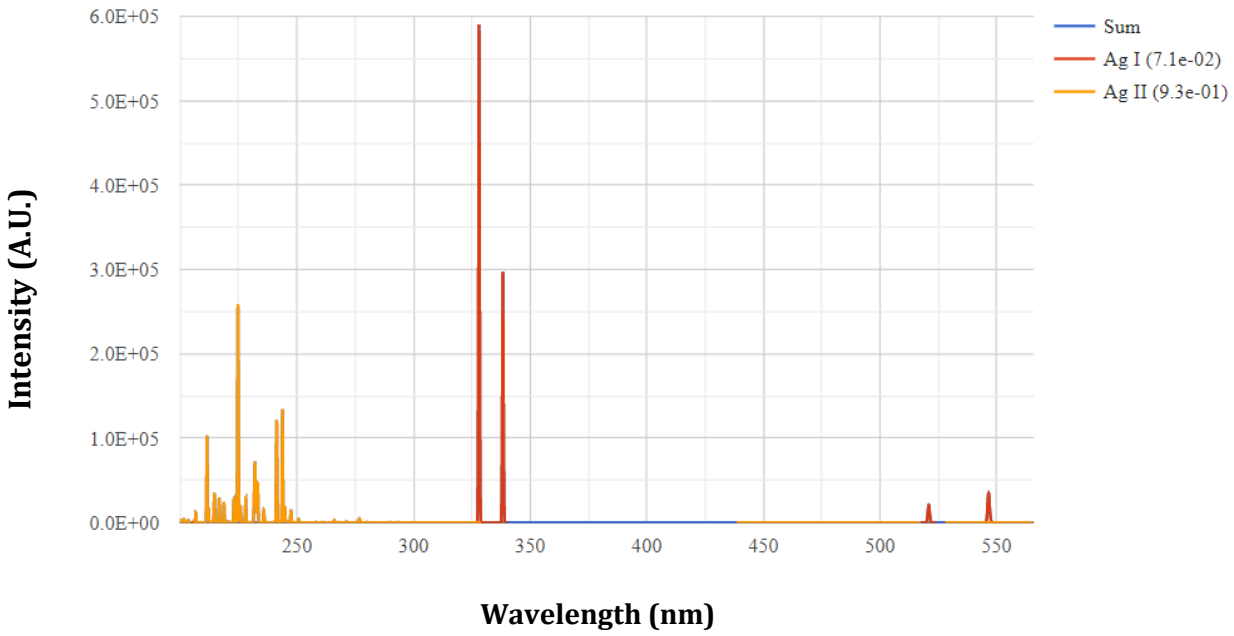

b) **Experimental LIBS Spectrum for Ag**

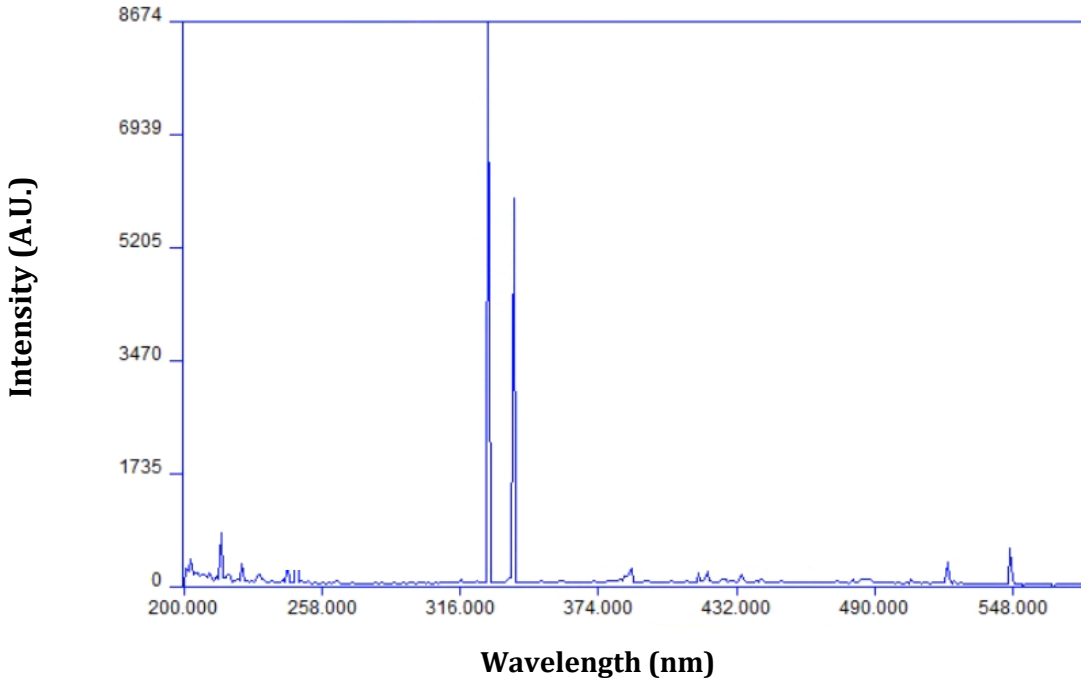

Figure 7.1: a) Silver LIBS emission spectrum referenced from the NIST LIBS spectral database[116] vs. b) Silver MPLIBS emission spectrum collected using our apparatus. The Ag I emission lines were detected in our spectra after ablating silver micron powder deposited upon nitrocellulose filters. The carbon emission peak has been removed.

The observed elemental emission lines of silver were then carefully compared to our bacterial emission lines of interest. The emission wavelengths are resolvable to within a hundredth of a nanometer and no direct overlap of silver peaks was observed with the bacteria peaks. Before combining the silver MPs with bacteria samples, the amount of silver powder to be deposited on the surface of the filters had to be determined with the goal of finding a reproducible method for depositing that known amount.

7.4 Metal Powder Deposition and Surface Coverage

In initial experiments, flocked swabs were placed ever so slightly in contact with the silver powder and used to transfer powder by brushing against the surface of nitrocellulose filters. This method could be done quickly, although the amount of silver powder transferred was not consistent. The filters were tested with LIBS and all of them resulted in massive scorching of the filter surfaces after a single laser ablation shown in Figure 7.2. After ablation, the powder within closest proximity to the ablation crater is pushed away, resulting in less scorching for subsequent laser pulses.

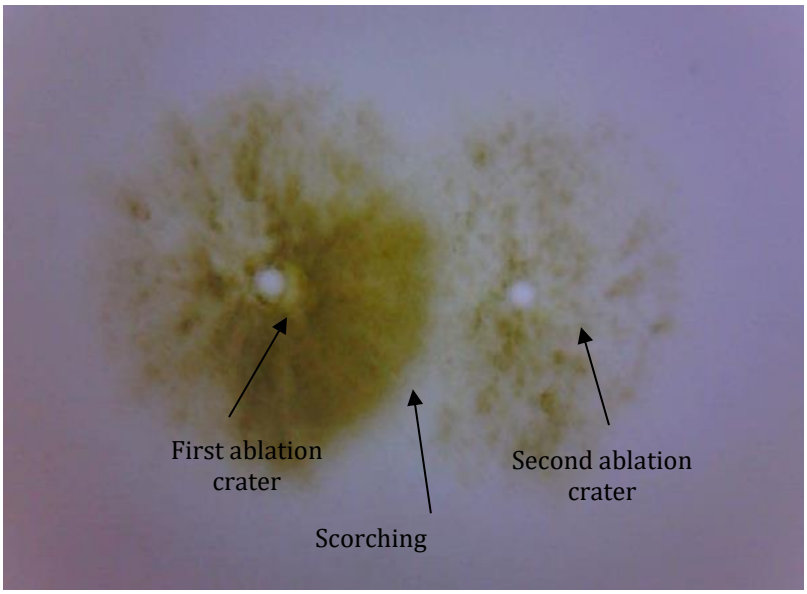

Figure 7.2: LIBS ablation craters and surrounding burning, centered on nitrocellulose filter surface coated with trace silver micron powder.

The amount of silver was reduced by brushing the swab against a filter even more lightly, and subsequently lowered by brushing the surface of that filter against other filters to transfer the silver powder in trace amounts. Using this new transfer process, ten filters were weighed before and after depositing silver microparticles using an EA microbalance, courtesy of Janeen Auld and Lara Watanabe of the University of Windsor Department of Chemistry and Biochemistry. This weighing technique is displayed in Figure 7.3.

Figure 7.3: Silver coated nitrocellulose filters inserted into EA microbalance. Two filters are placed on the balances to provide a reference counterweight.

The average filter mass without silver was 21.364 micro grams and was 21.377 micro grams after addition of the silver powder. The average amount of silver MPs deposited on the surface of the filters was 0.013 micro grams. At this level, the silver powder is barely visible on the surface of the filters to the naked eye. The filters were then tested with LIBS to check the reproducibility of the resulting spectra. The intensities of the two most prominent silver emission lines located at 328.06 nm and 338.31 nm in the LIBS spectra, were measured from 8 different locations on a filter with silver MPs deposited using the chamber deposition technique. The intensities had fluctuations of approximately 12% with 3105 ± 387 (A.U.) and 1922 ± 235 (A.U) respectively. Filters prepared in this way did not produce scorch marks during laser ablation. Examples of the filter surface with silver MPs and the resulting laser ablation craters are shown in Figure 7.4 below. These tests also show the sensitivity of the LIBS method to elemental concentrations or contaminations. In a typical LIBS spectrum, it is the optical emission from only nanograms or picograms of the analyte element that is being detected.

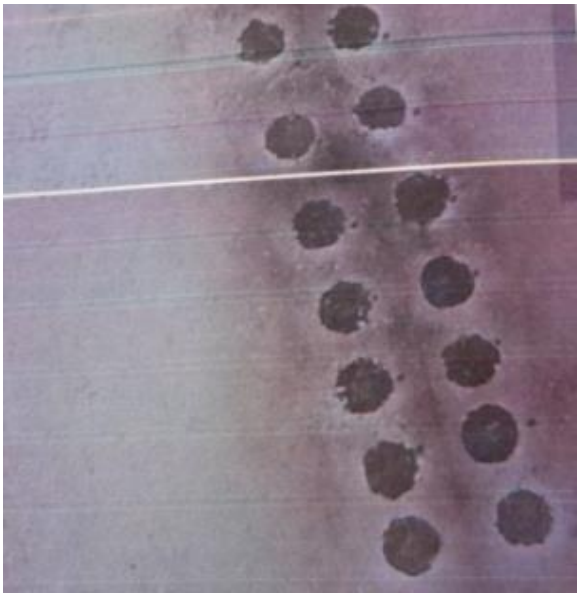

Figure 7.4: Zoomed in image of nitrocellulose filter with silver powder brushed along filter surface, captured using OASIS camera software. Craters displayed reproducibility among resulting LIBS spectra and visible ablation craters.

A technique to disperse the smallest of the silver particles and deposit them more uniformly upon the nitrocellulose filters was developed shortly after. Opening the container of silver microparticles produces a fine mist as the powder is agitated by the removal of the lid. This result of agitation and "settling" in air due to gravity gave rise to the idea of designing and constructing a silver deposition chamber. The fabrication of the chamber will be discussed in the following section.

7.5 Silver Microparticle Chamber

The chamber was drawn out schematically and the pieces were custom built by the machine shop out of plexiglass. The chamber and its components are shown in Figure 7.5. The chamber consists of a cube-shaped box with a rectangular slot opening that can be blocked by a plug/stopper. When the stopper is removed, a longer rectangular piece can be inserted into the chamber. This long piece contains a hinged end and a small circular region where a filter paper can be secured. Silver powder was inserted into the chamber. The chamber can be held in one hand and shaken easily. The stopper and long piece prevent contaminant materials from entering or any of the powder from escaping with a tight seal. Each filter can be inserted into the chamber and after shaking the chamber, the mist of smaller dispersed silver particles settles upon the exposed surface of the filter.

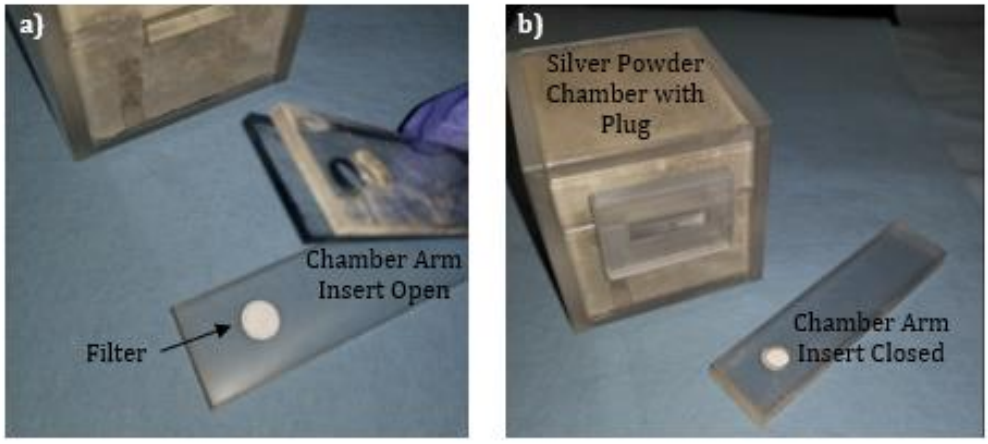

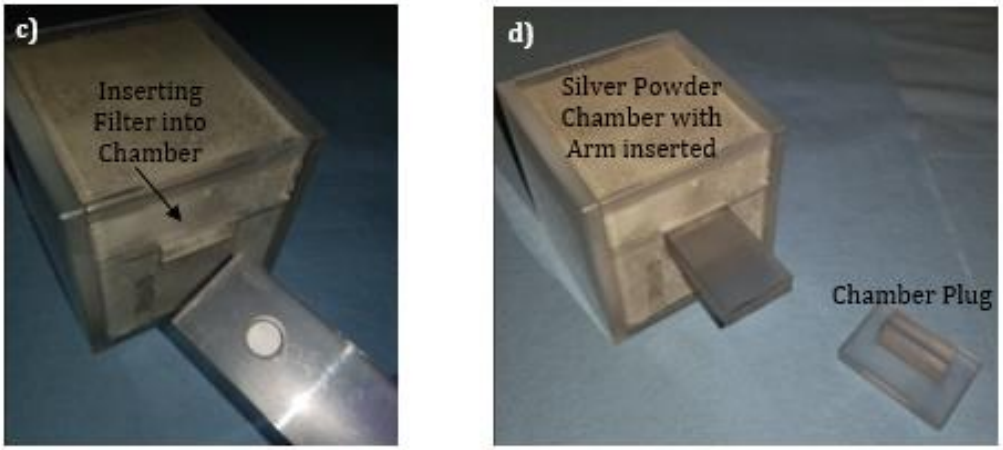

Figure 7.5: Silver powder deposition chamber and components. a) Filter positioned on base of chamber arm insert. b) Arm insert is closed to secure filter in place. Roof of arm insert contains a circular opening with diameter 8.15 mm. Chamber opening is sealed shut with plug and can be shaken for desired amount of time to agitate silver microparticles within. c) Plug is removed, and arm insert with blank filter can be inserted into frontal chamber slot opening. d) Inserted arm piece allows silver microparticles to fall uniformly upon the exposed filter surface.

The powder is uniformly distributed among the central region of the filters and barely visible where the LIBS ablation occurs, and after testing no scorching was observed on these filters. This method was used to produce several silver coated filters that bacteria could be deposited onto using the previously described centrifuge cone apparatus. The results of the LIBS ablation of bacteria deposited with silver MPs present are investigated in section 7.7.

7.6 Silver Surface Coverage

Three individual times are considered in this technique, the shaking time, the waiting time, and the settling time. A shaking time of 30 seconds was chosen specifically and held consistent to deposit silver MPs on the following filters. Additionally, a 10 second waiting time before inserting the filter was taken after the chamber was shaken. This was the minimum time at which the plug could be removed, and the chamber arm could be slid through the chamber opening. For longer waiting times, fewer silver MPs are deposited, until after a long enough time,

presumably none will be deposited. The settling time was the amount of time the filter was in the box with Ag MPs settling upon its surface due to gravity. Various settling times were attempted to investigate the most uniform and reproducible amount of surface coverage with the silver powder. This coverage was at a level that was barely visible to the naked eye.

Five pairs of filters were weighed before and after adding silver MPs, for settling time periods of 10, 20, 30, 40 and 50 second intervals. The calculated surface area coverage for the five pairs of filters is plotted in Figure 7.6. In one case, a 10 second settling time did not deposit enough powder to be measured by the microbalance and in the case of the 50 second settling times, too much powder was deposited on the surface. The ability to detect silver particles accurately below the nanogram range is not physically achievable with our current equipment, so a settling time in between our lower and upper deposition limits was chosen. Based on the consistency and observable coverage of each pair of filters, the 30 second settling time was chosen as the most reproducible deposition time.

Ten additional filters were prepared using the silver deposition chamber and weighed using the EA microbalance. The diameter of the circular opening of the long chamber arm insert was measured multiple times using a digital caliper to determine the area of the exposed filter surface for powder deposition. The average amount of silver MPs deposited and measured by the EA microbalance on the surface of the filters after a 30 second shaking period was 0.039 micro grams, contained within a central circular area of 52.18 mm^2. This amount of silver powder was almost triple that of the brushing technique, although the excess silver was contained around the edges of the nitrocellulose filters where the long piece clamps the filters in place. This excess powder is likely due to the sliding of the long piece in and out of the chamber, which pushes some powder into the circular opening. Small amounts of the silver powder also attach itself onto the bottom side of the filters as well. Future work for this technique will include removing the chamber arm piece with the silver chamber held upside down to attempt to reduce this excess powder from building up.

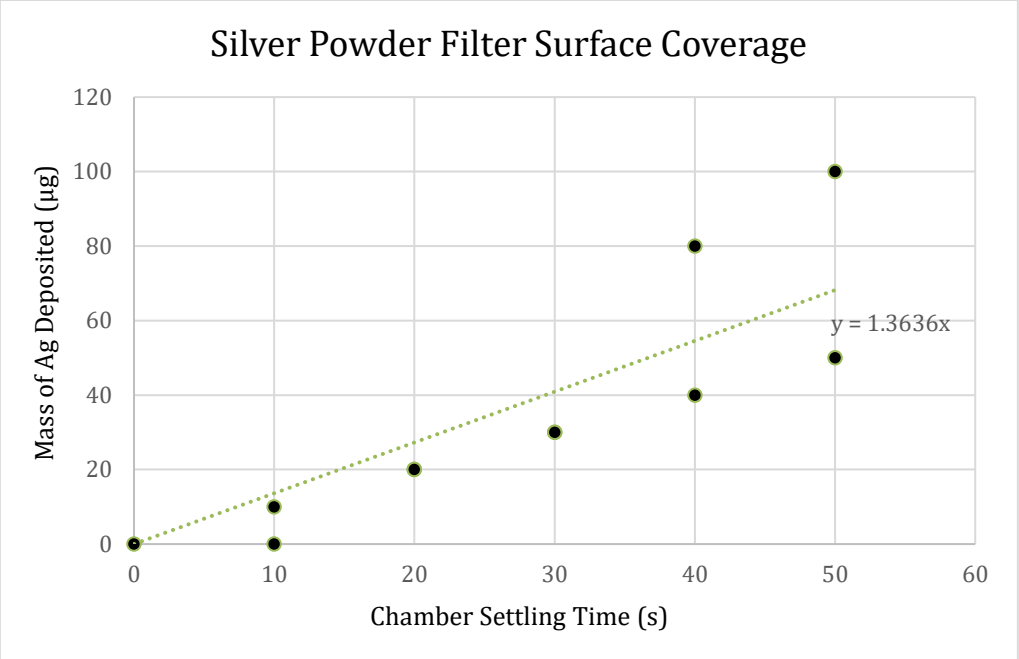

Figure 7.6: Plot of the mass of silver microparticles deposited on nitrocellulose filters using the custom silver chamber relative to the time-period of filter exposure to agitated powder. The chamber was shaken for 30 seconds and the filters were inserted into the chamber as silver powder settled on exposed filter surfaces. The silver microparticles were deposited at a rate of 1.36 µg/s upon the inserted filters. The mass deposition of silver MPs was more reproducible for 20 s and 30 s settling periods.

The mass differences measured by the EA microbalance and the settling times were used to quantify the surface coverage of silver powder on the filters. The mass deposition rate of the silver MPs on the nitrocellulose filters along with the exposed circular area of the filters was used to calculate a surface coverage density rate of 0.026 µg/mm^2·or 2.6 x 10^{-8} µg/µm^2. In the figure 7.7 below, the laser ablation craters can be seen to be approximately 75 microns in diameter, giving a circular ablation area of 4.4 x 10^3 µm^2. Assuming a uniform silver surface coverage density yields a silver ablation mass of 1.1 x 10^{-4} µg = 0.11 ng = 110 pg per laser shot. This is a very small amount of additional mass per laser ablation event. The measured mass of silver MPs was assumed to be linear with respect to the settling time in the low concentration regime. The next step is to build a new ROI file to analyze the silver emission line intensities in the LIBS spectra. A silver ratio model would be used to quantify the silver MPLIBS intensity versus the settling times and deposition times to

determine how the enhancement rate evolves during settling periods and whether the rate is optimized for a specific amount of time or if it plateaus and becomes saturated.

7.7 Effectiveness and Enhancement

Diluted bacteria samples were prepared in sets of two from the same initial concentrated specimens for species of *E. coli, M. smegmatis, P. aeruginosa* and *E. cloacae,* and tested with LIBS. Each pair of samples were deposited onto an unaltered nitrocellulose filter and a nitrocellulose filter coated with trace amounts of silver MPs deposited using the custom silver chamber. SEM images of the silver powder and the bacteria coverage upon silver coated filters are illustrated in Figure 7.7.

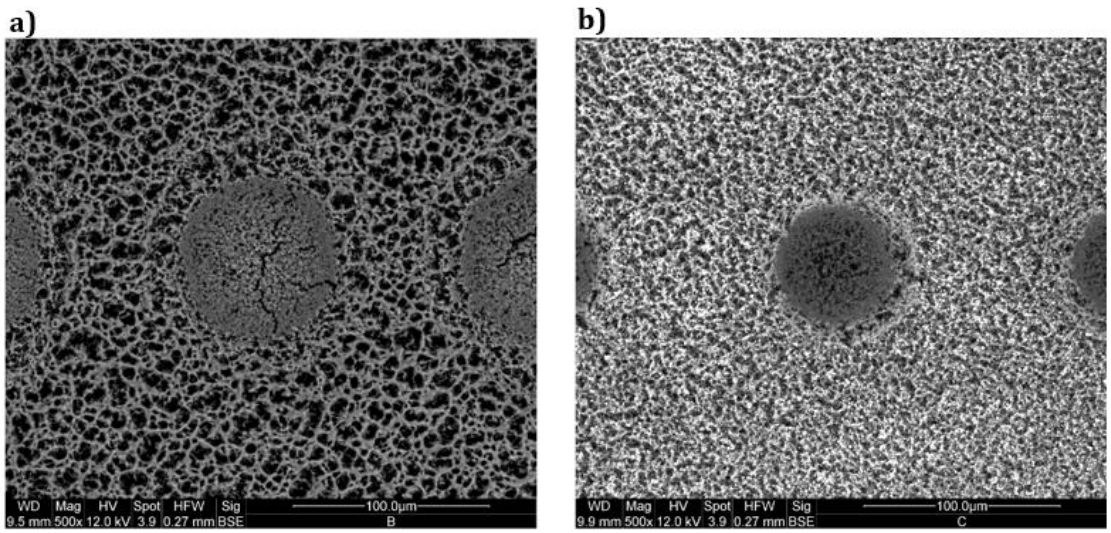

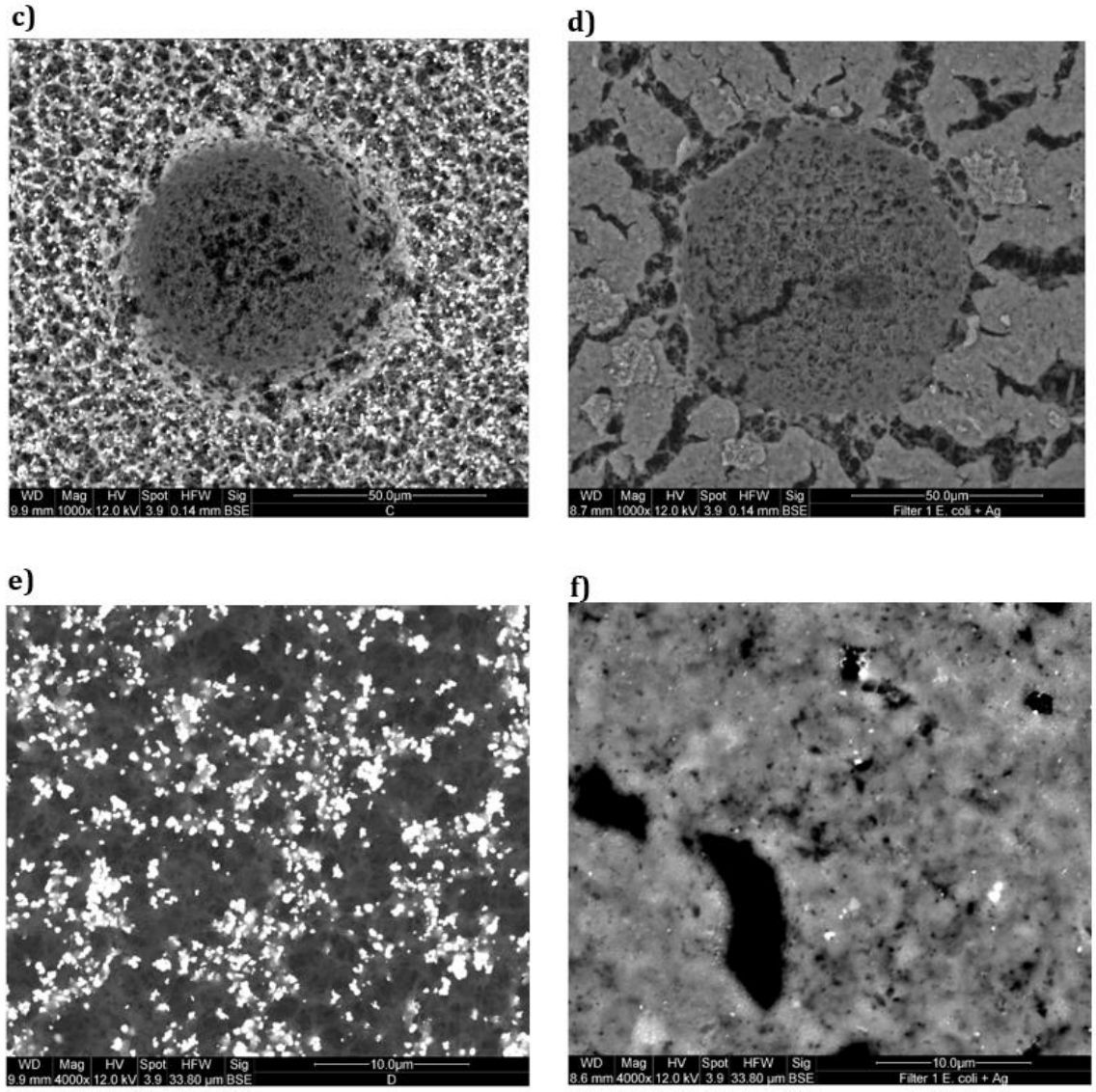

Figure 7.7: SEM images acquired of a) LIBS ablation crater on blank nitrocellulose filter 500x magnification. b) LIBS ablation crater on nitrocellulose filter coated with silver MPs deposited using the silver chamber 500x magnification Ablation crater is approximately 75 µm in diameter. c) LIBS ablation crater on nitrocellulose filter coated with silver MPs deposited using the silver chamber 1000x magnification. Silver MPs appear as bright white dots in the SEM images. d) LIBS ablation crater on nitrocellulose filter coated with silver MPs deposited using the silver chamber, with Escherichia coli bacterial cells deposited onto the silver coated filter 1000x magnification. Equivalent amounts of silver MPs are present in the bacteria samples but the majority are hidden underneath the layer of bacteria. Ablation crater is approximately 75 µm in diameter. e) Silver MPs deposited on nitrocellulose filter 4000x magnification. Silver MP are approximately 0.5 – 1 micron size compared to the 10 micron scale. f) Silver MPs and Escherichia coli bacterial cells deposited on nitrocellulose filter 4000x magnification. Larger silver MPs and silver MPs closer to the surface are detailed in white, while a majority of the silver MPs are

hidden underneath the layer of bacteria. Individual bacteria are not distinguishable or clearly visible in these SEM images.

The SEM images show the silver microparticles in detail between the pores of the nitrocellulose filtration media. The ablation crater produced in the presence of silver MPs appears visibly deeper than the ablation crater on the blank nitrocellulose filter. There is a visible difference between filters coated with silver MPs when bacteria are absent versus when bacteria are present. The bacterial lawn forms a layer on top of the filter surface and a portion of the silver MPs on the surface of the filter remain exposed between bacterial cells. The laser pulse breaks this lawn during the ablation process exposing additional silver MPs and the porous filtration media beneath.

After ablation, the 19 key elemental emission intensities including C, P, Ca, Mg and Na were compared to quantify any differences in the resultant bacterial LIBS spectra. The ratios between the spectral intensities with and without silver MPs present for each species of bacteria are presented in Table 7.1.

Table 7.1 Elemental enhancement ratios for bacteria samples

	Elemental LIBS Spectral Emission Enhancement				
Bacteria Species	**C**	**P**	**Mg**	**Ca**	**Na**
Escherichia coli	1.2	4.6	3.9	5.4	3.9
Mycobacterium smegmatis	1.2	1.7	2.7	8.4	6.7
Pseudomonas aeruginosa	1.3	1.1	6.9	27.3	1.0
Enterobacter cloacae	1.2	4.4	6.9	2.2	1.3

The first column of Table 7.1 contains the species of bacteria that were tested via LIBS, with and without the addition of silver microparticles on the nitrocellulose filters. The remaining columns show the overall enhancement ratios for the elements of interest (averaged from the 19 key elemental emission lines present in bacterial LIBS spectra). All of the elemental emission lines, including carbon, phosphorous, magnesium, calcium and sodium were enhanced with the presence of silver

microparticles on the filter surface during LIBS testing compared to bacteria samples that were prepared from identical stock solutions but deposited upon filters without the addition of silver microparticles. The carbon intensity was enhanced by 20-30% which did not exceed the limitations of our spectrometer, while the other elements were significantly enhanced. The most prominent elemental enhancement is the calcium peaks of the *Pseudomonas* LIBS spectral data. Further testing of this species will be conducted to determine if such an enhancement is reproducible. Another important feature to note is that for *Escherichia* and *Enterobacter*, the phosphorous peaks became evident and observable in the enhanced LIBS bacterial spectra, which is usually not the case.

The intensities for the vast majority of emission peaks were enhanced for all bacterial species, but the enhancement was not consistent between each bacterium or each element. The evidence supports random independent fluctuations between each specific elemental enhancement. This enhancement of elemental emission intensities could be crucial to improve the trace element detection capability of LIBS and could provide a means to potentially eliminate "empty spectra" that resemble blank water samples. The major drawback of microparticle enhanced LIBS is that a new spectral library would have to be created to begin to identify, classify and discriminate different species and genera of bacteria using this enhancement technique.

PLSDA discriminations were conducted for each bacteria sample deposited on a nitrocellulose filter that contained silver MPs against multiple filters coated with silver MPs containing no bacteria cells to prove that blank silver spectra do not classify as any of our bacteria with LIBS. All these discriminations resulted in 100% classification accuracy. This result was expected for silver spectra that contained none of the key emission peaks aside from carbon, compared to bacteria spectra. A PLSDA discrimination was also conducted for an *E. coli* sample deposited on a silver coated filter against the LIBS spectra of *E. coli* with and without deposited silver MPs to prove that spectra obtained from bacteria samples enhanced with silver MPs present are not identical to the spectra obtained from the same bacteria species deposited on blank filters. This discrimination is shown in Figure 7.8.

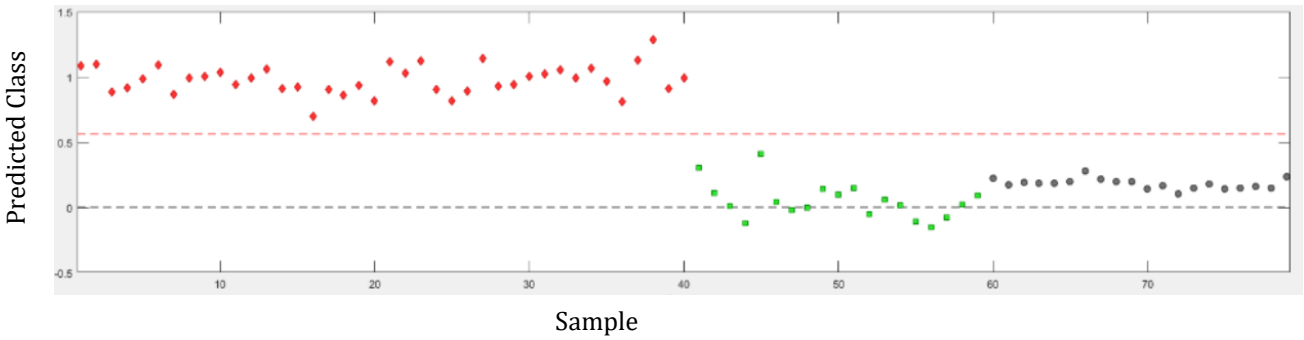

Figure 7.8: Example of PLS-DA discrimination of LIBS spectral data obtained from Escherichia coli deposited on nitrocellulose filter (class 1), Escherichia coli deposited on Ag coated nitrocellulose filter (class 2) and unknown class Escherichia coli deposited on Ag coated nitrocellulose filter (class 3) . In this test, the pure bacteria class is classified with a Predictor score of "1" and the bacteria samples combined with silver powder are classified with a Predictor score of zero. The Bayesian threshold for classification is indicated by the dashed red line. All data points subsequently tested that possessed a predictor score lower than the value of the Bayesian threshold were classified correctly. Unknown filter spectra of bacteria and silver powder was discriminated from the pure bacteria cells with 100% sensitivity and 100% specificity.

This set of experiments provided proof of concept that the addition of metallic microparticles did not decrease the ability of LIBS to accurately classify and discriminate bacterial species. We are convinced that the addition of easy to obtain and cheaply available silver microparticles does enhance the intensity of all our observed emission lines in each of our bacterial species. We do not currently know the complete mechanism behind this MP enhancement, but we do know that this effect is not the same as the plasmon resonance in NELIBS. Furthermore, we know that the presence of metals, which in general ablate much more easily than any other target substrates due to their thermal properties and their ability to donate electrons to the plasma, causes a higher temperature and a higher number of seed electrons in the plasma. The increased number of these electrons results in an enhanced emission from the same number of atoms as the metal microparticles produce a hotter analytic laser-induced plasma. We would have to study this mechanism further by collecting more bacterial spectra deposited on silver MP coated filters with LIBS. Further exploration into microparticle enhanced LIBS and whether enhancement using metallic powders on the micron scale to improve our overall limit of detection can

then be performed to determine the feasibility of LIBS as a technique to detect bacteria deposited in this way. No research utilizing microparticles for bacteria identification, classification or discrimination has been published to our knowledge based on our extensive review of bacteria LIBS research. The potential formation of a new field of microparticle enhanced laser-induced breakdown spectroscopy or MPLIBS could result from further research by our lab group.

References

[104] Dell'Aglio, M., Alrifai, R., & De Giacomo, A. (2018). Nanoparticle enhanced laser induced breakdown spectroscopy (NELIBS), a first review. *Spectrochimica Acta Part B: Atomic Spectroscopy*, *148*, 105-112. https://doi.org/10.1016/j.sab.2018.06.008

[105]Vinod, M., & Gopchandran, K. G. (2014). Au, Ag and Au: Ag colloidal nanoparticles synthesized by pulsed laser ablation as SERS substrates. *Progress in Natural Science: Materials International*, *24*(6), 569-578. https://doi.org/10.1016/j.pnsc.2014.10.003

[106] Qayyum, H., Ali, R., Rehman, Z. U., Ullah, S., Shafique, B., Dogar, A. H., ... & Qayyum, A. (2019). Synthesis of silver and gold nanoparticles by pulsed laser ablation for nanoparticle enhanced laser-induced breakdown spectroscopy. *Journal of Laser Applications*, *31*(2), 022014. https://doi.org/10.2351/1.5086838

[107] De Giacomo, A., Salajkova, Z., & Dell'Aglio, M. (2019). A quantum chemistry approach based on the analogy with π-system in polymers for a rapid estimation of the resonance wavelength of nanoparticle systems. *Nanomaterials*, *9*(7), 929.https://doi.org/10.3390/nano9070929

[108] Liao, W., Lin, Q., Xie, S., He, Y., Tian, Y., & Duan, Y. (2018). A novel strategy for rapid detection of bacteria in water by the combination of three-dimensional surface-enhanced Raman scattering (3D SERS) and laser induced breakdown spectroscopy (LIBS). *Analytica chimica acta*, *1043*, 64-71. https://doi.org/10.1016/j.aca.2018.06.058

[109] The World Health Organization, The World Health Report 1996: fighting disease, fostering development, (Geneva, Switzerland, 1996)

[110] Dell'Aglio, M., Salajková, Z., Mallardi, A., Mezzenga, R., Van't Hag, L., Cioffi, N., ... & De Giacomo, A. (2019). Application of gold nanoparticles embedded in the amyloids fibrils as enhancers in the laser induced breakdown spectroscopy for the metal quantification in microdroplets. *Spectrochimica Acta Part B: Atomic Spectroscopy*, *155*, 115-122. https://doi.org/10.1016/j.sab.2019.04.002

[111] De Giacomo, A., Gaudiuso, R., Koral, C., Dell'Aglio, M., & De Pascale, O. (2014). Nanoparticle Enhanced Laser Induced Breakdown Spectroscopy: Effect of nanoparticles deposited on sample surface on laser ablation and plasma emission. *Spectrochimica Acta Part B: Atomic Spectroscopy*, *98*, 19-27. https://doi.org/10.1016/j.sab.2014.05.010

[112] De Giacomo, A., Gaudiuso, R., Koral, C., Dell'Aglio, M., & De Pascale, O. (2014). Nanoparticle Enhanced Laser Induced Breakdown Spectroscopy: Effect of nanoparticles deposited on sample surface on laser ablation and plasma

emission. *Spectrochimica Acta Part B: Atomic Spectroscopy*, *98*, 19-27. https://doi.org/10.1016/j.sab.2014.05.010

[113] Saloň, I., Hanuš, J., Ulbrich, P., & Štěpánek, F. (2016). Suspension stability and diffusion properties of yeast glucan microparticles. *Food and Bioproducts Processing*, *99*, 128-135. https://doi.org/10.1016/j.fbp.2016.04.010

[114] Paulick, A. E. (2018). *Development of Laser-Induced Breakdown Spectroscopy as a Rapid Diagnostic Tool for Bacterial Infection*, Master's thesis, University of Windsor. https://scholar.uwindsor.ca/etd/7653

[115] Prevo, B. G., & Velev, O. D. (2004). Controlled, rapid deposition of structured coatings from micro-and nanoparticle suspensions. *Langmuir*, *20*(6), 2099-2107. https://doi.org/10.1021/la035295j

[116] https://physics.nist.gov/PhysRefData/ASD/LIBS/libs-form.html

Chapter 8: Conclusions and Future Work

8.1 Clinical Goal

The overarching goal of our LIBS research for past, present and future students has been to showcase and deliver laser-induced breakdown spectroscopy as an effective diagnostic tool for rapid bacterial identification and discrimination. In order to better understand bacterial LIBS and advance towards this goal, the main focus of my thesis has been to improve our deposition technique, investigate methods to enhance obtained bacterial LIBS spectra, improve the classification and discrimination ability using preprocessing methods and chemometric algorithms, and to increase the efficiency of collecting reproducible bacterial LIBS spectra for the construction of a robust spectral library.

The aim of this work was to evaluate the effectiveness of the LIBS technique on samples that were collected and prepared in a procedure that could be directly implemented into a clinical environment using patient specimens (i.e. samples collected using swabs). Experiments were designed and conducted to address various issues related to the testing of these swabbed samples. The two major issues that were considered in realistic samples included dealing with the low numbers of bacterial cells that are inherently present in actual clinical specimens (i.e. sputum, urine, blood and spinal fluid samples) as well as the presence of biological and inorganic contaminants that must be separated in order to concentrate the bacteria before LIBS ablation. The latter issue of separation will be addressed more comprehensively in future work by testing biological patient samples. (The acquisition and testing of patient samples was put on hold due to the safety precautions and restrictions currently implemented during the Covid-19 pandemic.)

Signal optimization and enhancement techniques were both used to eliminate sterile (i.e. blank) LIBS spectra that appear to resemble bacteria LIBS spectra and to boost bacteria LIBS spectra of reduced cell concentrations in various suspensions in order to improve the limit of detection to a level that would be clinically relevant. A library of bacteria LIBS spectra was acquired to showcase the effectiveness of chemometric techniques at classifying bacteria at the genus and strain levels.

The sensitivity and specificity of these bacterial LIBS classifications were investigated with the combined use of discriminant function analysis (DFA) and partial least-squares discriminant analysis (PLS-DA). Before preprocessing methods and the rejection of 'bad bacteria LIBS spectra', the chemometric algorithms resulted in a sensitivity of 66.37% and a specificity of 81.82% using DFA and a sensitivity of 65.78% and a specificity of 79.70% using PLS-DA when classifying a five-genus library comprised of *Escherichia, Pseudomonas, Staphylococcus, Mycobacterium* and *Enterococcus.* It was concluded that there is not a significant difference in discrimination ability between DFA and PLS-DA. These values are expected to improve as bacterial spectra are added to the library and as our LIBS technique is optimized to account for misclassified spectra.

These promising results support the ability of chemometric algorithms to correctly classify bacteria that have been collected and prepared using the methods described and developed in this work. These experiments also showcase the feasibility of building an extensive library of LIBS spectra collected from a wide variety of environmentally and medically relevant pathogens. By doing so, a patient sample can be taken, tested with LIBS, and the pathogen can be properly identified by comparing the LIBS spectra to the library using chemometrics. In the event the infections are not part of the existing library, the new pathogens can continuously be incorporated to build an ever-growing master library.

The current protocol involves the collection of bacteria using pathology swabs, centrifuging the suspension through a custom-fabricated cone device and concentrating the bacterial cells in a liquid suspension onto a small circular deposition area 1 mm in diameter upon a nitrocellulose filter medium. A pulse of high-intensity laser light focused onto the circular deposition allows a sensitive measurement of the elemental composition of the cells, leading to the detection and identification of the bacteria. By reducing the cell concentration in various suspensions, the limit of detection (LOD) may be calculated. It is important to note that our apparatus are positioned on an optical table that measures 3 m by 1 m and includes a large 1064 nm Nd-YAG laser, a spectrometer, a computer and a precise optical system of mirrors and lenses in order to ablate targets in an argon filled

chamber. The laser is a class 4 and requires protective laser safety goggles to be worn when the laser is in use. The size of the equipment and the number of components that must be carefully aligned would make it difficult for a clinician to conduct LIBS tests with our current setup. Handheld and bench-top LIBS devices, an example of which is displayed in Figure 8.1, have been built and are currently used in rapid elemental analysis in several areas of research.[117]

Figure 8.1: Image of a Z-200 handheld LIBS analyzer device produced by Analytik and a zoomed in screen view of elemental analysis.[118] This is one of many companies that produce portable LIBS instruments with friendly operating systems and numerous analytical apps to test a variety of sample materials. Image adapted from https://analytik.co.uk/product/z-200-handheld-libs-laser-analyser/

A portable LIBS instrument that could easily load samples and acquire spectral data without the need for safety goggles would be ideal for a clinical LIBS device.

Our group has studied the durability and repeatability of LIBS analysis over several years. The previous mounting procedures of our group achieved an initial LOD of ~50000 colony forming units (CFU) per laser ablation event with the use of a well-plate for concentrated bacterial deposition. This initial method was established using materials and equipment that are inexpensive and typically used in clinical

environments, however the minimum number of bacteria required for detection using LIBS was too high to be clinically relevant. The following procedure involved the design and implementation of the centrifuge insert, which resulted in a LOD of ~90000 CFU per laser ablation event. This method provided a rapid protocol for mounting bacteria of low titer specimens to improve reproducible signal reliability. While this did not immediately improve the LOD, the combination of the custom fabricated metal cone with the centrifuge insert reduced the LOD to ~5000, an entire order of magnitude greater than the previous two procedures.

It is believed that by improving the LOD of LIBS by an additional order of magnitude, we would be within a clinically relevant range since typical retrieval rates for a nasal swab are on the order of hundreds of colony forming units.[119] The number of bacteria present and the sensitivity and specificity of identifying the bacteria from different locations (i.e. throat swab vs. pus from an infected site) could vary drastically. Further work regarding specimens collected from different areas and sources would have to be investigated more extensively to prove whether LIBS would be appropriate for specific regions of the body.

Using signal optimization and enhancement techniques, the improvement of the current LOD by an order of magnitude is within reason and further results will indicate whether the LIBS technique is advantageous as a diagnostic tool for clinical specimens collected via swabs. Our current results demonstrate the robustness of LIBS measurements on test samples prepared in laboratory settings and the accuracy of LIBS combined with chemometric algorithms at detecting and discriminating bacteria. This method could be optimized and implemented to provide a method of bacterial identification that reduces the risk of bacterial infection to microbiologists, clinicians, and patients as well as a means to provide rapid appropriate treatment of infectious diseases. This would be a crucial medical achievement towards combating infections that can kill within hours of the onset of symptoms and towards preventing the emergence of antibiotic resistant strains of bacteria that result from generally prescribed antibiotics.

Not only could the implementation of LIBS into medical practice assist with preventing antibiotic resistant bacteria, but this technique could also be used to

specifically detect bacteria capable of antibiotic resistance using the acquired LIBS signals. In the linear dynamic range, the LIBS signal is linearly dependent on the number of bacterial cells present in the sample. Bacterium that are susceptible to antibiotics would not be able to reproduce after administering the drug and the LIBS signals would remain more constant. Bacterium that are resistant would be able to reproduce and multiply in the presence of the drug and as the number of cells increase, the LIBS signals would also increase. The doubling time for most known bacteria ranges between 15 minutes to 1 hour and could be factored into the expected LIBS signal measurements. By taking a LIBS spectrum before and after the bacterial cells are treated with antibiotics, the signals can provide evidence as to whether the species is resistant to a specific antibiotic. If the LIBS signal remained constant or lowered after administering the drug, then the cells were halted by that particular type of antibiotic. In the case where the LIBS signal remained proportional to that of the expected number of cells or increased substantially after factoring in the doubling times, the cells were unaffected by that particular type of antibiotic.

As part of this research, the limit of identification was investigated by calibrating the chemometric algorithms to improve the external validation accuracy of highly diluted specimens. Manipulation of the library with outlier elimination techniques such as histogram binning and water threshold levels was explored to remove misclassified spectra. The reduction of elemental contaminants contributing to extraneous background signals using improved cleaning and preparation methods along with the fabrication of newer inserts and cones using 3-D printing technology is underway. The addition of silver microparticles to enhance signal intensities is also being currently investigated to produce a standardized protocol that minimizes the bacterial limit of detection while maximizing classification accuracy. The presence of metallic MPs has demonstrated an enhancement of nearly all the bacterial LIBS emission intensities of interest for multiple bacteria species, some of which have more than doubled in the presence silver micron powder. Additional experiments will be conducted to map out different waiting times versus different settling times after shaking, to produce a grid of results to determine optimal silver deposition conditions. Additional ideas, concepts, and areas of interest of our group for future

projects relating to LIBS bacterial discrimination will be discussed in the following sections of this chapter.

8.2 Future Work

Laser-induced breakdown could be potentially improved and optimized towards the goal for diagnostic detection and classification of bacteria in a clinical setting with the implementation of several current and newly proposed approaches. For LIBS to become an accepted point-of-care medical diagnostic technology there are three key factors that the LIBS technique must accomplish. Firstly, the technique must be able to be performed on inexpensive disposable substrates to streamline and optimize the mounting procedure of samples. Secondly, the technique must rely on simple preparation and testing procedures that would utilize tools and equipment familiar to clinicians that would be available in a medical environment. Lastly, the technique must achieve a clinically relevant bacterial LOD.

It is important to note that the ICCD of our spectrometer imposes a physical limitation when generating LIBS spectra. In theory, the LOD could be reduced entire magnitudes by increasing the amplification of our spectrometer to greater levels. The issue is that any elemental emission signal that has too great an intensity could damage the ICCD. Current amplification settings were chosen such that the carbon line that is inherent to the nitrocellulose filtration media and by far the largest emission peak in our bacterial LIBS spectra, is at an intensity that does not exceed signal overflow. Removing the carbon emission line by customizing the spectrometer, for example adding in notch filters to attenuate the wavelength range of carbon or using two spectrometers designed to measure a range below 247.856 nm and another above 247.856 nm are very expensive solutions and prevent the ability to analyze the carbon atoms present in sample cells. Our group has tested other substrate materials and a better material for bacterial deposition has not been found, although removing or replacing the carbon line with another material would pose the physical limitation of amplification for another emission peak. The following section outlines multiple areas of research that our group would like to explore in future work related to LIBS

enhancement and the detection, identification, classification, and discrimination of bacteria.

Investigation into nanoparticle enhanced laser-induced breakdown is a potential pathway that will depend on the resulting effectiveness or success of microparticle enhanced laser-induced breakdown spectroscopy that is currently being investigated. The production or acquisition of high purity metallic NPs could be both difficult and expensive, which would not be advantageous towards implementing LIBS as a rapid diagnostic tool. NPs can be deposited and used directly to boost spectral emission intensities of patient samples, improve laser ablation efficiency, and detect trace metals. Further studies to determine the optimal surface concentration and placement of NPs for enhancement and the overall accuracy of NELIBS testing of bacteria are a viable option to reach a clinically relevant bacterial LOD.

Our current procedure of LIBS bacteria ablation collects 20 – 30 spectra per sample filter. Collecting multiple spectra per filter is crucial towards building a robust spectral library for accurate discrimination of newly tested samples. Measuring several spectra in a laboratory setting and adding spectra together to form an "add all spectrum" requires substantially more time than acquiring a single LIBS spectrum. We theorize that in a clinical setting, the collection of a single LIBS spectrum would be more ideal for analyzing patient samples. The entire specimen would be ablated by the laser and tested to detect and classify bacterial infections. With the use of a portable LIBS instrument and streamlined swabbing preparation procedures, the entire process could be conducted within minutes to provide rapid diagnostic results. While the use of a larger laser spot size does not currently help establish a larger spectral library, the adjustment of the optics in our lab to ablate entire samples in future experiments could support single spectrum analysis for bacterial classification. The relative time of preparing the samples and shooting the samples would have to be investigated to determine the optimal number of samples that should be tested in a clinical setting to provide the most accurate diagnosis.

During LIBS experiments, the sound of the LIP formation provides a subtle notification of the emission intensities in the collected spectra. The plasma spark

shock wave produced during laser ablation could be recorded acoustically to establish whether plasmas that produce stronger spectra have a unique sound compared to plasmas that result in weaker spectra. The corresponding acoustic signatures could be indicative of whether a spectrum should be rejected during data collection and improve the reproducibility of bacterial LIBS testing. The design and implementation of a device to measure acoustic signals during laser ablation could combine the expertise of sonography and similar fields with LIBS technology. This is an idea of a project that could be investigated by future group members to account for shot-to-shot variation of bacterial targets and improve the repeatability of the LIBS signals.

All of the previous work involving testing bacteria using LIBS has involved the use of chemometric algorithms to compare the LIBS spectra of different bacteria. This work was focused on the feasibility of using LIBS in a clinical setting and discriminating bacteria using chemometric techniques including DFA and PLS-DA. Bacteria classification is not limited to chemometrics and could be tested with additional techniques including artificial neural networks (ANN) or the combination of LIBS with other forms of spectroscopy.

ANNs are trained by processing examples, spectra in our case, with known inputs and results. ANNs form probability weighted associations between the known inputs and results which are stored within the network. The network is built up of connected nodes that operate similar to biological neurons in the brain.[120] The connections between these artificial neurons transmit signals in order to process inputs and adjust as outputs proceed. The weighted associations determined by non-linear functions increase and decrease as signals are transmitted dependent upon the strength of each neuron connection. The neurons form multiple layers with the ability to perform various transformations on input signals. The signals can be sent between layers and travel to each layer multiple times before determining the difference between output results and expected predictions.

It has also been proposed that the LIBS technique could be improved by combining the compositional information of the spectral data with the structural information provided by Raman spectroscopy. Raman spectroscopy is a technique

that measures shifts in the frequency of incident laser light. These shifts are caused by Stokes and anti-Stokes scattering. Incident photons interact with a sample material and either absorb the materials energy (anti-Stokes) or release energy (Stokes) into the material during inelastic scattering.[121] The vibrational modes of the molecules are altered by the corresponding changes in energy between the material and incident photons. The molecular information of Raman spectroscopy and elemental information of laser-induced breakdown spectroscopy could be integrated to create more unique bacterial fingerprints for a dual discrimination technique. The alternate discrimination with ANNs and the combination of LIBS with Raman spectroscopy could potentially improve the sensitivity and accuracy for a more robust bacterial classification technique.

One of the most commonly asked questions with respect to LIBS, especially because we use LIBS on bacteria, is whether laser-induced breakdown on virus samples is possible. This is definitely a topic of interest and importance with the need for rapid diagnosis of viral infections such as Covid-19. Few studies have been conducted using LIBS on viruses and our group has never worked with viruses.[122,123] A major advantage of working with our bacterial samples is that they are non-pathogenic species and provide a much safer working environment than one working with infectious organisms such as viruses. Aside from being more dangerous to handle, prepare and test with LIBS, viruses are also many times smaller than bacteria cells. Bacteria are on the scale of 1 – 3 μm while viruses are on the scale of 1000 to 10000 times smaller.[124] For example, the Corona virus is 80 to 160 nm in size.[125] Another issue is that viruses do not contain the trace metals that bacterial cells contain. These trace metals are the key components that we observe in our bacterial LIBS spectra. The LOD and enhancement ability of LIBS would have to be significantly increased from our current levels to begin testing viruses for viral detection and discrimination. Advancements towards viral LIBS requires a laboratory with higher biosafety protocols and expertise in the field of virology.

References

[117] Rakovský, J., Čermák, P., Musset, O., & Veis, P. (2014). A review of the development of portable laser induced breakdown spectroscopy and its applications. *Spectrochimica Acta Part B: Atomic Spectroscopy*, *101*, 269-287. https://doi.org/10.1016/j.sab.2014.09.015

[118] *Z-200 HANDHELD LIBS ANALYSER*, Analytik. https://analytik.co.uk/product/z-200-handheld-libs-laser-analyser/

[119] Warnke, P., Frickmann, H., Ottl, P., & Podbielski, A. (2014). Nasal screening for MRSA: different swabs–different results!. *PLoS One*, *9*(10), e111627.https://doi.org/10.1371/journal.pone.0111627

[120] Manzoor, S., Moncayo, S., Navarro-Villoslada, F., Ayala, J. A., Izquierdo-Hornillos, R., de Villena, F. M., & Caceres, J. O. (2014). Rapid identification and discrimination of bacterial strains by laser induced breakdown spectroscopy and neural networks. *Talanta*, *121*, 65-70. https://doi.org/10.1016/j.talanta.2013.12.057

[121] Efremov, E. V., Ariese, F., & Gooijer, C. (2008). Achievements in resonance Raman spectroscopy: Review of a technique with a distinct analytical chemistry potential. *Analytica chimica acta*, *606*(2), 119-134. https://doi.org/10.1016/j.aca.2007.11.006

[122] Gottfried, J. L. (2011). Discrimination of biological and chemical threat simulants in residue mixtures on multiple substrates. *Analytical and bioanalytical chemistry*, *400*(10), 3289-3301. https://doi.org/10.1007/s00216-011-4746-4

[123] Multari, R. A., Cremers, D. A., & Bostian, M. L. (2012). Use of laser-induced breakdown spectroscopy for the differentiation of pathogens and viruses on substrates. *Applied optics*, *51*(7), B57-B64. https://doi.org/10.1364/AO.51.000B57

[124] Leung, W. W. F., & Sun, Q. (2020). Electrostatic charged nanofiber filter for filtering airborne novel coronavirus (COVID-19) and nano-aerosols. *Separation and Purification Technology*, 116886. https://doi.org/10.1016/j.seppur.2020.116886

[125] Sahin, A. R., Erdogan, A., Agaoglu, P. M., Dineri, Y., Cakirci, A. Y., Senel, M. E., ... & Tasdogan, A. M. (2020). 2019 novel coronavirus (COVID-19) outbreak: a review of the current literature. *EJMO*, *4*(1), 1-7. https://doi.org/10.14744/ejmo.2020.12220

Appendix A

Table A: Complete list of bacteria that have ever been tested in a LIBS apparatus, as well as an identification of the substrate upon which this analysis was performed, the state of the bacteria, the specific chemometric routine used in identification, and the type of laser utilized in the test[126]

Micro-organism	Form	Chemometric utilized	Laser wavelength (nm)[a]
Acinetobacter baumannii ATCC BAA-1789	Colony on blood agar	PCA/PLS1	1064
Acinetobacter baylyi	Pellet, freeze-dried powder	Hyperspace projection of trace elements	810 (fs)
Acinetobacter calcoaceticus [FJ816073][b]	Colony on glass slide	PCA/PLS-RA	800 (fs)
Arhodomonas sp. [EU308280]	Colony on glass slide	PCA/PLS-RA	800 (fs)
Bacillus anthracis var. Sterne	Thin lawn[c] on nylon filter	None	1064
Bacillus anthracis var. Sterne	Thin lawn on agar, glass slide	PCA/PLS1	1064
Bacillus atrophaeous	Spore, aerosol stream	None	1064
Bacillus atrophaeous	Dried film on Al disk, steel disk, polycarbonate disk	NN, MLSRA,PLS-DA	1064
Bacillus atrophaeous	Pellet, freeze-dried powder	SVM	1064
Bacillus aureus	Spore, EDB trap	None	355
Bacillus cereus 6E1	Thin lawn on silver membrane filter	PCA, linear correlation, and SIMCA	1064
Bacillus cereus ATCC 14603	Pellet, freeze-dried powder	SVM	1064
Bacillus globigii[d] BG-1	Pellet, freeze-dried powder	None	1064
Bacillus globigii BG-1	Spore, aerosol stream	None	1064
Bacillus globigii BG-2	Pellet, freeze-dried powder	None	1064
Bacillus globigii BG-2	Spore, aerosol stream	None	1064

Bacillus globigii var. niger	Thin lawn on silver membrane filter	PCA, linear correlation, and SIMCA	1064
Bacillus globigii var. niger	Continually refreshed dense aerosol cloud (from powder) and aerosol stream	PCA	1064
Bacillus globigii var. niger	Powder on double-sided sticky tape	No, linear correlation, PCA, PLS-DA	1064x2 (DP)
Bacillus globigii 168	Colony (wet) on LB medium	None	532
Bacillus globigii	Thin film lawn on cellulose nitrate membrane filter	None	810 (fs), 1064
Bacillus globigii	Pellet, freeze-dried powder	Hyperspace projection of trace elements	810 (fs)
Bacillus globigii	Dried powder on solid substrate	PCA, HCA, PCA+LDA	1064
Bacillus globigii ATCC 23857	Colony on blood agar	PCA/PLS1	1064
Bacillus megaterium QM B1551	Colony (wet) on LB medium	None	532
Bacillus megaterium PV361	Colony (wet) on LB medium	None	532
Bacillus stearothermophilus ATCC 12979	Pellet, freeze-dried powder	SVM	1064
Bacillus thurengensis	Pellet, freeze-dried powder	None	1064
Bacillus thurengensis var. kurstaki	Thin lawn on silver membrane filter	PCA, linear correlation, and SIMCA	1064
Bacillus thurengensis var. kurstaki	Thin lawn on nylon filter	None	1064
Bacillus thurengensis T34	Colony (wet) on LB medium	None	532
Bacillus thuringiensis ATCC 51912	Pellet, freeze-dried powder	SVM	1064
Bacillus sp. [GQ392044]	Colony on glass slide	PCA/PLS-RA	800 (fs)
Bacillus sp. [GQ226038]	Colony on glass slide	PCA/PLS-RA	800 (fs)
Bacillus sp. [HM026606]	Colony on glass slide	PCA/PLS-RA	800 (fs)

Enterobacter cloacae [FJ194527]	Colony on glass slide	PCA/PLS-RA	800 (fs)
Enterobacter cloacae ATCC 13047	Thin lawn on nutrient-free agar	DFA, PLS-DA	1064
Enterobacter sp. [CP000653]	Colony on glass slide	PCA/PLS-RA	800 (fs)
Enterobacter sp. [GU586319]	Colony on glass slide	PCA/PLS-RA	800 (fs)
Enterobacter sp.[FJ194525]	Colony on glass slide	PCA/PLS-RA	800 (fs)
Erwinia chrysanthemi	Pellet, freeze-dried powder	Hyperspace projection of trace elements	810 (fs)
Escherichia coli	Pellet, freeze-dried powder	None	1064
Escherichia coli	Thin lawn on cellulose nitrate membrane filter	None	810 (fs), 1064
Escherichia coli	Pellet, freeze-dried powder	Hyperspace projection of trace elements	810 (fs)
Escherichia coli IHII/pHT315	Colony (wet) on LB medium	None	532
Escherichia coli K-12 (AB), Hfr-K12, HF4714, C (Nino C), O157:H7, ATCC 25922	Thin lawn on nutrient-free agar	DFA, PLS-DA	1064
Escherichia coli	Thin lawn on cellulose nitrate membrane filter	DFA, PLS-DA	1064
Escherichia coli O157:H7 ATCC 4389	Thin lawn on ground beef, bologna, chicken, milk, eggshell, lettuce, drain, cutting board, swab	PCA/PLS1	1064
Escherichia coli	Thin lawn on filter paper	None	1064
Escherichia coli	Thin lawn on filter paper and sausage	None	1064
Escherichia coli DH5α	Freeze-dried powder	PCA,PLS2	1064
Escherichia coli	Thin lawn on silicon wafer	DFA	266
Escherichia coli OV2	Colony on LB, MacConkey, Brucella agar	NN	1064

Escherichia coli ATCC 15597	Dried film on Al disk, steel disk, polycarbonate disk	PLS-DA	1064
Escherichia coli K12 ATCC 10798	Colony on blood agar	PCA/PLS1	1064
Escherichia coli	Thin lawn on glass slide	None	1064
Escherichia coli MC6-RP11, QCB1	Colony on LB agar	NN	1064
Escherichia coli K12	Thin lawn on plexiglass	PCA/SIMCA	1064, 775 (fs)
Escherichia coli	Unknown	K-means classifier and NN	1064
Escherichia coli CCM 3954	Colony on MH agar	PCA, Self-Organizing Maps (NN)	532
Escherichia coli K12, ATCC 25922	Thin lawn on silicon wafer	PCA, HCA	1064
Escherichia coli ATCC 25254	Thin lawn on plexiglass substrate	None	1064
Francisella tularensis vaccine strain	Thin lawn on agar, glass slide	PCA/PLS1	1064
Klebsiella pneumoniae ATCC 13882	Colony on blood agar	PCA/PLS1	1064
Klebsiella pneumonia K21P, K18P, K17P, K16R, K11CM, K11P, K7P,K6P, K3C, K2P	Colony on LB agar	NN	1064
Listeria innocua	Pellet, freeze-dried powder	PCA, Mahalanobis discriminant analysis (MDA)	266
Methylophilus methylotrophus [AB193724]	Colony on glass slide	PCA/PLS-RA	800 (fs)
Methylophilus sp. [AY436800]	Colony on glass slide	PCA/PLS-RA	800 (fs)
Methylophilus sp. [EU375653]	Colony on glass slide	PCA/PLS-RA	800 (fs)
Methylophilus sp. [GQ175365]	Colony on glass slide	PCA/PLS-RA	800 (fs)
Micrococcus luteus	Thin lawn on glass slide	None	1064
Mycobacterium smegmatis wild-type, TE, TA	Thin lawn on nutrient-free agar	DFA, PLS-DA	1064

Mycobacterium smegmatis	Thin lawn on cellulose nitrate membrane filter	DFA, PLS-DA	1064
Paenibacillus sp. [AY728023]	Colony on glass slide	PCA/PLS-RA	800 (fs)
Pantoea agglomerans [FJ611822]	Colony on glass slide	PCA/PLS-RA	800 (fs)
Proteus mirabilis	Pellet, freeze-dried powder	None	1064
Pseudomonas aeruginosa M841	Colony on LB, MacConkey, Brucella agar medium	NN	1064
Pseudomonas aeruginosa	Thin lawn on nutrient-free agar	DFA	1064
Pseudomonas aeruginosa	Thin lawn on cellulose nitrate membrane filter	DFA, PLS-DA	1064
Pseudomonas aeruginosa [HM036358]	Colony on glass slide	PCA/PLS-RA	800 (fs)
Pseudomonas aeruginosa ATCC 33580	Colony on blood agar	PCA/PLS1	1064
Pseudomonas aeruginosa PA1-PA19	Colony on LB agar	NN	1064
Pseudomonas putida	Pellet, freeze-dried powder	PCA, Mahalanobis discriminant analysis (MDA)	266
Salmonella enterica serovar Typhimurium[e]	Thin lawn on silicon wafer	DFA	266
Salmonella enterica ATCC 8324	Thin lawn on ground beef, bologna, chicken, milk, eggshell, lettuce, drain, cutting board, swab	PCA/PLS1	1064
Salmonella pollorum 1JVC, 1/1Km, 2/1Km	Colony on LB agar	NN	1064
Salmonella salamae 2JVC, 1/2Km, 2/2Km	Colony on LB agar	NN	1064
Salmonella typhymurium LB5010	Colony on LB, MacConkey, Bucella agar medium	Neural networks	1064
Salmonella typhimurium SL-1344, 1/22Km, 2/22Km	Colony on LB agar	NN	1064

Salmonella typhymurium	Pellet, freeze-dried powder	PCA, Mahalanobis discriminant analysis (MDA)	266
Salmonella typhymurium	Thin lawn on silicon wafer	PCA, HCA	1064
Shewanella oneidensis	Pellet, freeze-dried powder	Hyperspace projection of trace elements	810 (fs)
Staphylococcus aureus	Pellet, freeze-dried powder	None	1064
Staphylococcus aureus MRSA: LP9, MM61, MM66, MM66-4	Freeze-dried powder	PCA,PLS2	1064
Staphylococcus aureus	Thin lawn on nutrient-free agar	DFA,PLS-DA	1064
Staphylococcus aureus	Thin lawn on silicon wafer	DFA	266
Staphylococcus aureus SH1000, SH1000-1, RN4220, RN4220-fail, MRSA: LP9, MM61, MM66, MM66-4	Colony on blood agar	PCA/PLS1	1064
Staphylococcus aureus	Pellet, freeze-dried powder	PCA, Mahalanobis discriminant analysis (MDA)	266
Staphylococcus aureus	Unknown	K-means classifier and NN	1064
Staphylococcus aureus	Thin lawn on silicon wafer	PCA, HCA	1064
Staphylococcus aureus CCM 4223, CCM 4750 (MRSA), CCM 3953 (MSSA)	Colony on MH agar	PCA, Self-Organizing Maps (NN)	532
Staphylococcus aureus ATCC 25923	Thin lawn on plexiglass substrate	None	1064
Staphylococcus epidermidis	Thin lawn on nutrient-free agar	DFA,PLS-DA	1064
Staphylococcus epidermidis	Thin lawn on cellulose nitrate membrane filter	DFA, PLS-DA	1064
Staphylococcus pseudointermedius	Colony on MH agar	PCA, Self-Organizing Maps (NN)	532

Staphylococcus saprophyticus	Thin lawn on nutrient-free agar	DFA, PLS-DA	1064
Staphylococcus sciuri	Colony on MH agar	PCA, Self-Organizing Maps (NN)	532
Streptococcus mutans	Thin lawn on nutrient-free agar	DFA, PLS-DA	1064
Streptococcus viridans	Thin lawn on nutrient-free agar	DFA,PLS-DA	1064

[a]all lasers have ns pulse duration unless otherwise noted
[b]Genbank accession number
[c]Lawn usually denotes a liquid suspension deposited on a substrate then allowed to dry for a variable amount of time to form a thin, dry or semi-dry film. A colony means a growth accumulation region not in suspension or dispersed in a liquid.
[d]*Bacillus globigii* is also known as *Bacillus subtilis*
[e]*S. enterica* serovar Typhimurium is commonly referred to by its serovar identification only as *S. typhimurium* or by its more proper taxonomic identification, *S*. Typhimurium

References

[126] Rehse, S. J. (2019). A review of the use of laser-induced breakdown spectroscopy for bacterial classification, quantification, and identification. *Spectrochimica Acta Part B: Atomic Spectroscopy*, *154*, 50-69. https://doi.org/10.1016/j.sab.2019.02.005

Appendix B

Table B: Complete list of RM3 ratios used for discrimination of LIBS bacterial spectra

Complete List of RM3 Ratios					
p1/c	p2/na2	p4/na1	p6/cai1	mgii4/caii2	caii3/na2
p1/mgii1	p3/c	p4/na2	p6/na1	mgii4/caii3	caii4/c
p1/mgii2	p3/mgii1	p5/c	p6/na2	mgii4/caii4	caii4/na1
p1/mgii3	p3/mgii2	p5/mgii1	mgii1/c	mgii4/cai1	caii4/na2
p1/mgii4	p3/mgii3	p5/mgii2	mgii1/caii2	mgii4/na1	cai1/c
p1/mgi1	p3/mgii4	p5/mgii3	mgii1/caii3	mgii4/na2	cai1/na1
p1/mgi2	p3/mgi1	p5/mgii4	mgii1/caii4	mgi1/c	cai1/na2
p1/caii2	p3/mgi2	p5/mgi1	mgii1/cai1	mgi1/caii2	c/na1
p1/caii3	p3/caii2	p5/mgi2	mgii1/na1	mgi1/caii3	c/na2
p1/caii4	p3/caii3	p5/caii2	mgii1/na2	mgi1/caii4	mgi1/mgii1
p1/cai1	p3/caii4	p5/caii3	mgii2/c	mgi1/cai1	mgi1/mgii2
p1/na1	p3/cai1	p5/caii4	mgii2/caii2	mgi1/na1	mgi1/mgii3
p1/na2	p3/na1	p5/cai1	mgii2/caii3	mgi1/na2	mgi1/mgii4
p2/c	p3/na2	p5/na1	mgii2/caii4	mgi2/c	mgi2/mgii1
p1/mgii1	p4/c	p5/na2	mgii2/cai1	mgi2/caii2	mgi2/mgii2
p2/mgii2	p4/mgii1	p6/c	mgii2/na1	mgi2/caii3	mgi2/mgii3
p2/mgii3	p4/mgii2	p6/mgii1	mgii2/na2	mgi2/caii4	mgi2/mgii4
p1/mgii4	p4/mgii3	p6/mgii2	mgii3/c	mgi2/cai1	cai1/caii2
p2/mgi1	p4/mgii4	p6/mgii3	mgii3/caii2	mgi2/na1	cai1/caii3
p2/mgi2	p4/mgi1	p6/mgii4	mgii3/caii3	mgi2/na2	cai1/caii4
p2/caii2	p4/mgi2	p6/mgi1	mgii3/caii4	caii2/c	
p2/caii3	p4/caii2	p6/mgi2	mgii3/cai1	caii2/na1	
p2/caii4	p4/caii3	p6/caii2	mgii3/na1	caii2/na2	
p2/cai1	p4/caii4	p6/caii3	mgii3/na2	caii3/c	
p2/na1	p4/cai1	p6/caii4	mgii4/c	caii3/na1	

Vita Auctoris

NAME:	Jeremy C. Marvin
PLACE OF BIRTH:	Windsor, Ontario
YEAR OF BIRTH:	1994
EDUCATION:	B. Sc. [Honours] Medical Physics, 2016 University of Windsor, Windsor, Ontario
	M. Sc. Physics, 2020 University of Windsor, Windsor, Ontario